BioMedicine March 2014, Vol. 4, No. 1, Pages 1-6 DOI 10.7603/s40681-014-0001-6

Review article

EZH2: novel therapeutic target for human cancer

Long-Yuan Li [a,b,c,*]

[a] Graduate Institute of Cancer Biology, China Medical University, Taichung 404, Taiwan
[b] Center for Molecular Medicine, China Medical University Hospital, Taichung 404, Taiwan
[c] Department of Biotechnology, Asia University, Taichung 413, Taiwan

Received 31st of December 2013 Accepted 15th of January 2014

Keywords:
EZH2;
Polycomb repressive complex;
Chromatin modification;
Methylation

ABSTRACT

Enhancer of Zeste homlog 2 (EZH2) is a catalytic subunit of epigenetic regulator Polycomb repressive complex 2 (PRC2), which trimethylates Lys 27 of histone H3, leading to silencing of the target genes that are involved in a variety of biological processes including tumor progression and stem cell maintenance. However, in addition to its canonical PRC2-dependent transcriptional repression function, EZH2 also acts as a gene activator in a noncanonical PRC2-independent manner. Overexpression of EZH2 has been detected in diverse cancers, and is associated with tumor malignancy. Moreover, activating mutations and inactivating mutations of EZH2 are also associated with certain types of cancer. Given EZH2's multi-faceted function and role in cancer, context-specific strategy for targeting EZH2/EZH2-mediated signaling could serve as future targeted therapy/personalized medicine for human cancer.

1. Introduction

Epigenetic regulation, including DNA methylation and demethylation [1], histone modification, incorporation of histone variants [2, 3], and non-coding RNAs [4], plays a key role in modulating chromatin state and gene expression without altering DNA sequence. Aberrations of epigenetic regulators and chromatin modifications have proven links with human disease: e.g., cancer. Polycomb group proteins (PcGs) are crucial epigenetic regulators that form chromatin-modifying complexes, whose composition may be cell-context-dependent. In mammals, two major PcG complexes, Polycomb repressive complex 1 (PRC1) and 2 (PRC2), have been identified [5, 6]. Core components of PRC1 complex contain ring finger protein RING1A/B, B lymphoma Mo-MLV insertion region 1 (BMI1), chromobox homolog (CBX), PHC, and SCML subunits [5-7]. The PRC1 establishes repressive chromatin structure via E3 ubiquitin ligase RING1A/B that monoubiquitylates Lys 119 of histone H2A (H2AK119ub1) [8, 9]. Core subunits of PRC2, conserved from Drosophila to mammals, include suppressor of Zeste 12 (SUZ12), embryonic ectoderm development (EED), retinoblastoma suppressor associated protein 46/48 (RbAp46/48), and histone methyltransferase (HMTase) EZH2, which catalyzes trimethylation of histone H3 at Lys 27 (H3K27me3) to generate another epigenetic silencing mark [10-14] (**Fig. 1A**). However, study also reveals RING1B can maintain chromatin compaction and repress gene expression independent of its histone ubiquitination activity [15]. PcG proteins suppress transcription by forming chromatin loops with DNA methylation, which may impede DNA access to transcription factors [16]. Exact functions and molecular mechanisms underlying high-order chromatin configuration remain unexplored. Other than PcG proteins, Trithorax group (TrxG) proteins are known as critical to epigenetic regulation of senescence, cell cycle, DNA damage and stem cell biology. TrxG plays a role opposite to PcG: transcriptional activator of gene expression, modifying chromatin structure via trimethylation of histone H3 at Lys 4 (H3K4me3) [17]. It has been reported that many genes involved in development and differentiation concomitantly carry both repressive H3K27me3 and active H3K4me3 marks, known as bivalent chromatin domains. These bivalent loci are poised in a state ready for transcriptional activation or repression. Activated genes lose H3K27me3 and are enriched for H3K4me3; whereas repressed genes retain H3K27me3 or gain silencing marks like DNA methylation, but lose H3K4me3 [5].

EZH2, catalytic subunit of PRC2, is predominantly considered to trimethylates Lys 27 of histone H3, leading to silencing of target genes involved in cell cycle regulation, senescence, cell fate determination, cell differentiation and cancer [6]. Yet besides its PRC2-dependent transcriptional repression function, recent evidence indicates that EZH2 also mediates gene activation through methylating nonhistone proteins or forming transcriptional complexes with other factors to activate downstream target genes in a PRC2-independent fashion [18-22] (**Fig. 2**). Mounting evidence shows that overexpression/amplification or mutations of EZH2 have been detected in a variety of cancers, and are associated with tumor development and progression [23]. EZH2 also plays vital roles in stem cell maintenance and lineage differentiation [24-26]. Thus, EZH2/EZH2-mediated signaling deregulation contributes to numerous human pathologies, making this signaling an attractive therapeutic prospect and molecular marker to serve as targeted therapy/personalized treatment of human maladies, including cancers.

2. Domain structure and function of EZH2

2.1. Domain organization of EZH2

Human EZH2 was mapped to chromosome 7q35, which contains 20 exons and encodes 746 amino acids (**Fig. 1B**) [27]. EZH2 harbors functional domains: WD-40 binding domain (WDB), domains I-II, two SWI3, ADA2, N-CoR and TFIIIB (SANT) domains, cysteine-rich CXC domain and evolutionarily conserved carboxy-terminal Su(var)3-9, enhancer of zeste, trithorax (SET) domain. The SET domain of EZH2 is the catalytic domain required for HMTase activity [11, 14, 28, 29]. Moreover, complex of EZH2 with other PRC2 components, noncatalytic subunits EED and SUZ12, is necessary to gain robust HMTase activity [28, 30-34]. WDB is EED-interacting domain. Domain II is binding region for SUZ12, and SANT domains are for interaction with histone.

* Corresponding author.. Graduate Institute of Cancer Biology, China Medical University, Taichung 404, Taiwan.
E-mail address:lyl@mail.cmu.edu.tw (L.-Y.Li).

Published online: 12 February 2014

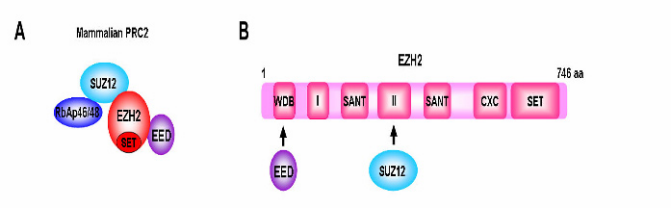

Figure 1. Core subunits of PRC2 and domain structure of EZH2. (A) Core subunits of mammalian PRC2 include suppressor of Zeste 12 (SUZ12), embryonic ectoderm development (EED), retinoblastoma suppressor-associated protein 46/48 (RbAp46/48), and histone methyltransferase (HMTase) EZH2, which catalyzes the trimethylation of histone H3 at Lys 27 (H3K27me3) to generate epigenetic silencing mark [10-14]. (B) Schematic diagram of EZH2 functional domains, WD-40 binding domain (WDB), domains I-II, two SWI3, ADA2, N-CoR and TFIIIB (SANT) domains, cysteine-rich CXC and evolutionarily conserved carboxy-terminal Su(var)3-9, enhancer of zeste, trithorax (SET) domain. EZH2's SET catalytic domain is needed for HMTase activity [11, 14, 28, 29]. WDB is EED-interacting domain. Domain II is binding region for SUZ12, SANT domains for interaction with histone

2.2. Polycomb-dependent transcriptional repression function of EZH2

As a catalytic subunit of PRC2, EZH2 is primarily considered as an epigenetic silencer for transcriptional repressing of gene expression, including a variety of tumor suppressor genes. With PRC2 recruited to target genes, EZH2 containing SET domain catalyzes trimethylation of histone H3 at Lys 27 (H3K27me3). Subsequently, the PRC1 subunit, CBX, recognizes and binds to H3K27me3 mark, then catalytic subunit of PRC1, RING1, monoubiquitylates Lys 119 of histone H2A (H2AK119ub1) to impede RNA polymerase II-dependent transcriptional elongation and repress gene transcription [5] (**Fig. 2A**). Although coordinated recruitment of PRC1/2 is widely quoted in the literature, genome-wide mapping of histone modifications and localization of PRC1 and 2 subunits by chromatin immunoprecipitation-sequencing found that some genes that lack H2AK119ub1 are also targeted by PRC2 [35]. Besides, some reports indicate PRC1 recruitment and PRC1-mediated H2AK119ub1 occurring independently of PRC2/H3K27me3 [36-38]. Moreover, Tavares et al. recently unraveled that RYBP-PRC1 complex, consisting of RING1 YY1 binding protein (RYBP) and PRC1 catalytic subunits, mediates H2AK119ub1 at normal level both in PRC2-null mESCs and wild type mESCs, portending PRC2/H3K27me3 as not needed for recruitment of RYBP-PRC1 complex and RYBP-PRC1-mediated H2AK119ub1 on PcG target loci [39]. These studies revealed that PRC1 and PRC2 may also regulate gene expression independent of each other.

Aside from well-recognized epigenetic gene silencing function, recent study demonstrated EZH2 interacts with and directly methylates non-histone target, cardiac transcription factor GATA4 at Lys 299. PRC2-mediated GATA4 methylation impaired its interaction with and acetylation by p300 to attenuate GATA4 transcriptional activity and gene expression [40] (**Fig. 2B**). Moreover, EZH2 binds and methylates RORα at Lys 38 which is recognized and ubiquitinated by DCAF1/DDB1/CUL4 ubiquitin ligase complex, giving rise to RORα degradation and transcriptional repression of RORα target genes [41] (**Fig. 2B**). These studies explore novel mechanism of PRC2-mediated gene suppression: EZH2 directly methylating transcriptional factor and inhibiting transcriptional activity.

Diverse epigenetic modification regulators can cooperatively fine-tune gene expression. Indeed, EZH2 physically interacts with and recruits DNA methyltransferases DNMT1, DNMT3A and DNMT3B to methylate CpG and establish a more deeply repressive chromatin state [42]. Yet knocking down EZH2 increases transcription of genes with minimal DNA methylation but not genes with heavily DNA hypermethylation [43, 44]. Several studies reveal EZH2 target genes pre-marked by PRC2-mediated H3K27me3 in normal cells as strongly correlated with genes becoming aberrantly hypermethylated in cancer cells, suggesting genes pre-marked H3K27me3 by PRC2 in normal development later become densely DNA-hypermethylated in the presence of oncogenic cues like abnormally elevated EZH2 expression [45-47]. Moreover, PRC2 interacts with histone deacetylase (HDAC), which may modify the histone mark by deacetylating H3K27 and relieving lysine side chain for methylation by PRC2, resulting in transcriptional silencing [48, 49]. These three groups of epigenetic silencing regulators EZH2, DNMTs and HDACs may contribute to modulating aberrant gene expression in cancer cells, and their functional connections have been observed in cancers of colon, breast, lung, liver, ovarian and prostate, as well as acute promyelocytic leukemia [46, 47, 50].

2.3. Polycomb-independent transcriptional activation function of EZH2

Apart form its transcriptional repression function, emerging studies uncover the noncanonical role of EZH2 showing that EZH2 also functions as an activator by methylating nonhistone proteins or forming transcriptional complexes with other factors to activate downstream target genes in a PRC2-independent manner [18-22] (**Fig. 2C**). Lee et al. demonstrated that in estrogen receptor (ER)-negative basal-like breast cancer cells, EZH2 physically interacts with nuclear factor-kappaB (NF-κB) components RelA/RelB as a ternary complex to activate a subset of NF-κB target genes independently of its HMTase activity [21] (**Fig. 2C, top**). In ER-positive luminal-like breast cancer cells, EZH2 also acts as an activator independently of its SET domain through association with ER and WNT signaling components TCF/β-catenin to activate ER target genes such as c-myc and cyclin D1 [20] (**Fig. 2C, middle left**). Similarly, Jung et al. revealed that EZH2 forms complex with DNA repair protein PCNA-associated factor (PAF) and TCF/β-catenin to promote WNT target gene transactivation independently of EZH2's HMTase activity, contributing to intestinal tumorigenesis [18] (**Fig. 2C, middle right**).

In contrast to methyltransferase activity of EZH2 dispensable for EZH2-mediated gene activation mentioned above, Xu et al. demonstrated methyltransferase activity of EZH2 is required for both EZH2-mediated transcriptional activation and androgen-independent growth of castration-resistant prostate cancer cells [22]. AKT-mediated EZH2 phosphorylation at Ser21 promotes EZH2 binding with androgen receptor (AR) and methylating AR or AR-associated proteins, resulting in transcriptional activation of a subset of its target genes [22] (**Fig. 2C, bottom left**). Recently, Kim et al. showed EZH2 phosphorylation at Ser21 by AKT is also required for EZH2 association with STAT3 and the enhanced STAT3 activity, that occur preferentially in glioma stem-like cells relative to non-stem tumor cells. Phosphorylated EZH2 interacts with and methylates STAT3 at Lys 180, which augments STAT3 activity by enhancing tyrosine phosphorylation of STAT3, resulting in transcriptional activation (**Fig. 2C, bottom right**) [19]. Such results contrast with EZH2-mediated methylation of GATA4 or RORα, which decrease their transcriptional activity [40, 41].

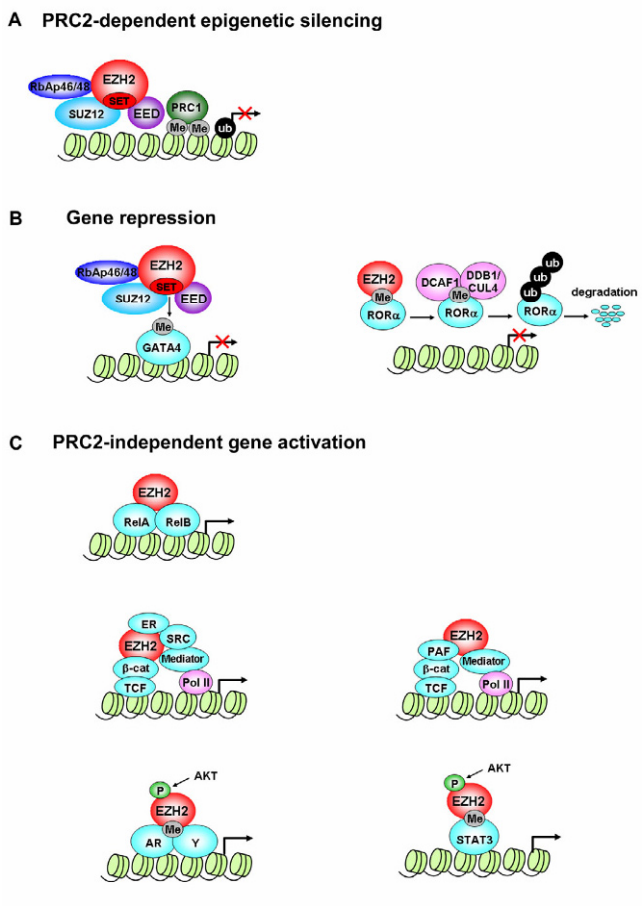

Figure 2. EZH2-mediated gene repression and activation mechanisms. (A) PRC2-dependent epigenetic silencing. With PRC2 (EZH2, EED, SUZ12, and RbAp46/48) recruited to target genes, EZH2 catalyzes trimethylation of histone H3 at Lys 27 (H3K27me3). PRC1 then recognizes and binds to H3K27me3 mark so as to monoubiquitylate Lys 119 of histone H2A (H2AK119ub1), resulting in epigenetic silencing. (B) EZH2-mediated gene repression via methylation of non-histone proteins. (Left) EZH2 interacts with and directly methylates cardiac transcription factor GATA4 at Lys 299. PRC2-mediated GATA4 methylation impairs interaction with and acetylation by p300, resulting in attenuated GATA4 transcriptional activity and gene repression [40]. (Right) EZH2 binds and methylates RORα at Lys 38 which is recognized and ubiquitinated by DCAF1/DDB1/CUL4 ligase complex, spawning RORα degradation and transcriptional repression of RORα target genes [41]. (C) PRC2-independent gene activation. (Top) EZH2 interacts with nuclear factor-kappaB (NF-κB) components RelA/RelB as ternary complex to activate gene expression [21]. (Middle left) EZH2 associates with ER and WNT signaling components TCF/β-catenin to activate ER target genes [20]. (Middle right) EZH2 forms complex with DNA repair protein PCNA-associated factor (PAF) and TCF/β-catenin to promote WNT target gene transactivation [18]. (Bottom left) AKT-mediated EZH2 phosphorylation at Ser21 promotes EZH2 binding with androgen receptor (AR) and methylating AR or AR-associated proteins, leading to transcriptional activation [22]. (Bottom right) EZH2 phosphorylation at Ser21 by AKT. Phosphorylated EZH2 interacts with and methylates STAT3 at Lys 180, augmenting STAT3 activity to yield transcriptional activation [19].

3. Roles of EZH2 in cancer progression

Overexpression/amplification or mutation of EZH2 have been found in a wide range of cancer types, including breast, prostate, lung, liver, colon, ovarian, bladder, glioblastoma and lymphoma. Elevated expression of EZH2 correlates with tumor malignancy, poor prognosis and poor patient survival [6]. Overexpression and amplification of EZH2 is barely detected in early stage of prostate cancers, but is more general in late stages. Increased copies of EZH2, with corresponding enhanced protein expression, are found in more than 50% of the hormone-refractory prostate cancers [51]. Similarly, tissue microarray analysis of breast caner tissue samples showed EZH2 highly expressed in invasive breast cancer and metastatic breast cancer compared with normal or atypical hyperplasia, plus associated with breast cancer aggressiveness and poor clinical outcome [52]. Ecotopic expression of EZH2 in breast epithelial cells promotes oncogenic transformation by measuring anchorage-independent growth and cell invasion [52]. In EZH2 transgenic mouse model, ovexpression of EZH2 in mammary epithelial cells using the mouse mammary tumor virus long terminal repeat causes epithelial hyperplasia, highlighting the potential role of EZH2 in tumor progression [53].

Various heterozygous mutations of EZH2 at tyrosine 641 (Y641) in the SET domain have been found in 22% of germinal center B-cell and diffuse large B-cell lymphoma (DLBCLs) and 7% of follicular lymphoma [54]. This Y641 somatic mutation causes a gain-of-function mutation, but Y641 mutant EZH2 exhibits catalytic activity toward substrates differently from wild-type (WT) EZH2. Y641 mutant EZH2 preferentially catalyzes tri-methylation of H3K27, but exhibits limited ability to catalyze the first mono- and di-methylation of H3K27. By contrast, WT EZH2 exerts highest catalytic activity for the first mono- and di-methylation of H3K27, but relatively weak catalytic activity for the tri-methylation of H3K27 [55]. Intriguingly, Y641 mutant EZH2 detected in B-cell lymphoma is always heterozygous. Thus, heterozygous Y641 mutant EZH2 can work along with WT EZH2 to raise H3K27me3 levels, which may be functionally like EZH2 overexpression [56]. Another heterozygous mutation of EZH2 at alanine 677 to glycine (A677G) is also identified in lymphoma cell lines and primary lymphoma samples with frequency less than 2-3% [55]. Similar to activating mutation of Y641 mutant EZH2, expression of A677G mutant EZH2 induces a global hypertrimethylation of H3K27. However, different from WT EZH2 and Y641 mutant, A677G mutant EZH2 efficiently methylates all three substrates (unmodified, mono- and dimethylated H3K27), indicating A677G mutant EZH2 deregulates H3K27 methylation without needing working with WT EZH2 as is the case for Y641 mutant EZH2 [55].

Mutations of EZH2 are detected in 10-13% of myelodyplasia-myeloproliferative neoplasm, 13% of myelofibrosis and 6% of various myelodysplastic syndrome subtypes, not occurring at single residue but throughout the gene. Most such mutations are nonsense and stop codon mutation, resulting in loss of HMTase activity, apparently unlike Y641 and A677 mutants [57], raising the possibility for EZH2 acting as a tumor suppressor. These studies indicate both activating and inactivating mutations of EZH2 can be associated with certain malignancy, their differential roles in regulating specific cohort of target genes that contribute to tumorigenesis may be context dependent and need to be explored further.

4. Targeting EZH2 or EZH2-mediated signaling for potential cancer therapy

Given its role in tumor progression and stem cell maintenance, EZH2 or

EZH2-mediated signaling may be attractive targets for potential cancer therapeutics. Several studies show the small molecule 3-deazaneplanocin A (DZNep), a S-adenosylhomocysteine hydrolase inhibitor, which inhibits methylation reaction and induces EZH2 degradation, suppresses various types of cancer growth and reduce tumor formation: e.g., glioblastoma cancer stem cells, ovarian cancer stem cell-like populations, prostate cancer/cancer stem cells [23]. Still, DZNep is not a specific EZH2 inhibitor; it also influences other processes that involve methylation reaction. Recently, several highly potent and selective inhibitors of EZH2, such as GSK126, GSK343, EPZ005687, EPZ-6438 and El1, have been discovered [58]. Among them, GSK126 and EPZ-6438 are the most potent and selective S-adenosyl-methionine (SAM)-competitive, small-molecule inhibitors of EZH2 methyltransferase activity. GSK126 could effectively suppress proliferation of EZH2 mutant DLBCL cell lines and inhibit tumor growth in xenograft mouse model of EZH2 mutant DLBCL *in vivo*, indicating pharmacological inhibition of EZH2 activity may show promise in treating DLBCL harboring activating mutations of EZH2 [59]. EPZ-6438 causes apoptosis and differentiation in SMARCB1 mutant malignant rhabdoid tumor (MRT) Cells, and completely inhibits growth of MRT xenografts in mice without tumor regrowth after dosing cessation [60]. This study reveals that inhibition of EZH2 activity may be a compelling therapeutics for a spectrum of cancers with genetic alterations conferring a proliferative dependency on EZH2 enzymatic activity despite EZH2 itself is not genetically changed in the cancers. EPZ-6438 also eliminates the growth of several EZH2 mutant xenografts including WSU-DLCL2 (Y641F), Pfeiffer (A677G), KARPAS-422 (Y641N) etc., and has been approved for human clinical trials in patients with advanced solid tumors or with B-cell lymphoma [58]. Moreover, down regulation of EZH2 expression by siRNAs or shRNAs has also been shown to inhibit cancer cell and tumor growth [23]. Besides direct blocking EZH2 activity/expression, EZH2-mediated tumorigenic signaling is another attractive therapeutic target. For example, study shows EZH2 up-regulating RAF1-ERK-β-catenin pathway, leading to promoting survival and proliferation of breast tumor initiating cells [23]. Inhibitors of RAF1-ERK signaling, such as sorafenib and AZD6244, are plausible therapeutic agents to eradicate breast tumor initiating cells.

5. Perspectives

EZH2, deregulated in a wide range of cancers, exerts its functions in distinct action modes (Fig. 2). Functioning in both PRC2-dependent (canonical) and -independent (noncanonical) manners to repress or activate target gene expression, it thus may contribute to tumorigenesis via both positive and negative regulation of gene activity in cell-context dependent manner. Currently, no EZH2 inhibitors are approved for treatment of human cancers; much effort has been made to develop EZH2 HMTase inhibitors. Since methyltransferase activity of EZH2 is not required for certain EZH2-mediated gene activation (Fig. 2C), alternative strategy aside from inhibiting EZH2 enzymatic activity warrants attention. In this regard, approaches based on disrupting interaction between EZH2 and other factors like ER/TCF/β-catenin and RelA/RelB might be potential therapeutic targets.

In addition to overexpression of EZH2 in cancers, activating mutations and inactivating mutations of EZH2 correlate with certain types of cancer, pointing to the complicated role of EZH2 mutants in cancer meriting further exploration: e.g., whether gain of EZH2 function mutant modulates a set of genes similar to or different from those regulated by inactivating mutation of EZH2. Given EZH2's multi-faceted role in cancer, insight into sophisticated regulatory mechanisms of EZH2/EZH2-mediated signaling will pave the way for developing context- or allele-specific (mutant EZH2-specific) strategy for targeting EZH2/EZH2-mediated signaling that could serve as future targeted therapy/personalized medicine for human cancer.

Acknowledgements

This work was supported by grants from National Science Council (NSC102-2321-B-039-002, NSC102-2325-B-039-002, NSC99-2632-B-039-001-MY3 to L.-Y.L.) and the Ministry of Health & Welfare (MOHW102-TD-PB-111-NSC105 to L.-Y.L.).

REFERENCES

[1] Rottach A, Leonhardt H, Spada F. DNA methylation-mediated epigenetic control. J Cell Biochem 2009;108:43-51.

[2] Henikoff S, Ahmad K. Assembly of variant histones into chromatin. Annu Rev Cell Dev Biol 2005;21:133-53.

[3] Kouzarides T. Chromatin modifications and their function. Cell 2007;128:693-705.

[4] Esteller M. Non-coding RNAs in human disease. Nat Rev Genet 2011;12:861-74.

[5] Margueron R, Reinberg D. The Polycomb complex PRC2 and its mark in life. Nature 2011;469:343-9.

[6] Sauvageau M, Sauvageau G. Polycomb group proteins: multi-faceted regulators of somatic stem cells and cancer. Cell Stem Cell 2010;7:299-313.

[7] Levine SS, Weiss A, Erdjument-Bromage H, Shao Z, Tempst P, Kingston RE. The core of the polycomb repressive complex is compositionally and functionally conserved in flies and humans. Mol Cell Biol 2002;22:6070-8.

[8] de Napoles M, Mermoud JE, Wakao R, Tang YA, Endoh M, Appanah R, et al. Polycomb group proteins Ring1A/B link ubiquitylation of histone H2A to heritable gene silencing and X inactivation. Dev Cell 2004;7:663-76.

[9] Wang H, Wang L, Erdjument-Bromage H, Vidal M, Tempst P, Jones RS, et al. Role of histone H2A ubiquitination in Polycomb silencing. Nature 2004;431:873-8.

[10] Cao R, Zhang Y. The functions of E(Z)/EZH2-mediated methylation of lysine 27 in histone H3. Curr Opin Genet Dev 2004;14:155-64.

[11] Cao R, Wang L, Wang H, Xia L, Erdjument-Bromage H, Tempst P, et al. Role of histone H3 lysine 27 methylation in Polycomb-group silencing. Science 2002;298:1039-43.

[12] Czermin B, Melfi R, McCabe D, Seitz V, Imhof A, Pirrotta V. Drosophila enhancer of Zeste/ESC complexes have a histone H3 methyltransferase activity that marks chromosomal Polycomb sites. Cell 2002;111:185-96.

[13] Kirmizis A, Bartley SM, Kuzmichev A, Margueron R, Reinberg D, Green R, et al. Silencing of human polycomb target genes is associated with methylation of histone H3 Lys 27. Genes Dev 2004;18:1592-605.

[14] Kuzmichev A, Nishioka K, Erdjument-Bromage H, Tempst P, Reinberg D. Histone methyltransferase activity associated with a human multiprotein complex containing the Enhancer of Zeste protein. Genes Dev 2002;16:2893-905.

[15] Eskeland R, Leeb M, Grimes GR, Kress C, Boyle S, Sproul D, et al. Ring1B compacts chromatin structure and represses gene

expression independent of histone ubiquitination. Mol Cell 2010;38:452-64.
[16] Tiwari VK, McGarvey KM, Licchesi JD, Ohm JE, Herman JG, Schubeler D, et al. PcG proteins, DNA methylation, and gene repression by chromatin looping. PLoS Biol 2008;6:2911-27.
[17] Schuettengruber B, Martinez AM, Iovino N, Cavalli G. Trithorax group proteins: switching genes on and keeping them active. Nat Rev Mol Cell Biol 2011;12:799-814.
[18] Jung HY, Jun S, Lee M, Kim HC, Wang X, Ji H, et al. PAF and EZH2 induce Wnt/beta-catenin signaling hyperactivation. Mol Cell 2013;52:193-205.
[19] Kim E, Kim M, Woo DH, Shin Y, Shin J, Chang N, et al. Phosphorylation of EZH2 activates STAT3 signaling via STAT3 methylation and promotes tumorigenicity of glioblastoma stem-like cells. Cancer Cell 2013;23:839-52.
[20] Shi B, Liang J, Yang X, Wang Y, Zhao Y, Wu H, et al. Integration of estrogen and Wnt signaling circuits by the polycomb group protein EZH2 in breast cancer cells. Mol Cell Biol 2007;27:5105-19.
[21] Lee ST, Li Z, Wu Z, Aau M, Guan P, Karuturi RK, et al. Context-specific regulation of NF-kappaB target gene expression by EZH2 in breast cancers. Mol Cell 2011;43:798-810.
[22] Xu K, Wu ZJ, Groner AC, He HH, Cai C, Lis RT, et al. EZH2 oncogenic activity in castration-resistant prostate cancer cells is Polycomb-independent. Science 2012;338:1465-9.
[23] Chang CJ, Hung MC. The role of EZH2 in tumour progression. Br J Cancer 2012;106:243-7.
[24] Chen YH, Hung MC, Li LY. EZH2: a pivotal regulator in controlling cell differentiation. Am J Transl Res 2012;4:364-75.
[25] Chen YH, Yeh FL, Yeh SP, Ma HT, Hung SC, Hung MC, et al. Myocyte enhancer factor-2 interacting transcriptional repressor (MITR) is a switch that promotes osteogenesis and inhibits adipogenesis of mesenchymal stem cells by inactivating peroxisome proliferator-activated receptor gamma-2. J Biol Chem 2011;286:10671-80.
[26] Wei Y, Chen YH, Li LY, Lang J, Yeh SP, Shi B, et al. CDK1-dependent phosphorylation of EZH2 suppresses methylation of H3K27 and promotes osteogenic differentiation of human mesenchymal stem cells. Nat Cell Biol 2011;13:87-94.
[27] Cardoso C, Mignon C, Hetet G, Grandchamps B, Fontes M, Colleaux L. The human EZH2 gene: genomic organisation and revised mapping in 7q35 within the critical region for malignant myeloid disorders. Eur J Hum Genet 2000;8:174-80.
[28] Ketel CS, Andersen EF, Vargas ML, Suh J, Strome S, Simon JA. Subunit contributions to histone methyltransferase activities of fly and worm polycomb group complexes. Mol Cell Biol 2005;25:6857-68.
[29] Muller J, Hart CM, Francis NJ, Vargas ML, Sengupta A, Wild B, et al. Histone methyltransferase activity of a Drosophila Polycomb group repressor complex. Cell 2002;111:197-208.
[30] Nekrasov M, Wild B, Muller J. Nucleosome binding and histone methyltransferase activity of Drosophila PRC2. EMBO Rep 2005;6:348-53.
[31] Han Z, Xing X, Hu M, Zhang Y, Liu P, Chai J. Structural basis of EZH2 recognition by EED. Structure 2007;15:1306-15.
[32] Pasini D, Bracken AP, Jensen MR, Lazzerini Denchi E, Helin K. Suz12 is essential for mouse development and for EZH2 histone methyltransferase activity. EMBO J 2004;23:4061-71.
[33] Cao R, Zhang Y. SUZ12 is required for both the histone methyltransferase activity and the silencing function of the EED-EZH2 complex. Mol Cell 2004;15:57-67.
[34] Montgomery ND, Yee D, Chen A, Kalantry S, Chamberlain SJ, Otte AP, et al. The murine polycomb group protein Eed is required for global histone H3 lysine-27 methylation. Curr Biol 2005;15:942-7.
[35] Ku M, Koche RP, Rheinbay E, Mendenhall EM, Endoh M, Mikkelsen TS, et al. Genomewide analysis of PRC1 and PRC2 occupancy identifies two classes of bivalent domains. PLoS Genet 2008;4:e1000242.
[36] Schoeftner S, Sengupta AK, Kubicek S, Mechtler K, Spahn L, Koseki H, et al. Recruitment of PRC1 function at the initiation of X inactivation independent of PRC2 and silencing. EMBO J 2006;25:3110-22.
[37] Sing A, Pannell D, Karaiskakis A, Sturgeon K, Djabali M, Ellis J, et al. A vertebrate Polycomb response element governs segmentation of the posterior hindbrain. Cell 2009;138:885-97.
[38] Leeb M, Pasini D, Novatchkova M, Jaritz M, Helin K, Wutz A. Polycomb complexes act redundantly to repress genomic repeats and genes. Genes Dev 2010;24:265-76.
[39] Tavares L, Dimitrova E, Oxley D, Webster J, Poot R, Demmers J, et al. RYBP-PRC1 complexes mediate H2A ubiquitylation at polycomb target sites independently of PRC2 and H3K27me3. Cell 2012;148:664-78.
[40] He A, Shen X, Ma Q, Cao J, von Gise A, Zhou P, et al. PRC2 directly methylates GATA4 and represses its transcriptional activity. Genes Dev 2012;26:37-42.
[41] Lee JM, Lee JS, Kim H, Kim K, Park H, Kim JY, et al. EZH2 generates a methyl degron that is recognized by the DCAF1/DDB1/CUL4 E3 ubiquitin ligase complex. Mol Cell 2012;48:572-86.
[42] Vire E, Brenner C, Deplus R, Blanchon L, Fraga M, Didelot C, et al. The Polycomb group protein EZH2 directly controls DNA methylation. Nature 2006;439:871-4.
[43] McGarvey KM, Greene E, Fahrner JA, Jenuwein T, Baylin SB. DNA methylation and complete transcriptional silencing of cancer genes persist after depletion of EZH2. Cancer Res 2007;67:5097-102.
[44] Kodach LL, Jacobs RJ, Heijmans J, van Noesel CJ, Langers AM, Verspaget HW, et al. The role of EZH2 and DNA methylation in the silencing of the tumour suppressor RUNX3 in colorectal cancer. Carcinogenesis 2010;31:1567-75.
[45] Ohm JE, McGarvey KM, Yu X, Cheng L, Schuebel KE, Cope L, et al. A stem cell-like chromatin pattern may predispose tumor suppressor genes to DNA hypermethylation and heritable silencing. Nat Genet 2007;39:237-42.
[46] Schlesinger Y, Straussman R, Keshet I, Farkash S, Hecht M, Zimmerman J, et al. Polycomb-mediated methylation on Lys27 of histone H3 pre-marks genes for de novo methylation in cancer. Nat Genet 2007;39:232-6.
[47] Widschwendter M, Fiegl H, Egle D, Mueller-Holzner E, Spizzo G, Marth C, et al. Epigenetic stem cell signature in cancer. Nat Genet 2007;39:157-8.
[48] van der Vlag J, Otte AP. Transcriptional repression mediated by the human polycomb-group protein EED involves histone deacetylation. Nat Genet 1999;23:474-8.
[49] Tie F, Furuyama T, Prasad-Sinha J, Jane E, Harte PJ. The Drosophila Polycomb Group proteins ESC and E(Z) are present in a complex containing the histone-binding protein p55 and the histone deacetylase RPD3. Development 2001;128:275-86.
[50] Villa R, Pasini D, Gutierrez A, Morey L, Occhionorelli M, Vire E, et al. Role of the polycomb repressive complex 2 in acute promyelocytic leukemia. Cancer Cell 2007;11:513-25.
[51] Saramaki OR, Tammela TL, Martikainen PM, Vessella RL, Visakorpi T. The gene for polycomb group protein enhancer of zeste homolog 2 (EZH2) is amplified in late-stage prostate cancer. Genes Chromosomes Cancer 2006;45:639-45.
[52] Kleer CG, Cao Q, Varambally S, Shen R, Ota I, Tomlins SA, et al. EZH2 is a marker of aggressive breast cancer and promotes

neoplastic transformation of breast epithelial cells. Proceedings of the National Academy of Sciences of the United States of America 2003;100:11606-11.

[53] Li X, Gonzalez ME, Toy K, Filzen T, Merajver SD, Kleer CG. Targeted overexpression of EZH2 in the mammary gland disrupts ductal morphogenesis and causes epithelial hyperplasia. Am J Pathol 2009;175:1246-54.

[54] Morin RD, Johnson NA, Severson TM, Mungall AJ, An J, Goya R, et al. Somatic mutations altering EZH2 (Tyr641) in follicular and diffuse large B-cell lymphomas of germinal-center origin. Nat Genet 2010;42:181-5.

[55]McCabe MT, Graves AP, Ganji G, Diaz E, Halsey WS, Jiang Y, et al. Mutation of A677 in histone methyltransferase EZH2 in human B-cell lymphoma promotes hypertrimethylation of histone H3 on lysine 27 (H3K27). Proceedings of the National Academy of Sciences of the United States of America 2012;109:2989-94.

[56] Sneeringer CJ, Scott MP, Kuntz KW, Knutson SK, Pollock RM, Richon VM, et al. Coordinated activities of wild-type plus mutant EZH2 drive tumor-associated hypertrimethylation of lysine 27 on histone H3 (H3K27) in human B-cell lymphomas. Proceedings of the National Academy of Sciences of the United States of America 2010;107:20980-5.

[57] Chase A, Cross NC. Aberrations of EZH2 in cancer. Clin Cancer Res 2011;17:2613-8.

[58] Helin K, Dhanak D. Chromatin proteins and modifications as drug targets. Nature 2013;502:480-8.

[59] McCabe MT, Ott HM, Ganji G, Korenchuk S, Thompson C, Van Aller GS, et al. EZH2 inhibition as a therapeutic strategy for lymphoma with EZH2-activating mutations. Nature 2012;492:108-12.

[60] Knutson SK, Warholic NM, Wigle TJ, Klaus CR, Allain CJ, Raimondi A, et al. Durable tumor regression in genetically altered malignant rhabdoid tumors by inhibition of methyltransferase EZH2. Proceedings of the National Academy of Sciences of the United States of America 2013;110:7922-7.

BioMedicine March 2014, Vol. 4, No. 1, Pages 7-15 DOI 10.7603/s40681-014-0002-5

Review article

Evolving Personalized Therapy for Castration-Resistant Prostate Cancer

Hsin-Ho Liu[a,b,c†], Yuh-Shyan Tsai[a,d†], Chen-Li Lai[a,d†], Chih-Hsin Tang[e], Chih-Ho Lai[a,e], Hsi-Chin Wu[e,f]*, Jer-Tsong Hsieh[a,g]**, Che-Rei Yang[e,f]***

[a] Department of Urology, University of Texas Southwestern Medical Center, Dallas, Texas, USA
[b] Division of Urology, Department of Surgery, Taichung Tzu Chi General Hospital, Taichung, Taiwan
[c] Department of Bio-Industrial Mechatronics Engineering, National Taiwan University, Taipei, Taiwan
[d] Department of Urology, Medical College and Hospital, National Cheng Kung University, Tainan, Taiwan
[e] School of Medicine, China Medical University, Taichung, Taiwan
[f] Department of Urology, China Medical University Hospital, Taichung, Taiwan
[g] Graduate Institute of Cancer Biology, China Medical University, Taichung, Taiwan

Received 28th of November 2013 Accepted 31st of December 2013

Keywords:
Prostate cancer;
Personalized cancer therapy;
Castration-resistant prostate cancer

ABSTRACT

With advances in molecular biologic and genomic technology, detailed molecular mechanisms for development of castration-resistant prostate cancer (CRPC) have surfaced. Metastatic prostate cancer (PCa) no longer represents an end stage, with many emerging therapeutic agents approved as effective in prolonging survival of patients from either pre- or post-docetaxel stage. Given tumor heterogeneity in patients, a one-size-fits-all theory for curative therapy remains questionable. With the support of evidence from continuing clinical trials, each treatment modality has gradually been found suitable for selective best-fit patients: e.g., new androgen synthesis inhibitor arbiraterone, androgen receptor signaling inhibitor enzalutamide, sipuleucel-T immunotherapy, new taxane carbazitaxel, calcium-mimetic radium-223 radiopharmaceutical agent. Moreover, several emerging immunomodulating agents and circulating tumor cell enumeration and analysis showed promise in animal or early phase clinical trials. While the era of personalized therapy for CRPC patients is still in infancy, optimal therapeutic agents and their sequencing loom not far in the future.

1. Current therapeutic regimen in prostate cancer

Prostate cancer (PCa) is the lead malignancy among males in Western countries, accounting for 28% (238,590) of newly diagnosed cancers in United States in 2013 [1]. It has been the second common cause of cancer deaths in men (behind lung cancer) for two decades [1, 2]. Treatment for clinically localized PCa aims at cure, typically by surgery or radiation. Emerging technologies have also been used for selected patients in low-risk PCa: e.g., high-intensity focused ultrasound (HIFU), cryotherapy, radiofrequency ablation and photodynamic therapy. For advanced PCa cases, androgen deprivation therapy (ADT) is standard treatment. The majority of advanced PCa patients respond to initial ADT temporarily but inevitably progress from androgen-dependent stage to CRPC. Effective treatment at this stage is largely limited to chemotherapy. Indeed, prior to 2010, only docetaxel chemotherapy shows survival benefit in CRPC. With the most effective standard chemotherapeutic regimens, mean increase in survival time is two months, highlighting the need for more effective treatments [3, 4]

Figure 1 plots common clinical course of PCa from localized stage to CRPC. Interpretation of castration resistance pathway could lead to identification of new pathway-targeted therapeutics. Incidence and mortality rates vary widely across geographic regions and ethnic groups [5]. Of note, Asians have substantially lower prevalence than African Americans and Caucasians, indicating linkage between genetic background and susceptibility [6]. Exact molecular mechanisms of prostate carcinogenesis are not fully elucidated, but it is evident that genetic factors at both germline and somatic levels play key roles in carcinogenesis. It has been increasingly recognized that cancer cells are heterogeneous within the same lesion at both genetic and epigenetic levels, which could translate into functional heterogeneity: e.g., self-renewal properties, tumor-initiating ability [7]. Significant tumor heterogeneity appears within primary and metastatic tumor lesions as well as individual cases, challenging standard approach to cancer management and highlighting the need for personalized cancer therapy.

*Corresponding authors, Department of Urology, China Medical University Hospital, Taichung, Taiwan
**Corresponding author, Department of Urology, University of Texas Southwestern Medical Center, Dallas, Texas, USA
E-mail addresses: wuhc@mail.cmuh.org.tw (H.C-Wu), JT.Hsieh@UTSouthwestern.edu (J.-T, Hsieh), cryang@mail.cmuh.org.tw (C.-R. Yang)
†Equal contribution to this work.

Published online: 13 February 2014

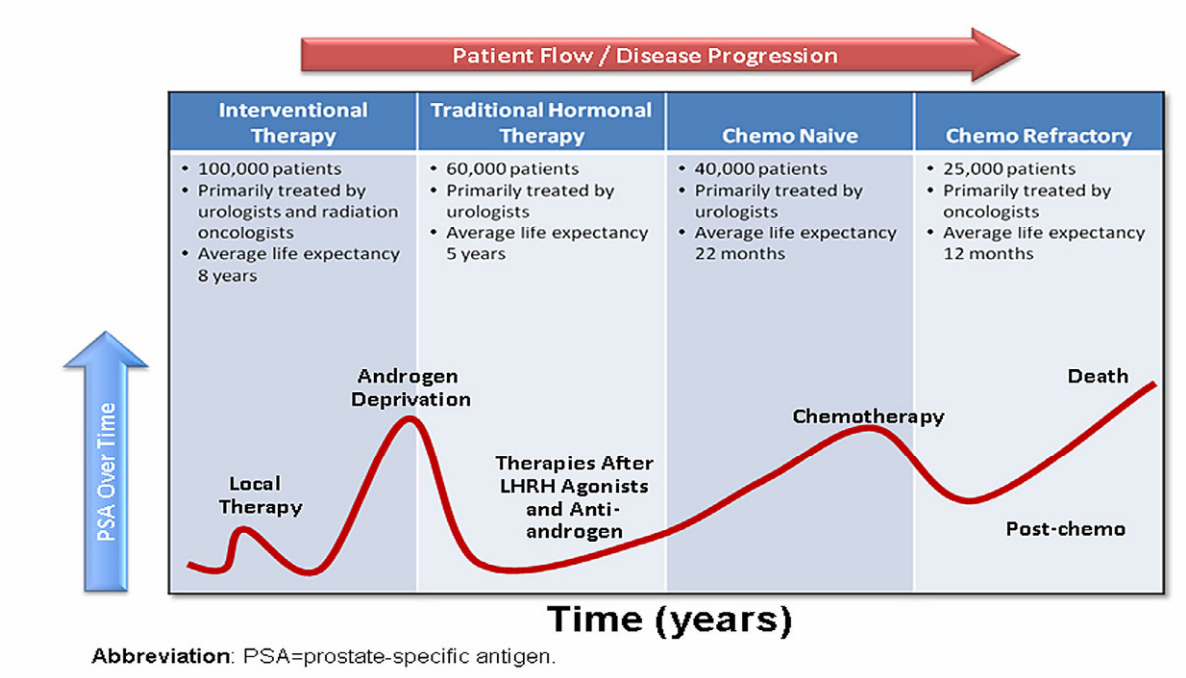

Figure 1. Common clinical course of PCa progression from localized stage to CRPC. PSA level is used as a surrogate for cancer burden; the figure shows PSA rising at the time of initial diagnosis, returning to normal via first-line treatment (radiation or surgery), then rising again as cancer recurs. Again it is reduced by hormonal therapy. When CRPC occurs, PSA again rises and minimally impacted by chemotherapy. After chemotherapy fails, PSA rises until the patient dies. Permission from Dr. Ganesh Raj (Department of Urology, University of Texas Southwestern Medical Center).

2 New strategies in CRPC therapy

In the case of advanced PCa, ADT is standard treatment, which initially reduced tumor burden and prostate-specific antigen (PSA) level to low or undetectable level. Most PCa ultimately recurs despite of ADT, presenting with progressively rising of PSA level, termed CRPC. Docetaxel was regarded as the only reasonable option before 2010. Additionally, there is no therapeutic agent for patients who experience progression after first-line docetaxel. Recent years have seen a number of novel anticancer drugs for CRPC clinics. The past three years can be considered exceptional due to positive outcomes in Phase III trials. Key antitumor agents showing positive results include taxane cabazitaxel [8, 9], vaccine sipuleucel-T [10], cytochrome p450 17 (CYP17) inhibitor abiraterone [11, 12], androgen-receptor antagonist enzalutamide (formerly known as MDV-3100) [13-15], and radioisotope alpharadin (radium 223) [16]. Other promising agents including denosumab [17], orteronel [18], ipilimumab [19] and cabozantinib [20, 21] are currently under study. These novel agents are appropriately applied to the CRPC treatment pathway to maximize therapeutic efficacy.

Cabazitaxel, a second-generation taxane, demonstrably improves overall survival when added to prednisone versus mitoxantrone plus prednisone in TROPIC (treatment of hormone-refractory metastatic PCa previously treated with docetaxel-containing regimen) trial: median overall survival is 15.1 months versus 12.7 months in CRPC patients with progression after docetaxel treatment [8]. Progression-free survival also improves in the cabazitaxel-prednisone treatment arm.

Sipuleucel-T, an active cellular immunotherapy, is a type of therapeutic cancer vaccine consisting of autologous peripheral-blood mononuclear cells (PBMCs), including antigen-presenting cells (APCs) activated *ex vivo* with a recombinant fusion protein (PA2024) [10]. PA2024 consists of a prostate-specific acid phosphatase (PAP) fused with granulocyte-macrophage colony-stimulating factor (GM-CSF), an immune-cell activator. This regimen can reduce death risk by 22%, representing a 4.1-month improvement in median survival [10]. In conclusion, sipuleucel-T prolonged overall survival among asymptomatic metastatic CRPC (mCRPC) patients. Adverse events are more frequently reported in the sipuleucel-T group, including chills, fever, and headache with mainly Grade 1 or 2 in severity.

Abiraterone acetate blocks androgen biosynthesis by inhibiting 17α-hydroxylase/C17,20-lyase (CYP17). The COU-AA-301 and COU-AA-302 trials established the role of abiraterone in mCRPC patients with or without previous docetaxel chemotherapy. In COU-AA-301 trial, overall survival as primary endpoint was longer with abiraterone acetate-prednisone than with placebo-prednisone (14.8 vs. 10.9 months; P<0.001) [11]. In COU-AA-302 trial, radiographic progression-free survival was also longer with abiraterone-prednisone group than with prednisone alone (16.5 vs. 8.3 months; P<0.001) [12]. Hence abiraterone acetate significantly prolongs overall survival of mCRPC patients, with or without previous docetaxel chemotherapy.

Enzalutamide, a novel androgen receptor signaling inhibitor, competitively inhibits binding of androgens to the androgen receptor (AR), inhibits AR nuclear translocation, and inhibits association of the AR with DNA [22]. The AFFIRM trail (A multinational phase 3, randomized double-blind, placebo-controlled efficacy and safety study of oral MDV3100 in progressive CRPC previously treated with docetaxel-based chemotherapy) confirms that enzalutamide could benefit men with post-docetaxel CRPC [15]. Enzalutamide is well-tolerated and prolongs overall survival with median survival of 18.4 months, slows disease progression, and improves quality of life in men with post-docetaxel CRPC. It reduces risk of death by 37% relative to placebo [14, 15].

Table 1. Novel strategies for CRPC therapy

Category	Mechanism/ Drug	Reference
Taxane	Inhibits microtubule depolymerization	
	Docetaxel	[3,4]
	Cabazitaxel	[8,9]
Immunotherapy	Autologous immunotherapy	
	Sipuleucel-T	[10,65,66,67]
	Immune checkpoint inhibitor	
	Ipilimumab	[69]
	Tremelimumab	[70]
AR signaling inhibitor	Androgen receptor antagonist	
	Enzalutamide	[14,15]
	CYP17 inhibitor	
	Abiraterone acetate	[11,12,41]
	Orteronel	[46,47]
	Galeterone	[46,47]
	VT-464	[47]
	HSP90 chaperone inhibitors	
	Geldanamycin	[44]
	Histone deactylase inhibitors	
	Vorinostat (SAHA)	[44]
Tyrosine kinase inhibitor	Against MET and VEGFR2	
	Cabozantinib	[20,21]
PI3K pathway inhibitor	PI3K Inhibitors	[36]
	XL147	
	BEZ235	
	GDC-0941	
	AKT inhibitors	[36]
	GSK690693	
	MK2206	
	mTOR inhibitors	[36]
Alpha-pharmaceuticals	Irradiation causes double-strand DNA break	
	Alpharadin	[16]

Radium-223 (alpharadin), calcium-mimetic radiopharmaceutical, has high bone affinity. Alsympca (ALpharadin in SYMptomatic Prostate Cancer) Phase III trial shows improved overall survival: median duration 14 months [16]. Time to first skeletal-related event (SRE) also improves, with median duration of 13.6 months.

Cabozantinib (XL184), an orally bioavailable tyrosine kinase inhibitor, shows potent activity against MET and VEGF Receptor 2 (VEGFR2). It suppresses MET and VEGFR2 signaling, rapidly inducing apoptosis of endothelial and tumor cells, resulting in tumor regression. It can also block progression of osteolytic and osteoblastic lesions [20, 21]

3. Personalized therapy

It is well documented that response to standard therapy differs among patients diagnosed with the same cancer. Obviously, a one-size-fits-all concept is not expected to achieve identical outcome; individualized approach is needed. Progress in understanding intricate molecular mechanisms for transformation of normal cells into cancer, plus aberrant control of complementary pathways, leads us into a more complex world for diagnosis and treatment. Oncology has entered an era with treatment individualized or customized, therapy based on molecular and genetic traits of a tumor and its microenvironment, tailored to improve outcomes and decrease both toxicity and health-care costs. Personalized cancer therapy targets aberrations that drive tumor progression, administering the right therapy for the right person at the right time. Success requires identification of novel validated markers for prognosis, treatment response, resistance and toxicity. Chief task in practice is modifying therapy for diverse tumor nature with inadequate, limited prognostic tools [23, 24].

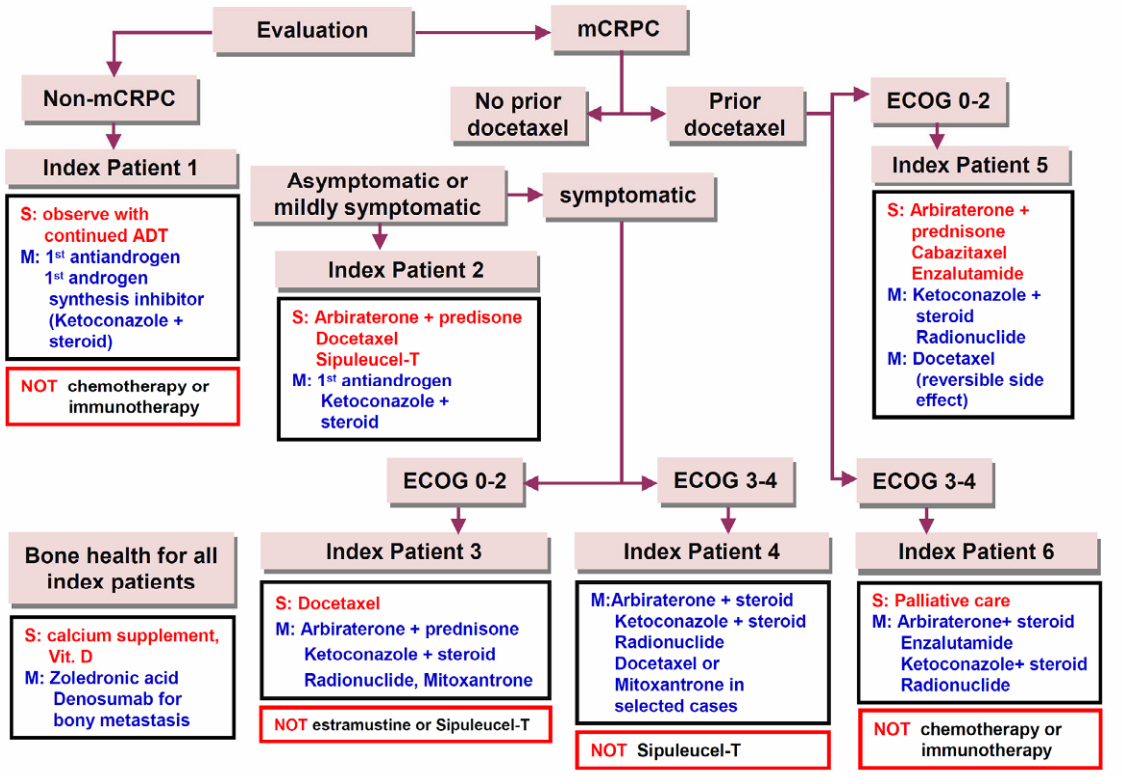

Figure 2. Modified version of the algorithm of American Urological Association guideline that represents personalized therapy prototype for CRPC (adapted from [25]). S: suggesting treatment for therapeutic agents; M: considering treatment for therapeutic agents; Black rectangle: suggesting treatment for categorized therapeutic agents; Red rectangle: not recommending treatment.

The American Urological Association (AUA) announced clinical guidelines for CRPC in May, 2013 [25]. With several Food and Drug Administration (FDA)-approved therapeutic agents for mCRPC debuting over the past three years, urologists and other clinicians face challenges with multiple treatment options. Potential sequencing of these agents further makes clinical decision-making more complex than ever. To assist in clinical decision-making, AUA developed six index patients to represent the most commonly encountered in clinical practice, which based on the presence or absence of metastatic disease, the degree of symptoms, the patients' performance status, and the prior docetaxel-based chemotherapy. Such guidelines constitute a prototype of personalized therapy for CRPC (Figure 2).

4. Genomic strategy for targeting therapy in CRPC

Large-scale cancer genomic characterization projects offer critical new insights into molecular classification of cancers and have potential to identify new therapeutic targets [26]. PCa exhibits heterogeneous epidemiological and clinical aspects, likely a reflection of underlying genomic diversity. From a molecular viewpoint, cancer can result from a combination of single nucleotide variants (SNVs), small insertions and deletions (indels), chromosomal rearrangements, aberrant DNA methylation and copy number alterations (CNAs), which engenders different expressions of oncogenes or tumor suppressors. In the long run, gathering the entire genomic and transcriptomic landscape of PCa, as well as defining frequency of alteration in several common signal transduction pathways, can further correlate genomic alterations to clinical outcome.

4.1 Copy number and transcriptome profiles define core pathway alterations

Copy number alterations (CNAs) can result in amplification of oncogenes or deletion of tumor suppressor genes; these changes contribute significantly to cancer etiology. Consistent and common findings from global analyses of CNAs within PCa include *TMPRSS2-ERG* fusion (around 50%) [27, 28], 8p loss (30-50%) and 8q gain (20-40%) [29, 30]. Focal amplifications of *AR* (Xq12) and *MYC* (8q24), and homozygous focal deletions of *PTEN* (10q23) and *NKX3.1* (8p21) are frequently identified in PCa [31, 32]. Recent CNA study of 218 primary and metastatic tumors added a key role for somatic copy number increases of *NCOA2* gene, which encodes an AR coactivator [30]. In detail, besides above descriptions, peaks of deletion targeting *RB1* on 13q14.2, *TP53* on 17p31.1, interstitial 21q22.2-3 deletion spanning *ERG* and *TMPRSS2* [30], deletions on 12p13.31-p12.3, which spans *ETV6* and *DUSP16* as well as *CDKN1B* [29] were reported. Most common amplified loci include *MYC* on 8q24.21 and *NCOA2* on 8q13.3. Focal amplification of *AR* (Xq12) is likewise common but restricted to metastatic tumors. Among mutated genes, the most common is androgen receptor (*AR*); other oncogenes like *IDH1, IDH2, PIK3CA, KRAS,* and *BRAF* do not commonly mutate in PCa [30]. There is no great correlation between histology (Gleason score) and CNAs; the latter could serve as an independent clinical marker from Gleason score [33]. Integrating CNAs, transcriptome, and mutation data can further conduct core pathway analysis for PCa. Three recognized cancer pathways, PI3K, RAS/RAF, and RB, are ordinarily altered in primary PCa (range: 34-43%) and metastases (74-100%). Of particular interest is PI3K pathway, altered in nearly half the primaries and all metastases examined [30]. Loss of PTEN function is well documented in PCa: estimated frequency around 40% [34]. PTEN negatively regulates PI3K/Akt pathway; loss of PTEN activity may lead to permanent PI3K/Akt activation. Frequency of PI3K pathway alteration rises substantially when *PTEN* alteration is considered with *INPP4B* and *PHLPP* phosphatase alterations recently implicated in PI3K regulation, the *PIK3CA* gene itself, and regulatory subunits *PIK3R1* and *PIK3R3* [26]. Exploring novel PI3K pathway inhibitors may reap therapeutic benefit [35, 36].

4.2. Genetic alterations highly associated with TMPRSS2-ERG

A recent rearrangement involving the androgen-regulated *TMPRSS2* and members of the ETS transcription factor family (*ERG, ETV1, ETV4*) has been identified in a majority of prostate cancers [27, 37]. Further functional studies of *TMPRSS2-ERG* have shown modest evidence of oncogenic activity with cooperating transforming events [27, 28]: *TMPRSS2-ERG* fusion as the single most established PCa molecular lesion [27], meaning expression of N-terminally truncated ERG protein under control of *TMPRSS2* androgen-responsive promoter [38]. Significant regions of copy-number loss link with *TMPRSS2-ERG* fusion: spanning tumor suppressors *PTEN* and *TP53*, plus another spanning 3p14 multigenic region. The 3p14 deletion, whose association with *TMPRSS2-ERG* loomed predominant, appeared only in PCa [30, 39]. Homogeneous distribution of *TMPRSS2-ERG* fusion in 19% of high-grade prostatic intraepithelial neoplasia (PIN) lesions and in 50% of localized PCa suggests this fusion as either occurring after onset or associated with early events predisposing to clinical progression [38]. Recent genomic studies show how ERG binds to AR-regulated genes and alters AR signaling in PCa cells via epigenetic silencing, invariable with a role in inhibiting prostate epithelial differentiation and turning on EZH2 expression, which initiates stem cell-like de-differentiation and carcinogenesis [40]. Population-based studies hint ETS fusion-positive cancer as aggressive in nature and support early detection-based efforts. Commercially available urine test for *TMPRSS2-ERG* is technically feasible nowadays; in PSA-screened cohorts it shows sensitivity of 30-50% and specificity >90%. Examination for *TMPRSS2-ERG* may detect 15-20% of men harboring PCa but with normal DRE (digital rectal examination) and PSA levels, including a substantial proportion of those who harbor high-grade Gleason disease [41]. Most 5' end ETS fusion partners are androgen responsive; targeting androgen signals may act at least in part by inhibition of ETS fusion. Recent studies indicated a highly specific CYP17 inhibitor, abiraterone acetate, ablating androgen and estrogen syntheses that drive *TMPRSS2-ERG* fusions, inducing regression in >50% of CRPC cases [42]. Hormone-dependent overexpression of ERG persisted in CRPC, and *TMPRSS2-ERG* tumors manifested a subgroup of PCa remaining exquisitely sensitive to CYP17 blockade [43]. Also, ETS gene-fusion status may serve as a prospective character of androgen dependence in CRPC state [44]. As deregulated transcription factors, ETS fusions may drive PCa via induction of downstream target genes, maybe offering a target as therapeutic strategy.

4.3 Androgen receptor (AR) signaling pathway

AR signaling is essential for growth and differentiation of a normal prostate and is responsible for treatment failure in CRPC or metastatic PCa. The contribution of AR to prostate tumorigenesis and disease progression is incontrovertible. The exclusive requirement of PCa cells for AR activity is illuminated at clinic, wherein therapeutic suppression of AR signaling, typically achieved through ligand depletion and direct

AR antagonists, results in PSA decline and objective tumor regressions. Conventional therapy currently focuses on androgen-dependent activation of AR via its C-terminal ligand-binding domain (LBD). Mechanisms of therapeutic failure include AR amplification and/or overexpression, gain-of-function AR mutations, intracrine androgen production; overexpression of AR coactivators, expression of constitutively active splice variants of AR, and ligand-independent AR activation through growth factors, cytokines, or aberrant AR phosphorylation [45]. Among AR pathway genes, the most prominent finding is a peak of copy-number gain on 8q13.3 that spans the nuclear receptor coactivator gene *NCOA2* [30]. High frequency of *NCOA2* gain in primary tumors plus a known role as AR coactivator [46] lends insight into how these two genes collaborate in early PCa progression by enhancing AR transcriptional output. *NCOA2* functions as a driver oncogene in primary tumors by increasing AR signaling; in contrast, *AR* amplification is largely restricted to mCRPC and likely a mechanism of drug resistance rather than a natural step in tumor progression.

Recently developed androgen-ablative and AR antagonist strategies that achieve complete androgen ablation and sufficient suppression of AR signaling in the prostate improve efficacy of AR targeting and subsequent therapeutic outcome. A new means to deplete androgens is a selective CYP17 inhibitor, which inhibits both testicular-derived androgen production and tumor-derived androgen synthesis, meaning a great advance toward durable androgen depletion and suppression of AR activity. Despite strong rationale for aiming at CYP17, this target remains largely unexploited, with relatively few candidate agents progressing to clinical trials and only ketoconazole, an unspecific CYP17 inhibitor, in widespread clinical use [47]. Promising clinical results from abiraterone acetate in CRPC cases have recently been reported [11]; its efficacy has spawned clinical development of other androgen biosynthesis inhibitors. Orteronel (TAK-700), oral non-steroidal imidazole CYP17 inhibitor, is reportedly more selective for 17,20 lyase activity than abiraterone acetate, but according to recent data from Phase III clinical trial of ortoronel plus prednisone in treatment of progressive mCRPC, ortoronel plus prednisone would not demonstrate a pre-specified level of clinical efficacy. While ortoronel never met the primary endpoint of improved OS (HR=0.894, p=0.226), it did show advantage as secondary endpoint of radiographic progression-free survival (HR=0.755, p<0.001) and posed no major safety concern. Galeterone (VN/124-1, TOK-001), an oral agent, functions both as CYP17A1 inhibitor and anti-androgen, causing AR protein degradation. Preclinical data averred that galeterone may represent the next generation of therapy for cases of CRPC and disease that has progressed despite treatment with enzalutamide. Phase III trails for galeterone are expected in the near future. VT-464, non-steroidal small molecular 17,20 lyase inhibitor, is also in early-phase testing for men with CRPC [48].

Direct AR antagonists are often combined with orchiectomy or GnRH agonists/antagonists, to inhibit AR signaling further. Docking of AR antagonists into the AR C-terminal LBD results in both passive AR inhibition, via competition for agonists, and active mechanism of AR inhibition: e.g., prevention of coactivator binding and inducement of corepressor recruitment. AR can be alternatively spliced so that the C-terminal domain is deleted, rendering AR constitutively active [49]. Splice variants are refractory to traditional androgen deprivation and AR antagonists, highlight that the new class of AR-inhibitory agents must be developed for successful management of tumors expressing truncated AR, wherein even total androgen ablation has no effect on receptor activity. Options for suppressing function of C-terminal-deficient ARs already exist. HSP90 inhibitors (geldanamycin) and agents modulating HSP90-histone deacetylase interactions (genistein) both show capacity for reducing overall AR levels as well as suppressing action of both full-length and truncated AR [45]. Several studies implicate AR N-terminal domain (NTD) as key mediator of ligand-independent AR activity in PCa cell. Alternative means to inhibit AR function by using a decoy molecule representing AR NTD demonstrably suppress tumor growth and hormonal progression [50]. Intratumor injection of lentivirus expressing AR NTD decoy fragment inhibited growth of established LNCaP xenografts [51]. Development of shorter decoy peptides to AR NTD means great challenges: e.g., how to retain both specificity for AR and antitumor activity, maintain peptide lability and requirement of nonlinear regions of AR NTD needed for protein-protein interactions. Lastly, it has been recently shown that AR may require histone deacetylases (HDACs) for transcriptional activation; HDAC inhibitors cooperate with AR-directed therapeutics to enhance cellular response. Novel understanding of AR function during disease progression has scored breakthroughs in novel AR antagonists and ligand-depletion strategies. Stratification of CRPC patients according to disparate AR reactivation may reap the greatest benefit: e.g., for recurrence associated with AR mutations or splice variants inducing resistance to AR antagonists, it is unlikely that the latter would help. This advance is expected to provide new insight into CRPC mechanisms, serving as a base for personalized medicine.

4.4. Epigenetic alterations

Epigenetics is defined as heritable changes in gene expression caused by mechanisms other than altered DNA sequence. Unlike many other genetic changes, epigenetic processes are reversible and do not change DNA sequence or quantity, though they enhance genomic instability that might lead to oncogenic activation and inactivation of tumor suppressors [52]. Among types of epigenetic change, the most crucial are DNA methylation and histone modification, both prominent in cancer progression. DNA methylation causes gene-silencing either by inhibiting access of target binding sites to transcriptional activators and/or by promoting binding of methyl-binding domain proteins, which interact with HDACs that promote chromatin condensation into transcriptionally repressive conformations. DNA methylation is thought to alter chromosome structure and define regions for transcriptional regulation. Covalent modification of multiple DNA sites by methylation is heritable and reversible, involved in regulating a gamut of biological processes [53]. Several classes of drugs, including inhibitors of DNA methyltransferases and HDACs, are known to modify epigenetic information in a fashion not specific to genes. AR may require HDACs for transcriptional activation; HDAC inhibitors may cooperate with AR-directed therapeutics to elicit enhanced cellular response. HDAC inhibitors show promise as therapeutic targets with potential to reverse aberrant epigenetic states associated with PCa.

5. Personalizing treatments with circulating tumor cells (CTCs)

CTCs appear in the bloodstream, having detached from their tumor of origin. A major cause of cancer-associated mortality is tumor metastasis, which depends on successful dissemination to the whole body, mainly

through blood. Therefore, CTCs shed into vasculature and possibly on the way to potential metastatic sites arouse obvious interest. Studies in past years have shown CTCs as markers predicting cancer progression and survival in metastatic [54-57] or even early-stage cancer patients [58]. Assessment CTC using CellSearch has been cleared by the FDA as a prognostic indicator for patients with metastatic breast, prostate, and colorectal cancers [54, 59]. Increasing CTC numbers correlate with aggressive disease, increased metastasis, and decreased time to relapse in CRPC [55, 60, 61]. CTCs could serve as a real-time monitor for progression and marker for survival and thus have potential to guide therapeutic management, indicate therapy effectiveness or necessity, even while metastases are still undetectable, and offer insights into mechanisms of drug resistance. Thus, CTCs not only could be used as a surrogate endpoint marker in clinical trials [62], but also could become a treatment target [63]. Discrepancy in gene expression between primary tumors and CTCs, as well as heterogeneity within the CTC population, can be observed frequently. To such a degree, it is possible to identify their tissue of origin via expression profiling to detect organ-specific metastatic signatures. This could help to localize small metastatic lesions and afford valuable insight into further diagnostic and therapeutic strategies [64].

Although CTC counts are of prognostic relevance, CTC enumeration is not yet validated as a surrogate of clinical benefit. Technical challenge in this field consists of finding tenuous tumor cells (a few CTCs mixed with approximately 10 million leukocytes and 5 billion erythrocytes in 1 ml of blood) and distinguishing them from epithelial non-tumor cells and leukocytes. It should be feasible with advanced technology that allows automated and high-throughput separation, visualization and quantification of cancer cells from blood [59]. Ability to evaluate longitudinally gene amplifications, mutations, deletions or translocations playing crucial roles in CRPC pathogenesis with CTCs lends unique insight into underlying and evolving biology of tumor, without need for invasive biopsies [65]. This will also allow analysis of molecular changes that occur secondary to treatment pressures and intra-patient tumor heterogeneity that may otherwise have been missed with tumor biopsies. It also allows patient sub-classification according to molecular profiles of risk, prognosis and likely response [66]. Molecular characterization of CTCs may lend insight into underlying mechanisms of resistance to cancer therapy and develop biomarkers to support rational molecular stratification of patients with CRPC to novel antitumor agents. Ultimately, deep sequencing of DNA from CTCs will permit detection of tumor heterogeneity of CRPC, in order to dissect clonal evolution and aid understanding of clones' association with drug resistance. Future research on CTC enumeration may pinpoint a robust biomarker with strong statistical association to clinical benefit from treatment, which may be employed as a surrogate for true outcome in patients with CRPC. Moreover, CTCs may expedite anticancer drug design, minimizing delay in development and regulatory approval of effective agents for CRPC, reducing the number of patients undergoing ineffective regimen.

6. Personalized immunotherapy for PCa

The concept of immune modulation, which aims at generating a meaningful antitumor immune response, has been extensively evaluated in melanoma and renal cell carcinoma. This principle has been extended to PCa, known as slow-growing and more indolent, which can allow sufficient time for generating effective antitumor immune response. Moreover, recent studies indicated that PCa is more immunogenic than considered earlier, with evidence of PCa-specific autoantibodies in blood samples of patients. Sipuleucel-T is the first immunotherapy approved by the US FDA in April 2010 [10]. It is indicated for treatment of asymptomatic or minimally symptomatic mCRPC based on IMPACT (Immunotherapy for Prostate AdenoCarcinoma Treatment) trial, making it the first of its kind vaccine therapy approved for advanced solid tumors. Sipuleucel-T is active cellular cancer vaccine, stimulating immune response to PCa. First, leukopheresis is followed by enrichment of PBMCs, which are incubated with targeted immunogen PA2024, a PAP recombinant fusion protein, and GM-CSF before intravenous administration. Once infused, autologous PBMCs are thought to mature into functional APCs, and activate PAP-specific CD4+ and CD8+ T cells. These activated T cells then home in on tumor lesions, mediating an antitumor response [67-69]. The IMPACT trial, a Phase III, randomized, double-blind, placebo-controlled study, enrolled 512 patients with asymptomatic or minimally symptomatic mCRPC without visceral metastases. Patients were assigned in a 2:1 ratio to receive sipuleucel-T or placebo administered intravenously every two weeks for total three infusions. The primary and secondary endpoints in this study were median overall survival and time to objective disease progression. The sipuleucel-T group had a relative reduction of 22% in risk of death as compared with the placebo group, representing a 4.1-month improvement in median survival (25.8 vs. 21.7 months); 36-month survival probability was 31.7% in the sipuleucel-T versus 23.0% in the placebo group. But secondary endpoint, time to objective disease progression, was not met, similar in both groups. Immune responses to the immunizing antigen were observed in patients receiving sipuleucel-T. Adverse events such as chills, fever and headache were more frequently reported in the sipuleucel-T than in the placebo group [10]. Recent studies in tumor immunology have also focused on the concept of immune checkpoints, a series of molecules that function to limit an ongoing immune response [68, 70]. The ability of cancer cells to evade anti-tumor T-cell activity in microenvironment has recently been accepted as a hallmark of cancer progression. Blocking of one or more such immune checkpoints with monoclonal antibodies (mAbs) has been shown to rescue otherwise exhausted antitumor T cells. Blocking checkpoints to recover existing antitumor immune responses might presumably be more effective than inducing a *de novo* antitumor response through vaccination. Both pilimumab (MDX-010) and tremelimumab (CP-675206) are clinical applications of checkpoint inhibitors, antibodies specific for cytotoxic T lymphocyte antigen 4 (CTLA-4). Ipilimumab is an antagonistic mAbs that recognizes CTLA-4, an immunomodulatory molecule expressed by activated T cells, and to CD80 on APCs. It was proven active both in PSA response and clinical improvement, with or without radiotherapy in mCRPC patients [71]. Because anti-CTLA-4 mAbs target the immune system instead of the tumor, they hold potential advantages over traditional antitumor mAbs, chemotherapy, and immunotherapy (vaccines and cytokines). Other antibodies with neutralizing function, such as CD137, CD40, and PD-1 (programmed cell death 1), are currently in various stages of preclinical and clinical evaluation.

Most treatment regimens for advanced cancer highlight a combination of chemotherapy drugs, or concurrent radio-chemotherapy, raising a possibility that immunotherapy may need combination with conventional therapy to achieve maximal effect. Fortunately,

conventional cancer treatments have immunological benefits [72], making combinatorial trials attractive. In sum, there is strong rationale for combined immunotherapies and/or combining immunotherapy with conventional therapy, but such combination increases complexity for clinical trial design; issues of dosing and sequence become a great challenge.

7. Conclusions and perspectives

In the past decade, cancer therapy has slowly but steadily transformed from a one-size-fits-all to a more personalized approach, each patient treated according to specific genetic defects of his/her own tumor. Appearance of genomic technologies has now provided the means to develop data that address complexity of biologic states. Practice of cancer therapy continually faces the challenge of matching the right therapeutic regimen with the right patient at the right time, balancing relative benefit with risk to attain optimal outcome. Cases with CRPC may represent myriad heterogeneity in terms of performance, comorbidity, and underlying molecular mechanisms. Prior to 2010, the sole agent for CRPC was docetaxel; positive results now available from clinical trials of cabazitaxel, sipuleucel-T, abiraterone, and enzalutamide mean we now have a plethora of agents to choose from. New AUA guidelines for CRPC treatment in 2013 represent a prototype of personalized therapy. Despite these recent advances, efforts in molecular therapeutics should continue and bring further changes in the PCa treatment paradigm. Moreover, many emerging personalized therapies are under scrutiny: e.g., immunotherapy and CTC-targeted therapy. Though personalized therapy for CRPC is still in its infancy, ideal therapy tailored for individual CRPC patients continues to advance.

Acknowledgments

We thank Dr. Ming-Chei Maa and Dr. Yuan-Man Hsu for valuable suggestions and editorial assistance. The authors thank Dr. Ganesh Raj (Department of Urology, University of Texas Southwestern Medical Center) for permission to use Figure 1 in this review. This work was funded by the National Science Council (NSC101-2314-B-006-011-MY3 and NSC101-2313-B-039-004-MY3), China Medical University (CMU102-S-28), and the Tomorrow Medicine Foundation.

Declaration of Interest: Authors declare no conflicts of interest for this work.

REFERENCES

[1] Siegel R, Naishadham D, Jemal A. Cancer statistics, 2013. CA Cancer J Clin 2013; 63:11-30.

[2] Silverberg E, Boring CC, Squires TS. Cancer statistics, 1990. CA Cancer J Clin 1990; 40:9-26.

[3] Berthold DR, Pond GR, Soban F, de Wit R, Eisenberger M, Tannock IF. Docetaxel plus prednisone or mitoxantrone plus prednisone for advanced prostate cancer: updated survival in the TAX 327 study. J Clin Oncol 2008; 26:242-5.

[4] Petrylak DP, Tangen CM, Hussain MHA, Lara Jr PN, Jones JA, Taplin ME, Burch PA, Berry D, Moinpour C, Kohli M, Benson MC, Small EJ, Raghavan D, Crawford ED. Docetaxel and estramustine compared with mitoxantrone and prednisone for advanced refractory prostate cancer. N Engl J Med 2004; 351:1513-20.

[5] Grönberg H. Prostate cancer epidemiology. Lancet 2003; 361:859-64.

[6] Hsing AW, Devesa SS. Trends and patterns of prostate cancer: what do they suggest? Epidemiol Rev 2001; 23:3-13.

[7] Meric-Bernstam F, Mills GB. Overcoming implementation challenges of personalized cancer therapy. Nat Rev Clin Oncol 2012; 9:542-48.

[8] de Bono JS, Oudard S, Ozguroglu M, Hansen S, Machiels J-P, Kocak I, Gravis Gl, Bodrogi I, Mackenzie MJ, Shen L, Roessner M, Gupta S, Sartor AO. Prednisone plus cabazitaxel or mitoxantrone for metastatic castration-resistant prostate cancer progressing after docetaxel treatment: a randomised open-label trial. Lancet 2010; 376:1147-54.

[9] Paller CJ, Antonarakis ES. Cabazitaxel: a novel second-line treatment for metastatic castration-resistant prostate cancer. Drug Des Devel Ther 2011; 5:117-24.

[10] Kantoff PW, Higano CS, Shore ND, Berger ER, Small EJ, Penson DF, Redfern CH, Ferrari AC, Dreicer R, Sims RB, Xu Y, Frohlich MW, Schellhammer PF. Sipuleucel-T immunotherapy for castration-resistant prostate cancer. N Engl J Med 2010; 363:411-22.

[11] de Bono JS, Logothetis CJ, Molina A, Fizazi K, North S, Chu L, Chi KN, Jones RJ, Goodman Jr OB, Saad F, Staffurth JN, Mainwaring P, Harland S, Flaig TW, Hutson TE, Cheng T, Patterson H, Hainsworth JD, Ryan CJ, Sternberg CN, Ellard SL, Fléchon A, Saleh M, Scholz M, Efstathiou E, Zivi A, Bianchini D, Loriot Y, Chieffo N, Kheoh T, Haqq CM, Scher HI. Abiraterone and increased survival in metastatic prostate cancer. N Engl J Med 2011; 364: 1995-2005.

[12] Ryan CJ, Smith MR, de Bono JS, Molina A, Logothetis CJ, Souza Pd, Fizazi K, Mainwaring P, Piulats JM, Ng S, Carles J, Mulders PFA, Basch E, Small EJ, Saad F, Schrijvers D, Van Poppel H, Mukherjee SD, Suttmann H, Gerritsen WR, Flaig TW, George DJ, Yu EY, Efstathiou E, Pantuck A, Winquist E, Higano CS, Taplin M-E, Park Y, Kheoh T, Griffin T, Scher HI, Rathkopf DE. Abiraterone in metastatic prostate cancer without previous chemotherapy. N Engl J Med 2013; 368:138-48.

[13] Scher HI, Beer TM, Higano CS, Anand A, Taplin ME, Efstathiou E, Rathkopf D, Shelkey J, Yu EY, Alumkal J, Hung D, Hirmand M, Seely L, Morris MJ, Danila DC, Humm J, Larson S, Fleisher M, Sawyers CL. Antitumour activity of MDV3100 in castration-resistant prostate cancer: a phase 1–2 study. Lancet 2010; 375:1437-46.

[14] Scher HI, Fizazi K, Saad F, Taplin ME, Sternberg CN, Miller K, Wit RD, Mulders P, Hirmand M, Selby B, De Bono JS. Effect of MDV3100, an androgen receptor signaling inhibitor (ARSI), on overall survival in patients with prostate cancer postdocetaxel: Results from the phase III AFFIRM study. J Clin Oncol 2012; 30(15) suppl:LBA1.

[15] De Bono JS, Fizazi K, Saad F, Taplin ME, Sternberg CN, Miller K, Mulders P, Chi KN, Armstrong AJ, Hirmand M, Selby B, Scher HI. Primary, secondary, and quality-of-life endpoint results from the phase III AFFIRM study of MDV3100, an androgen receptor signaling inhibitor. J Clin Oncol 2012; 30(5) suppl:4519.

[16] Nilsson S, Strang P, Aksnes AK, Franze`n L, Olivier P, Pecking A, Staffurth J, Vasanthan S, Andersson C, Bruland ØS. A randomized, dose–response, multicenter phase II study of radium-223 chloride for the palliation of painful bone metastases in patients with castration-resistant prostate cancer Eur J Cancer 2012; 48:678-86.

[17] Fizazi K, Carducci M, Smith M, Damião R, Brown J, Karsh L, Milecki P,

Shore N, Rader M, Wang H, Jiang Q, Tadros S, Dansey R, Goessl C. Denosumab versus zoledronic acid for treatment of bone metastases in men with castration-resistant prostate cancer: a randomised, double-blind study. Lancet 2011;377:813-22.

[18] Dreicer R, Agus DB, Bellmunt J, De Bono JS, Petrylak DP, Tejura B, Shi Y, Fizazi K. A phase III, randomized, double-blind, multicenter trial comparing the investigational agent orteronel (TAK-700) plus prednisone (P) with placebo plus P in patients with metastatic castration-resistant prostate cancer (mCRPC) that has progressed during or following docetaxel-based therapy. J Clin Oncol 2012;30(15) suppl:TPS4693.

[19] Small EJ, Tchekmedyian NS, Rini BI, Fong L, Lowy I, Allison JP. A pilot trial of CTLA-4 blockade with human anti-CTLA-4 in patients with hormone-refractory prostate cancer. Clin Cancer Res 2007; 13(6):1810-15.

[20] Yakes FM, Chen J, Tan J, Yamaguchi K, Shi Y, Yu P, Qian F, Chu F, Bentzien F, Cancilla B, Orf J, You A, Laird AD, Engst S, Lee L, Lesch J, Chou Y-C, Joly AH. Cabozantinib (XL184), a novel MET and VEGFR2 Inhibitor, simultaneously suppresses metastasis, angiogenesis, and tumor growth. Mol Cancer Ther 2011; 10(12):2298-308.

[21] Smith DC, Smith MR, Sweeney C, Elfiky AA, Logothetis C, Corn PG, Vogelzang NJ, Small EJ, Harzstark AL, Michael S. Gordon, Vaishampayan UN, Haas NB, Spira AI, Lara Jr PN, Lin CC, Srinivas S, Sella A, Schoffski P, Scheffold C, Weitzman AL, Hussain M. Cabozantinib in patients with advanced prostate cancer: results of a phase II randomized discontinuation trial. J Clin Oncol 2013; 31:412-19.

[22] Tran C, Ouk S, Clegg NJ, Chen Y, Watson PA, Arora V, Wongvipat J, Smith Jones PM, Yoo D, Kwon A, Wasielewska T, Welsbie D, Chen C, Higano CS, Beer TM, Hung DT, Scher HI, Jung M, Sawyers CL. Development of a second-generation antiandrogen for treatment of advanced prostate cancer. Science 2009; 324:787-90.

[23] Garman KS, Nevins JR, Potti A. Genomic strategies for personalized cancer therapy. Hum Mol Genet 2007; 16:226-32.

[24] van 't Veer LJ, Bernards R. Enabling personalized cancer medicine through analysis of gene-expression patterns. Nature 2008; 452:564-70.

[25] The clinical guideline for the therapy of castration-resistant prostate cancer, American Urological Association (AUA). http://www.auanet.org/education/guidelines/castration- resistant-prostate-cancer.cfm.

[26] The cancer genome atlas research network. Comprehensive genomic characterization defines human glioblastoma genes and core pathways. Nature 2008; 455:1061-68.

[27] Tomlins SA, Rhodes DR, Perner S, Dhanasekaran SM, Mehra R, Sun XW, Varambally S, Cao X, Tchinda J, Kuefer R, Lee C, Montie JE, Shah RB, Pienta KJ, Rubin MA, Chinnaiyan AM. Recurrent fusion of TMPRSS2 and ETS transcription factor genes in prostate cancer. Science 2005; 310:644-48.

[28] Tomlins SA, Laxman B, Varambally S, Cao X, Yu J, Helgeson BE, Cao Q, Prensner JR, Rubin MA, Shah RB, Mehra R, Chinnaiyan AM. Role of the TMPRSS2–ERG gene fusion in prostate cancer. Neoplasia 2008; 10:177-88.

[29] Lapointe J, Li C, Giacomini CP, Salari K, Huang S, Wang P, Ferrari M, Hernandez-Boussard T, Brooks JD, Pollack JR. Genomic profiling reveals alternative genetic pathways of prostate tumorigenesis. Cancer Res 2007; 67:8504-10.

[30] Taylor BS, Schultz N, Hieronymus H, Gopalan A, Xiao Y, Carver BS, Arora VK, Kaushik P, Cerami E, Reva B, Antipin Y, Mitsiades N, Landers T, Dolgalev I, Major JE, Wilson M, Socci ND, Lash AE, Heguy A, Eastham JA, Scher HI, Reuter VE, Scardino PT, Sander C, Sawyers CL, Gerald WL. Integrative genomic profiling of human prostate cancer. Cancer cell 2010; 18:11-22.

[31] Reynolds MA. Molecular alterations in prostate cancer. Cancer Lett 2008; 270 13-24.

[32] Grasso CS, Wu YM, Robinson DR, Cao X, Dhanasekaran SM, Khan AP, Quist MJ, Jing X, Lonigro RJ, Brenner JC, Asangani IA, Ateeq B, Chun SY, Siddiqui J, Sam L, Anstett M, Mehra R, Prensner JR, Palanisamy N, Ryslik GA, Vandin F, Raphael BJ, Kunju LP, Rhodes DR, Pienta KJ, Chinnaiyan AM, Tomlins SA. The mutational landscape of lethal castrate resistant prostate cancer. Nature 2012; 487:239-43.

[33] Spans L, Clinckemalie L, Helsen C, Vanderschueren D, Boonen S, Lerut E, Joniau S, Claessens F. The Genomic Landscape of Prostate Cancer. Int J Mol Sci 2013; 14:10822-51.

[34] Pourmand G, Ziaee AA, Abedi AR, Mehrsai A, Alavi HA, Ahmadi A, Saadati HR. Role of PTEN gene in progression of prostate cancer. Urol J 2007; 4:95-100.

[35] Fresno Vara JA, Casado E, de Castro J, Cejas P, Belda-Iniesta C, Gonza├lez-Baro├n M. PI3K/Akt signalling pathway and cancer. Cancer Treat Rev 2004; 30:193-204.

[36] Sarker D, Reid AHM, Yap TA, de Bono JS. Targeting the PI3K/AKT pathway for the treatment of prostate cancer. Clin Cancer Res 2009; 15:4799-805.

[37] Mosquera JM, Perner S, Genega EM, Sanda M, Hofer MD, Mertz KD, Paris PL, Simko J, Bismar TA, Ayala G, Shah RB, Loda M, Rubin MA. Characterization of TMPRSS2-ERG fusion high-grade prostatic intraepithelial neoplasia and potential clinical implications. Clin Cancer Res 2008; 3380-85.

[38] Perner S, Mosquera JM, Demichelis F, Hofer MD, Paris PL, Simko J, Collins C, Bismar TA, Chinnaiyan AM, Marzo AMD, Rubin MA. TMPRSS2-ERG fusion prostate cancer: an early molecular event associated with invasion. Am J Surg Pathol 2007; 31:882-88.

[39] Beroukhim R, Mermel CH, Porter D, Wei G, Raychaudhuri S, Donovan J, Barretina J, Boehm JS, Dobson J, Urashima M, Mc Henry KT, Pinchback RM, Ligon AH, Cho YJ, Haery L, Greulich H, Reich M, Winckler W, Lawrence MS, Weir BA, Tanaka KE, Chiang DY, Bass AJ, Loo A, Hoffman C, Prensner J, Liefeld T, Gao Q, Yecies D, Signoretti S, Maher E, Kaye FJ, Sasaki H, Tepper JE, Fletcher JA, Tabernero J, Baselga J, Tsao MS, Demichelis F, Rubin MA, Janne PA, Daly MJ, Nucera C, Levine RL, Ebert BL, Gabriel S, Rustgi AK, Antonescu CR, Ladanyi M, Letai A, Garraway LA, Loda M, Beer DG, True LD, Okamoto A, Pomeroy SL, Singer S, Golub TR, Lander ES, Getz G, Sellers WR, Meyerson M. The landscape of somatic copy-number alteration across human cancers. Nature 2010; 463:899-905.

[40] Yu J, Yu J, Mani RS, Cao Q, Brenner CJ, Cao X, Wang X, Wu L, Li J, Hu M, Gong Y, Cheng H, Laxman B, Vellaichamy A, Shankar S, Li Y, Dhanasekaran SM, Morey R, Barrette T, Lonigro RJ, Tomlins SA, Varambally S, Qin ZS, Chinnaiyan AM. An integrated network of androgen receptor, polycomb, and TMPRSS2-ERG gene fusions in prostate cancer progression. Cancer Cell 2010; 17:443-54.

[41] Thompson IM, Pauler DK, Goodman PJ, Tangen CM, Lucia MS, Parnes HL, Minasian LM, Ford LG, Lippman SM, Crawford ED, Crowley JJ, Charles A. Coltman J. Prevalence of prostate cancer among men with a prostate-specific antigen level ≤4.0 ng per milliliter. N Engl J Med 2004; 350:2239-46.

[42] Attard G, Reid AHM, Yap TA, Raynaud F, Dowsett M, Settatree S, Barrett M, Parker C, Martins V, Folkerd E, Clark J, Cooper CS, Kaye SB, Dearnaley D, Lee G, de Bono JS. Phase I clinical trial of a selective inhibitor of CYP17, abiraterone acetate, confirms that castration-resistant prostate cancer commonly remains hormone driven. J Clin Oncol 2008; 26: 4563-71.

[43] Attard G, Swennenhuis JF, Olmos D, Reid AHM, Vickers E, A'Hern R, Levink R, Coumans F, Moreira J, Riisnaes R, Oommen NB, Hawche G, Jameson C, Thompson E, Sipkema R, Carden CP, Parker C, Dearnaley D, Kaye SB, Cooper CS, Molina A, Cox ME, Terstappen LWMM, de Bono JS. Characterization of ERG, AR and PTEN gene status in circulating tumor cells from patients with castration-resistant prostate cancer. Cancer Res 2009; 69:

2912-18.

[44] Tomlins SA, Bjartell A, Chinnaiyan AM, Jenster G, Nam RK, Rubin MA, Schalken JA. ETS gene fusions in prostate cancer: from discovery to daily clinical practice. 2009; 56:275-86.

[45] Knudsen KE, Scher HI. Starving the addiction: new opportunities for durable suppression of AR signaling in prostate cancer. Clin Cancer Res 2009; 15:4792-98.

[46] Agoulnik IU, Vaid A, Bingman III WE, Erdeme H, Frolov A, Smith CL, Ayala G, Ittmann MM, Weigel NL. Role of SRC-1 in the promotion of prostate cancer cell growth and tumor progression. Cancer Res 2005; 65:7959-67.

[47] Vasaitis TS, Bruno RD, Njar VCO. CYP17 inhibitors for prostate cancer therapy. J Steroid Biochem Mol Biol 2011; 125:23-31.

[48] Ferraldeschi R, Pezaro C, Karavasilis V, de Bono JS. Abiraterone and novel antiandrogens: overcoming castration resistance in prostate cancer. Annu Rev Med 2013; 64:1-13.

[49] Dehm SM, Schmidt LJ, Heemers HV, Vessella RL, Tindall DJ. Splicing of a novel androgen receptor exon generates a constitutively active androgen receptor that mediates prostate cancer therapy resistance. Cancer Res 2008; 68:5469-77.

[50] Quayle SN, Mawji NR, Wang J, Sadar MD. Androgen receptor decoy molecules block the growth of prostate cancer. Proc Natl Acd Sci USA 2007; 104:1331-36.

[51] Godbole AM, Njar VCO. New insights into the androgen-targeted therapies and epigenetic therapies in prostate cancer. Prostate Cancer 2011; Article ID 918707.

[52] Jones PA, Baylin SB. The epigenomics of cancer. Cell 2007; 128:683-92.

[53] Majumdar S, Buckles E, Estrada J, Koochekpour S. Aberrant DNA methylation and prostate cancer. Current Genomics 2011; 12:486-505.

[54] Cristofanilli M, Budd GT, Ellis MJ, Stopeck A, Matera J, Miller MC, Reuben JM, Doyle GV, Allard WJ, Terstappen LWMM, Hayes DF. Circulating tumor cells, disease progression, and survival in metastatic breast cancer. N Engl J Med 2004; 351:781-91.

[55] de Bono JS, Scher HI, Montgomery RB. Circulating tumor cells predict survival benefit from treatment in metastatic castration-resistant prostate cancer. Clin Cancer Res 2008; 6302-09.

[56] Cohen SJ, Punt CJA, Iannotti N, Saidman BH, Sabbath KD, Gabrail NY, Picus J, Morse M, Mitchell E, Miller MC, Doyle GV, Tissing H, Terstappen LWMM, Meropol NJ. Relationship of circulating tumor cells to tumor response, progression-free survival, and overall survival in patients with metastatic colorectal cancer. J Clin Oncol 2008; 26:3213-21.

[57] Chaffer CL, Weinberg RA. A perspective on cancer cell metastasis. Science 2011; 331: 1559-64.

[58] Rhim AD, Mirek ET, Aiello NM, Maitra A, Bailey JM, McAllister F, Reichert M, Beatty GL, Rustgi AK, Vonderheide RH, Leach SD, Stanger BZ. EMT and dissemination precede pancreatic tumor formation. Cell 2011; 148:349-61.

[59] Allard WJ, Matera J, Miller MC, Repollet M, Connelly MC, Rao C, Tibbe AGJ, Uhr JW, Terstappen LWMM. Tumor cells circulate in the peripheral blood of all major carcinomas but not in healthy subjects or patients with nonmalignant diseases. Clin Cancer Res 2004; 10: 6897-904.

[60] Shaffer DR, Leversha MA, Danila DC, Lin O, Gonzalez-Espinoza R, Gu B, Anand A, Smith K, Maslak P, Doyle GV, Terstappen LWMM, Lilja H, Heller G, Fleisher M, Scher HI. Circulating tumor cell analysis in patients with progressive castration-resistant prostate cancer. Clin Cancer Res 2007; 13:2023-29.

[61] Danila DC, Heller G, Gignac GA, Gonzalez-Espinoza R, Anand A, Tanaka E, Lilja H, Schwartz L, Larson S, Fleisher M, Scher HI. Circulating tumor cell number and prognosis in progressive castration-resistant prostate cancer. Clin Cancer Res 2007; 13:7053-58.

[62] Olmos D, Arkenau HT, Ang JE, Ledaki I, Attard G, Carden CP, Reid AHM, A'Hern R, Fong PC, Oomen NB, Molife R, Dearnaley D, Parker C, Terstappen LWMM, de Bono JS. Circulating tumour cell (CTC) counts as intermediate end points in castration-resistant prostate cancer (CRPC): a single-centre experience. Ann Oncol 2009; 20:27-33.

[63] Alix-Panabières C, Pantel K. Circulating tumor cells: liquid biopsy of cancer. Clin Chem 2013; 59:110-18.

[64] Plaks V, Koopman CD, Werb Z. Circulating tumor cells. Science 2013;341:1186-8.

[65] Attard G, Bono JSd. Utilizing circulating tumor cells: challenges and pitfalls. Curr Opin Genet Dev 2010; 21:50-58.

[66] Yap TA, Swanton C, de Bono JS. Personalization of prostate cancer prevention and therapy: are clinically qualified biomarkers in the horizon? The EPMA Journal 2012; 3:3.

[67] Higano CS, Small EJ, Schellhammer P, Yasothan U, Gubernick S, Kirkpatrick P, Kantoff PW. Sipuleucel-T. Nat Rev Drug Discov 2010; 9:513-14.

[68] Drake CG. Prostate cancer as a model for tumour immunotherapy. Nat Rev Immunol 2010; 10:580-93.

[69] Higano CS, Schellhammer PF, Small EJ, Burch PA, Nemunaitis J, Yuh L, Provost N, Frohlich MW. Integrated data from 2 randomized, double-blind, placebo-controlled, phase 3 trials of active cellular immunotherapy with sipuleucel-T in advanced prostate cancer. Cancer 2009; 115:3670-79.

[70] Fong L, Small EJ. Anti–cytotoxic T-lymphocyte antigen-4 antibody: the first in an emerging class of immunomodulatory antibodies for cancer treatment. J Clin Oncol 2008; 26:5275-83.

[71] Slovin SF, Beer TM, Higano CS, Tejwani S, Hamid O, Picus J, Harzstark A, Scher HI, Lan Z, Lowy I. Initial phase II experience of ipilimumab (IPI) alone and in combination with radiotherapy (XRT) in patients with metastatic castration-resistant prostate cancer (mCRPC). J Clin Oncol 2009; 27(15s):5138.

[72] Nesslinger NJ, Sahota RA, Stone B, Johnson K, Chima N, King C, Rasmussen D, Bishop D, Rennie PS, Gleave M, Blood P, Pai H, Ludgate C, Nelson BH. Standard treatments induce antigen-specific immune responses in prostate cancer. Clin Cancer Res 2007; 13:1493-502.

BioMedicine March 2014, Vol. 4, No. 1, Pages 16-19 DOI 10.7603/s40681-014-0003-4

Original article

Contribution of personalized Cyclin D1 genotype to triple negative breast cancer risk

Liang-Chih Liu[a,#], Chen-Hsien Su[a,d,#], Hwei-Chung Wang[a,#], Wen-Shin Chang[a,d], Chia-Wen Tsai[a,b], Ming-Chei Maa[b], Chang-Hai Tsai[a], Fuu-Jen Tsai[c] and Da-Tian Bau[a,b,d,*]

[a]Terry Fox Cancer Research Laboratory, China Medical University Hospital, Taichung, Taiwan
[b]Graduate Institute of Basic Medical Science, China Medical University, Taichung, Taiwan
[c]Department of Medical Research, China Medical University Hospital, Taichung, Taiwan
[d]Graduate Institute of Clinical Medical Science, China Medical University, Taichung, Taiwan

# These authors contributed equally to this work

Received 8th of December 2013 Accepted 20th of December 2013

Keywords:
Cyclin D1;
Genotype;
Triple negative breast cancer

ABSTRACT

Aim: Cell cycle regulator *cyclin D1 (CCND1)* is a pivotal regulator for G1/S phase transition, playing a critical part in initiation of carcinogenesis. Triple negative breast cancer comprises a very heterogeneous group of cancer cells, but little is known about what is wrong in the genome of these patients. This study investigated contribution of *CCND1* genotype to individual triple negative breast cancer susceptibility.

Materials: In all, 2464 native Taiwan subjects consist of 1232 breast cancer cases and 1232 controls were enrolled in a hospital-based, case-control study. *CCND1* A870G (rs9344) genotyping was analyzed by polymerase chain reaction-restriction fragment length polymorphism (PCR-RFLP). Risk-stratified analyses correlated genotype and age-related characteristics of breast cancer subgroups.

Results: No significant difference was found between patient and control groups in distribution of genotypic and allelic frequencies in *CCND1* genotype, yet *CCND1* A870G (rs9344) GG genotype was far less prevalent in breast cancer patients younger than 55 years (OR=0.62, 95%CI=0.43–0.89, *P*=0.0362), with first menarche earlier than 12.2 years (OR=0.61, 95% CI=0.42–0.87, *P*=0.0241), with menopause earlier than 49.0 years (OR=0.57, 95%CI=0.39–0.82, *P*=0.0093), or showing triple-negative breast cancer (OR=0.28, 95%CI=0.13–0.62, *P*=0.0006). Such valuable findings suggest *CCND1* A870G (rs9344) as a predictive marker for triple negative breast cancer in Taiwanese women; the authors sincerely hope these help us fight the toughest subtype in clinical management.

1. Introduction

Breast cancer is one of the most common worldwide malignancies in women today; its morbidity and mortality have not decreased with development of anticancer drugs [1]. Breast cancer in Asia displays lower incidence than in Western populations, but is still the leading cancer among Asian women and an issue of extraordinary public health concern. Asian breast cancer is characterized by early tumor onset, showing a relatively younger median age at diagnosis. In Taiwan, breast cancer ranks second among cancers, noted for high incidence, high mortality, and early onset [2, 3]. Most women are exposed to well-known environmental risk factors for cancer, but only a portion of exposed individuals develop breast cancer, suggesting a wide variation in individual susceptibility.

Cyclin D1 (CCND1) plays a critical role in controlling G1/S phase transition of the cell cycle [4], which accomplishes this gate-keeping role by forming a complex with its partners CDK 4 or CDK6 [4,5]. Some reports demonstrate it as involved in some types of tumor growth in a CDK-independent pattern [6,7]. Dysregulation of CCND1 is commonly observed in human cancer, with overexpression of it frequently cited as a potential biomarker [8-10]. However, underlying mechanisms of CCND1 overexpression and its connection to breast cancer progression are poorly understood. Terry Fox Cancer Research Lab in China Medical University previously found that *CCND1* genotypes positively associated with other types of cancer in Taiwan [11-15]. We currently take interest not only in revealing the contribution of genotypes to breast cancer, but to its toughest subtype in clinical treatment: triple negative breast cancer.

This study's genotyping work ascertained correlation between *CCND1* A870G (rs9344) polymorphism and breast cancer risk in Taiwanese women. Additional analyses evaluated the contribution of this SNP to breast cancer patients with specific clinicopathological features, such as those of triple negative breast cancer.

2. Materials and methods

2.1. Study population

A total of 1232 patients diagnosed with breast cancer were recruited at the outpatient clinics of general surgery at China Medical University Hospital in Taichung, Taiwan. Clinical characteristics of patients (including histological details) were all defined by expert surgeons. Slides were reviewed and scored by two independent pathologists. For ER, PR, and p53 immunoassaying, nuclear stain in 10% of neoplastic cells served as positive cutoff, Ki67-labelling index of >30% considered positive. HER-2/neu results were derived according to the package insert and guidelines of the American Society of Clinical Oncology and College of American Pathologists [16]. All patients voluntarily participated, completing self-administered questionnaires and supplying peripheral blood samples. An equal number of age-matched non-breast cancer healthy volunteers as controls were selected after initial random sampling from the hospital's Health Examination Cohort. Exclusion criteria of the control group included previous malignancy, metastasized cancer from other or unknown origin, and any familial or genetic disease.

* Correspondence author. Terry Fox Cancer Research Lab, China Medical University Hospital, 2 Yuh-Der Road, Taichung, 404 Taiwan.
E-mail address: artbau2@gmail.com(D.-T.Bau).

Published online: 13 February 2014

Both groups completed a short questionnaire that included habits. Our study was approved by the Institutional Review Board of China Medical University Hospital (DMR96-IRB-240), written-informed consent obtained from all participants.

2.2. Genotyping conditions

Genomic DNA was prepared from peripheral blood leukocytes using a QIAamp Blood Mini Kit (Blossom, Taipei, Taiwan) and genotyping processes performed as in our prior studies [11-15]. Briefly, primers used for *CCND1* A870G were: forward 5'-GTG AAG TTC ATT TCC AAT CCG C-3', and reverse 5'-GGG ACA TCA CCC TCA CTT AC-3'. Polymerase chain reaction (PCR) cycling conditions were: one cycle at 94°C for 5 min; 35 cycles of 94°C for 30 s, 55°C for 30 s, and 72°C for 30 s, and a final extension at 72°C for 10 min.

2.3. RFLP conditions

After PCR procedure for *CCND1* A870G genotyping, resultant 167 bp PCR product was mixed with 2 U *Nci* I and incubated for 3 h at 37 C. The G form PCR products could be further digested, while A form could not. Two fragments 145 bp and 22 bp were present if the product was digestible G form. Then 10 l of product was loaded into a 3% agarose gel containing ethidium bromide for electrophoresis, genotype analysis performed by two researchers independently and blindly. Ten percent of the samples were randomly selected for direct sequencing, results entirely concordant.

2.4. Statistical analyses

To ensure controls representative of general population while precluding genotypic error, genotype frequency deviation of *CCND1* single nucleotide polymorphisms in controls from those expected under Hardy-Weinberg equilibrium was assessed using the goodness-of-fit test. Pearson's Chi-square or Fisher's exact test (when expected number in any cell was less than five) compared distribution of *CCND1* genotypes between groups, statistical *P*-value less than 0.05 recognized as significant.

3. Results

A total of 1232 patients diagnosed with breast cancer and an equal number of matched controls were enrolled, as compared and summarized in Table 1. Ages of patients and controls were well matched, as were age at menarche, age when bearing first child ($P>0.05$) (Table 1). As for individual behavior, tobacco smoking and alcoholism both emerged as risk factors for breast cancer in this population ($P<0.05$) (Table 1).

Table 2 plots frequencies of genotypes and alleles of *CCND1* A870G in breast cancer and control groups. First, results of genotyping analysis revealed distribution of *CCND1* A870G genotype do not significantly differ between patients and controls ($P=0.1949$) (Table 2). Odds ratios of AG and GG were 0.95 and 0.80 (95% CI= 0.79-1.15 and 0.62-1.03) compared to AA wild-type genotype. Second, we performed dominant and recessive comparison to find odds ratios of GG versus AA+AG and AG+GG versus AA were 0.82 and 0.92 (95%CI=0.66-1.03 and 0.77-1.10, $P=0.0931$ and 0.3793), respectively. Last, there was no significant difference between breast cancer and controls in distribution of allelic frequency (OR=0.92, 95%CI=0.82-1.03, $P=0.1442$): i.e., G allele (AG and GG) meant a slightly but not statistically protective effect against breast cancer compared to AA wild genotype (Table 2).

We took interest in association of clinicopathologic traits with *CCND1* A870G genotypes. Given diverse mechanisms of carcinogenesis in distinct subtypes of breast cancer, we analyzed linkage among *CCND1* A870G genotypes with age-related and clinicopathologic characteristics of breast cancer patients (Tables 3-4). Data showed GG genotype at *CCND1* A870G less prevalent in breast cancer patients younger than 55 years (OR=0.62, 95%CI=0.43–0.89, $P=0.0362$), with first menarche earlier than 12.2 years (OR=0.61, 95% CI=0.42–0.87, $P=0.0241$), with menopause earlier than 49.0 years (OR=0.57, 95%CI=0.39–0.82, $P=0.0093$), or with triple-negative breast cancer (OR=0.28, 95%CI=0.13–0.62, $P=0.0006$) (Tables 3-4). Different genotype distribution among breast cancer patients stratified by other factors, including first full pregnant (Table 3) and Ki67 status (Table 4), was not statistically significant.

Table 1. Distribution of demographic and life-style of breast cancer patients and matched controls

Characteristic	Controls (n = 1232)			Patients (n = 1232)			*P*-value
	n	%	Mean (SD)	n	%	Mean (SD)	
Age (years)							
< 40	359	29.1%		362	29.4%		0.89[a]
40-55	558	45.3%		547	44.4%		
> 55	315	25.6%		323	26.2%		
Age at menarche (years)			12.4 (0.7)			12.1 (0.6)	0.79[b]
Age at birth of first child (years)			29.4 (1.2)			29.8 (1.4)	0.63[b]
Age at menopause (years)			48.8 (1.8)			49.3 (2.0)	0.59[b]
Site							
Unilateral				1198	97.2%		
Bilateral				34	2.8%		
Family History							
First degree (Mother, sister and daughter)				55	4.5%		
Second degree				6	0.5%		
No history				1171	95%		
Habit							
Cigarette smokers	86	7.0%		170	13.8%		<0.0001[a]
Alcohol drinkers	91	7.4%		162	13.1%		<0.0001[a]

Statistic results based on [a] Chi-square or [b] unpaired *Student's t*-test.

Table 2. Intergroup distribution of *CCND1* A870G (rs9344) genetic and allelic frequencies

A870G (rs9344)	Controls	%	Patients	%	OR (95% CI)[a]	*P-value*[b]
Genetic frequency						
AA	303	24.6%	323	26.2%	1.00 (Reference)	0.1949
AG	725	58.8 %	736	59.7%	0.95 (0.79-1.15)	
GG	204	16.6%	173	14.1%	0.80 (0.62-1.03)	
Carrier comparison						
AA+AG	1028	83.4%	1059	85.9%	1.00 (Reference)	0.0931
GG	204	16.6%	173	14.1%	0.82 (0.66-1.03)	
AA	303	24.6%	323	26.2%	1.00 (Reference)	0.3793
AG+GG	929	75.4%	909	73.8%	0.92 (0.77-1.10)	
Allele frequency						
Allele A	1331	54.0%	1382	56.1%	1.00 (Reference)	0.1442
Allele G	1133	46.0%	1082	43.9%	0.92 (0.82-1.03)	

[a] OR: odds ratio, CI: confidence interval; [b] Based on Chi-square test

Table 3. Association of *CCND1* A870G genotypes with age-related related demographic characteristics

Characteristics	*CCND1 A870G* Controls N (%)	Cases n (%)	*P*-value[a]	Crude[b] OR (95% CI)[c]
Onset age				
< 55.0 years			**0.0362***	
AA	146 (23.06)	169 (27.57)		1.00 (Ref.[d])
AG	377 (59.56)	365 (59.54)		0.84 (0.64-1.09)
GG	110 (17.38)	79 (12.89)		**0.62 (0.43-0.89)***
AG+GG	487 (76.94)	444 (72.43)		0.79 (0.61-1.02)
≧55.0 years			0.8040	
AA	157 (26.21)	154 (24.88)		1.00 (Ref.[d])
AG	348 (58.10)	371 (59.94)		1.09 (0.83-1.42)
GG	94 (15.69)	94 (15.18)		1.02 (0.71-1.46)
AG+GG	442 (73.79)	465 (75.12)		1.07 (0.83-1.39)
Age at menarche				
< 12.2 years			**0.0241***	
AA	146 (23.70)	171 (27.85)		1.00 (Ref.[d])
AG	360 (58.44)	365 (59.45)		0.87 (0.66-1.13)
GG	110 (17.86)	78 (12.70)		**0.61 (0.42-0.87)***
AG+GG	470 (76.30)	443 (72.15)		0.80 (0.62-1.04)
≧12.2 years			0.9362	
AA	157 (25.49)	152 (24.60)		1.00 (Ref.[d])
AG	365 (59.25)	371 (60.03)		1.05 (0.80-1.37)
GG	94 (15.26)	95 (15.37)		1.04 (0.73-1.50)
AG+GG	459 (74.51)	466 (75.40)		1.05 (0.81-1.36)
Age at first birth of child				
< 29.6 years			0.4570	
AA	148 (24.03)	161 (26.26)		1.00 (Ref.[d])
AG	365 (59.25)	363 (59.22)		0.91 (0.70-1.19)
GG	103 (16.72)	89 (14.52)		0.79 (0.55-1.14)
AG+GG	468 (75.97)	452 (73.74)		0.89 (0.69-1.15)
≧29.6 years			0.3791	
AA	155 (25.16)	162 (26.17)		1.00 (Ref.[d])
AG	360 (58.44)	373 (60.26)		0.99 (0.76-1.29)
GG	101 (16.40)	84 (13.57)		0.80 (0.55-1.14)
AG+GG	461 (74.84)	457 (73.83)		0.95 (0.73-1.22)
Age at menopause				
< 49.0 years			**0.0093***	
AA	144 (23.38)	177 (28.64)		1.00 (Ref.[d])
AG	364 (59.09)	366 (59.22)		0.82 (0.63-1.06)
GG	108 (17.53)	75 (12.14)		**0.57 (0.39-0.82)***
AG+GG	472 (76.62)	441 (71.36)		**0.76 (0.59-0.98)***
≧49.0 years			0.7110	
AA	159 (25.81)	146 (23.78)		1.00 (Ref.[d])
AG	361 (58.60)	370 (60.26)		1.12 (0.85-1.46)
GG	96 (15.59)	98 (15.96)		1.11 (0.78-1.59)
AG+GG	457 (74.19)	468 (76.22)		1.12 (0.86-1.45)

[a] Based on Chi-square.

[b] Difference in the trend in statistical significance before any adjustment for individual habits such as smoking (pack-years).

[c] OR, odds ratio; CI, confidence interval.

[d] Ref., reference.

* Statistical significant

Table 4. Association of *CCND1* A870G genotypes with breast cancer risk stratified by clinicopathologic characteristics compared with non-cancer healthy controls

Character	Genotype, number (%)[a] AA	AG	GG	OR (95%CI)[b]	*P*-value[c]
Control	303 (24.6)	725 (58.8)	204 (16.6)	1.00 (Ref.[d])	
Triple-negative status					
No	159 (28.8)	316 (57.1)	78 (14.1)	0.73 (0.53-1.01)	0.1228
Yes	42 (40.4)	54 (51.9)	8 (7.7)	**0.28 (0.13-0.62)***	**0.0006***
Ki67 status					
Negative	76 (27.4)	156 (56.3)	45 (16.2)	0.88 (0.58-1.32)	0.6099
Positive	90 (26.6)	193 (57.1)	55 (16.2)	0.91 (0.62-1.33)	0.7447

[a] Triple-negative and Ki67 status data were available for 657 and 615 patients, respectively, all data given as number of patients (%) unless otherwise noted.

[b] OR, odds ratio; CI, confidence interval.

[c] Based on Chi-square.

[d] Ref., reference.

* Statistical significant

4. Discussion

For years, Terry Fox Cancer Research Lab in China Medical University has keeping on the anticancer task via the translational circle from genomic biomarker revealing, anticancer drug discovery, cell and animal model establishment for drug efficacy and genotype-phenotype correlation investigation, and clinical personalized application. In this hospital-based case-control study, our team has genotyped a famous SNP *CCND1* A870G studying its association with Taiwanese breast cancer risk in central Taiwan. With a collection of samples from a quite large population, we have found that the GG genotype in *CCND1* A870G plays a protective role for triple-negative breast cancer, and in early onset (< 55 years), early menarche (<12.2 years) and premenopausal (<49 years) Taiwanese women.

As a first step, we performed routine genotype work, but results showed *CCND1* A870G genotype not linked with breast cancer susceptibility. Since we have almost collected the largest breast cancer population in Taiwan (1232 cases and age-matched controls), strategy of investigating more subjects is less urgent. Estrogen exposure is widely viewed as closely related to breast cancer risk, with age undeniably the strongest demographic risk factor for most malignancies (75% occur in patients older than 55 years) [17]. With adequate sample size, we confidently rated the contribution of this SNP to breast cancer patients with specific clinicopathological features by stratification analysis. The estrogen- and age-related factors included onset age, age at menarche, age at first birth of child, and age at menopause (Table 3). Likewise, we wished to evaluate contribution of this SNP to triple negative breast cancer. This study identified 104 breast cancer patients with triple negative breast cancer. So-named because of its negative expression of ER, PR, and HER-2/neu [18], it is characterized by aggressiveness and higher rates of recurrence and metastasis. Interestingly, existing targeted therapies effective against other subtypes of breast cancer were ineffective in dealing with triple negative. It typically occurs in young patients, whose disease is associated with variations of BRCA1 and other genes: e.g., *hOGG1*, *EGFR2* [16, 19, 20]. Cyclin D1 (coded by *CCND1*) plays first gatekeeper in the cell cycle, whereas copy number alterations of *CCND1* were reported as differentially more frequent in triple negative breast cancer samples than those in other breast cancers

[21]. Still, no report investigates association of SNPs on *CCND1* with triple negative breast cancer risk. Our results proved genotype of *CCND1* A870G not correlated with breast cancer risk as in other malignancies [11-15]; more promising, stratified analysis showed GG genotype of *CCND1* A870G playing a protective role for triple-negative breast cancer (Table 4), as with early onset (<55 years), early menarche (<12.2 years) and/or premenopausal (<49 years) Taiwanese women (Table 3). It is also found that Ki67 status, reported as a potential indicator to triple negative breast cancer [22], were not associated with *CCND1* A870G genotype (Table 4).

Recent years have seen rapidly accumulated information on cancer genotyping as a great boost for translational medicine and personalized therapy. We still have a long way to go to make history in this field. The first successful step seemed fulfilled by cooperation between local clinicians and basic scientists. Since heredity plays a key role in cancer susceptibility, we must pay more attention to genetic conservation and independence of Taiwan from Western countries, respecting profound ethnic differences while pursuing globalization. Translational studies in Taiwan, participation of experts in nutrition and care-taking, together with cooperation of patients and relatives, warrant bolstering and encouragement. Our study highlights GG genotype of *CCND1* A870G playing a protective role in triple-negative breast cancer, as well as in early onset, early menarche and premenopausal Taiwanese women. We sincerely hope each successive piece of our work expedites personalized therapy and medication, plus the war against cancer, especially in our beloved Taiwan.

Acknowledgements

This work was supported by China Medical University Hospital (grant number: DMR-103-019) and the Terry Fox Cancer Research Foundation. The authors deeply appreciate help from Tsai-Ping Ho, Chieh-Lun Hsiao, Lin-Lin Hou, Chao-Yi Lai, Chia-En Miao, Tzu-Chia Wang, Yun-Ru Syu and Tissue Bank.

REFERENCES

[1] Jemal A, Center MM, DeSantis C and Ward EM. Global patterns of cancer incidence and mortality rates and trends. Cancer Epidemiol Biomarkers Prev 2010; 19:1893-907.

[2] Cheng SH, Tsou MH, Liu MC, Jian JJ, Cheng JC, Leu SY, et al. Unique features of breast cancer in Taiwan. Breast Cancer Res Treat 2000; 63:213-23.

[3] Kuo WH, Yen AM, Lee PH, Chen KM, Wang J, Chang KJ, et al. Cumulative survival in early-onset unilateral and bilateral breast cancer: an analysis of 1907 Taiwanese women. Br J Cancer 2009; 100:563-70.

[4] Sherr CJ. Cancer cell cycles. Science 1996; 274:1672-7.

[5] Sherr CJ. D-type cyclins. Trends Biochem Sci 1995; 20:187-90.

[6] Coqueret O. Linking cyclins to transcriptional control. Gene 2002; 299:35-55.

[7] Fu M, Wang C, Li Z, Sakamaki T and Pestell RG. Minireview: Cyclin D1: normal and abnormal functions. Endocrinology 2004; 145:5439-47.

[8] Jayasurya R, Sathyan KM, Lakshminarayanan K, Abraham T, Nalinakumari KR, Abraham EK, et al. Phenotypic alterations in Rb pathway have more prognostic influence than p53 pathway proteins in oral carcinoma. Mod Pathol 2005; 18:1056-66.

[9] Bova RJ, Quinn DI, Nankervis JS, Cole IE, Sheridan BF, Jensen MJ, et al. Cyclin D1 and p16INK4A expression predict reduced survival in carcinoma of the anterior tongue. Clin Cancer Res 1999; 5:2810-19.

[10] Michalides R, van Veelen N, Hart A, Loftus B, Wientjens E and Balm A. Overexpression of cyclin D1 correlates with recurrence in a group of forty-seven operable squamous cell carcinomas of the head and neck. Cancer Res 1995; 55:975-78.

[11] Shih LC, Tsai CW, Tsai MH, Tsou YA, Chang WS, Li FJ, et al. Association of cyclin D1 genotypes with nasopharyngeal carcinoma risk. Anticancer Res 2012; 32:1093-98.

[12] Hsia TC, Liu CJ, Lin CH, Chang WS, Chu CC, Hang LW, et al. Interaction of CCND1 genotype and smoking habit in Taiwan lung cancer patients. Anticancer Res 2011; 31:3601-05.

[13] Lin HH, Ke HL, Hsiao KH, Tsai CW, Wu WJ, Bau DT, et al. Potential role of CCND1 G870A genotype as a predictor for urothelial carcinoma susceptibility and muscle-invasiveness in Taiwan. Chin J Physiol 2011; 54:196-202.

[14] Lin HH, Ke HL, Hsiao KH, Tsai CW, Wu WJ, Bau DT, et al. CCND1 1722 polymorphism and potential relevance to upper tract urothelial cancer. Anticancer Res 2011; 31:1043-47.

[15] Tsai MH, Tsai CW, Tsou YA, Hua CH, Hsu CF and Bau DT. Significant association of cyclin D1 single nucleotide polymorphisms with oral cancer in taiwan. Anticancer Res 2011; 31:227-31.

[16] Wolff AC, Hammond ME, Schwartz JN, Hagerty KL, Allred DC, Cote RJ, et al. American Society of Clinical Oncology/College of American Pathologists guideline recommendations for human epidermal growth factor receptor 2 testing in breast cancer. Arch Pathol Lab Med 2007; 131:18-43.

[17] Edwards BK, Howe HL, Ries LA, Thun MJ, Rosenberg HM, Yancik R, et al. Annual report to the nation on the status of cancer, 1973-1999, featuring implications of age and aging on U.S. cancer burden. Cancer 2002; 94: 2766-92.

[18] Lee E, McKean-Cowdin R, Ma H, Spicer DV, Van Den Berg D, Bernstein L, et al. Characteristics of triple-negative breast cancer in patients with a BRCA1 mutation: results from a population-based study of young women. J Clin Oncol 2011; 29:4373-80.

[19] Liu X, Xiao N, Guo W, Wu Y, Cai Z, He Q, et al. The hOGG1 gene 5'-UTR variant c.-53G>C contributes to the risk of gastric cancer but not colorectal cancer in the Chinese population: the functional variation of hOGG1 for gastric cancer risk. J Cancer Res Clin Oncol 2011; 137:1477-85.

[20] Xie H, Xia K, Rong H and Chen X. Genetic polymorphism in hOGG1 is associated with triple-negative breast cancer risk in Chinese Han women. Breast 2013; 22:707-12.

[21] Zhang S, Shao Y, Hou G, Bai J, Yuan W, Hu L, et al. QM-FISH analysis of the genes involved in the G1/S checkpoint signaling pathway in triple-negative breast cancer. Tumour Biol 2013.

[22] Li XR, Liu M, Zhang YJ, Wang JD, Zheng YQ, Li J, et al. CK5/6, EGFR, Ki-67, cyclin D1, and nm23-H1 protein expressions as predictors of pathological complete response to neoadjuvant chemotherapy in triple-negative breast cancer patients. Med Oncol 2011; 28 Suppl 1:S129-34.

BioMedicine March 2014, Vol. 4, No. 1, Pages 20-23 DOI 10.7603/s40681-014-0004-3

Original article

Vascular Endothelial Growth Factor -460 C/T BstUI Gene Polymorphism is associated with Primary Open Angle Glaucoma

Hui-Ju Lin[a,b], Wen-Lu Chen[a,b], Ter-Hsin Chen[c], Yung-Jen Kung[d], Lei Wan[b,e,f]

[a]Department of Ophthalmology, China Medical University Hospital, Taichung, Taiwan
[b]School of Chinese Medicine, China Medical University, Taichung, Taiwan
[c]Graduate Institute of Veterinary Pathobiology, College of Veterinary Medicine, National Chung Hsing University, Taichung, Taiwan
[d]Department of Veterinary Medicine, National Chung Hsing University, Taichung, Taiwan
[e]Department of Biotechnology, Asia University, Taichung, Taiwan
[f]Department of Gynecology, China Medical University Hospital, Taichung, Taiwan

Received 8th of December 2013 Accepted 28th of December 2013

Keywords:
Primary open angle;
Glaucoma;
Genetic polymorphism;
Vasogenetic endogenous;
Growth factor;
Nitric oxide;
Hypoxia

ABSTRACT

***Background*:** Hypoxia and nitric oxide (NO) play important roles in the onset and progression of glaucoma. Vascular endothelial growth factor (VEGF) is one of the main factors responsive to hypoxia and NO. In this study, we investigated the association between the *BstU*I C/T VEGF gene polymorphism and primary open angle glaucoma (POAG).

***Methods**:* 60 POAG patients and 78 healthy volunteers were enrolled in this study. The most frequently observed polymorphism in the VEGF gene is *BstU*I C/T, which was located 460 nucleotides upstream of the gene. The polymorphism was observed using polymerase chain reaction-based restriction analysis.

***Results**:* Significant differences were observed in the distribution of the polymorphism between control subjects and POAG patients (p = 0.003). C/C homozygotes are absent in the control group; therefore, this genotype represents a suitable genetic maker for POAG.

Conclusions: Hypoxia and NO may be involved in the pathway whereby the VEGF-460 polymorphism regulates POAG. Furthermore, homozygous C/C VEGF genotype is a useful maker for Chinese POAG. ***Background*:** Hypoxia and nitric oxide (NO) play important roles in the onset and progression of glaucoma. Vascular endothelial growth factor (VEGF) is one of the main factors responsive to hypoxia and NO. In this study, we investigated the association between the *BstU*I C/T VEGF gene polymorphism and primary open angle glaucoma (POAG).

***Methods**:* 60 POAG patients and 78 healthy volunteers were enrolled in this study. The most frequently observed polymorphism in the VEGF gene is *BstU*I C/T, which was located 460 nucleotides upstream of the gene. The polymorphism was observed using polymerase chain reaction-based restriction analysis.

***Results**:* Significant differences were observed in the distribution of the polymorphism between control subjects and POAG patients (p = 0.003). C/C homozygotes are absent in the control group; therefore, this genotype represents a suitable genetic maker for POAG.

Conclusions: Hypoxia and NO may be involved in the pathway whereby the VEGF-460 polymorphism regulates POAG. Furthermore, homozygous C/C VEGF genotype is a useful maker for Chinese POAG.

1. Introduction

Various circulatory abnormalities have been cited as involved in etiology of glaucomatous optic neuropathy.[1,2] Prominent in the disease is vascular regulatory factor itself.[3] Among vascular factors, recent studies suggest possibility of endothelium-dependent vaso-regulatory system playing a key pathogenetic role.[4] Ability of cells to sense and respond to changes in oxygen tension is critical for many developmental, physiological, and pathological processes; hypoxia may play a direct role in pathogenesis of optic nerve head cupping, and visual field defects.[4,5] It is evident that hypoxia ranks among the crucial factors in pathogenesis of optic nerve damage and visual field defects in glaucoma. Yancey CM et al. proposed greater intraocular pressure (IOP) leading to decreased choroidal blood flow and outer retinal hypoxia, measured as lesser choroidal pO_2; this hypoxia is responsible for electroretinogram C-wave[5].

Nitric oxide (NO) is another vital endothelium-dependent vasoactive mediator acting as a potent vasodilator. Kotiloski H et al. observed that NO concentrations in aqueous humour were slightly higher in glaucoma patients than in controls.[4] Galassi F et al. also suggested disorders of NO regulatory processes as be involved in modulating blood supply to the optic nerve and in aqueous humour outflow.[1] Becquet et al. suggested NO acting at the level of ciliary muscle as well as on aqueous outflow pathway (trabecular meshwork, Schlemms' canal, and collecting channels), thus influencing ocular hydrodynamics.[6] It is also known that topical or intracameral application of NO donors alter aqueous humour outflow.[7] Neufeld AH et al. proved induction of nitric-oxide synthesis (NOS-2) in an optic nerve head moderately raising IOP level. Excessive NO production by NOS-2 is

*Corresponding author.. School of Chinese Medicine, China Medical University, No.91 Hsueh-shih Road, 404 Taichung, Taiwan
E-mail address: leiwan@mail.cmu.edu.tw (W. Lei).

Published online: 13 February 2014

cytodestructive to many tissues and neurotoxic to the central nervous system.[8] The exact nature of physiopathological interaction between NO vaso-regulation and how it influences aqueous humour outflow remain unclear, but there exists well-established relationship between NO and glaucoma.

Hypoxia modulates expression of a number of genes.[4,5,9-14] Among these, vascular endothelial growth factor (*VEGF*) gene is viewed as a critical mediator of endothelial sprouting at hypoxic sites.[9-14] It has been proven that NO up-regulates expression of *VEGF*,[12-14] which can be regulated by a variety of stimuli: hypoxia, cobaltous ion, nitric oxide (NO), growth factors, and cytokines.[15] Hypoxia is regarded as the most potent *VEGF* regulator, and NO has recently drawn much attention as a regulator.[16,17] Hypoxia and NO play important roles in pathogenesis of glaucoma. We correlated VEGF *BstU*I C/T gene polymorphism with primary open angle glaucoma (POAG).

2. Materials and Methods

We enrolled POAG patients from the Department of Ophthalmology at China Medical University Hospital from May to July 2003. All patients received serial ophthalmic examination: IOP, visual acuity, gonioscopy, autoperimetry, optic disc examination, and retinal examination. The control group volunteers were selected from patients receiving routine physical examination and were examined by the same ophthalmologist. Volunteers were all free of any systemic disease, patients with ocular disease other than POAG eliminated. POAG patients met at least one of the following criteria. Visual field: 1). At least two abnormal visual field tests by Humphrey automated perimetry, as defined by computer-based objective criteria. 2). Presence of one or more absolute defects in central visual field 30°, with ophthalmologic interpretation as glaucomatous visual field loss. Optic disca: 1). Either horizontal or vertical cup-to-disc ratio 0.6 or more. 2). Narrowest remaining neuroretinal rim of 20% or fewer disc diameters.Ophthalmologic: Patients with other possible causes of disc or field changes other than POAG were excluded.

We tabulated VEGF-460 polymorphism in all subjects, comparing its prevalence between control and POAG groups. Odds ratio calculated diverse allele frequencies. This study was conducted out with approval from the Human Study Committee of China Medical College Hospital. Informed consent was obtained from all participants. Genomic DNA was prepared from peripheral blood by Extractor WB kit (Wako, Japan). Polymerase chain reactions (PCRs) for genes were carried out in a total volume of 50 μl, containing genomic DNA; 2-6 *p*mole of each primer; 1X Taq polymerase buffer (1.5 mM $MgCl_2$); and 0.25 units of AmpliTaq DNA polymerase (Perkin Elmer, Foster City, CA). Primers for genes are forward 5'-TGTGCGTGTGGGGTTGAGCG-3'and reverse 5'-TACGT GCGGACAGGGCCTGA-3' according to Watson et al.[2] PCR amplification used programmable thermal cycler GeneAmp PCR System 2400 (Perkin Elmer). The 175 bp PCR product was mixed with 2 units of *Bst*U I (Takara, Japan) and the reaction buffer as per manufacturer's instructions. Restriction site was located -460 bp upstream of exon I, (C to T); transcription site "C" was cuttable. Two fragments measuring 155 bp and 20 bp were present if product was digestable. Uncuttable band was 175 bp on gel. Reaction was incubated for 2 hours at 37℃, 10 µl of the products loaded onto a 3% agarose gel containing ethidium bromide for electrophoresis. Polymorphism was categorized as "TT" (cuttable) and "CC" (uncuttable) homozygote or "TC" heterozygote (Figure 1).

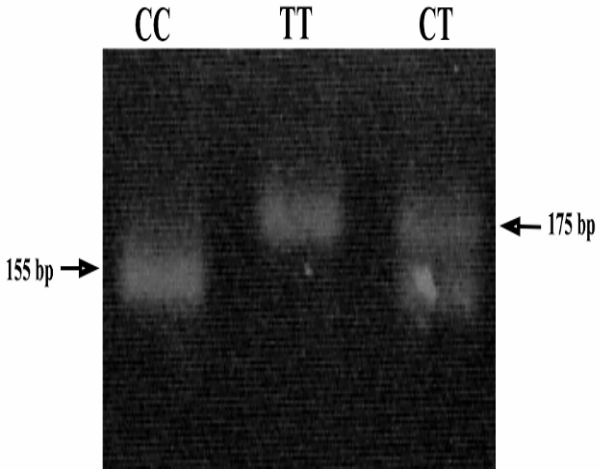

Figure 1. PCR products of VEGF-460 gene C/T polymorphism present on 3% agarose gel. Lane 1 "CC" homozygote: the two *BstU*I cuttable bands were 155 bp and 20 bp. Lane 2 "TT" homozygote: "T" was *BstU*I uncuttable site, and the fragment was measured 175 bp. Lane 3 "TC" heterozygote.

For statistical analysis of the allelic frequency distribution in this polymorphism, both groups were compared using the chi-square test. The software used for the calculation was the SPSS® system. When the assumption of the chi-square test was violated (i.e. when 1 cell had an expected count of <1, or > 20% of the cells had an expected count of <5), the Fisher's exact test was performed. A *p*-value of <0.05 was considered statistically significant.

3. Results

The POAG group consisted of 60 patients, the control group 78 healthy volunteers. The latter ranged in age from 22 to 70 (mean: 53) years and had no ophthalmic disease, all Chinese and unrelated, including 40 women and 38 men. POAG patients ranged in age from 20 to 70 (mean: 48) years, were unrelated, including 30 women and 30 men. All patients were followed up two to eight (average of five) years. Ten received trabeculectomy, two of these at two different sites; fifty used topical drugs to control intraocular pressure. Each patient used an average of 1.3 types of anti-glaucomatous drugs. Ten patients required no drugs to control IOP following trabeculectomy. Table 1 plots VEGF genotype frequencies between groups: significant difference appears in C/C polymorphism distribution between normal controls and POAG patients (p = 0.003). Distribution in the POAG group was "T/T" homozygote, 43.3%; "C/T" heterozygote, 43.3%; and "C/C" homozygote, 13.4%. Distribution of CC homozygote was sharply higher in the POAG group.

Table 1. Distribution of VEGF gene –460 *BstU*I polymorphism between healthy control subjects and POAG patients exam by Fisher's exact test

	TT	TC	CC	Total	*p*-valve
Control	38 (48.7%)	40 (51.3%)	0 (0%)	78 (100.0%)	0.003
POAG	26 (43.3%)	26 (43.3%)	8 (13.4%)	60 (100.0%)	

Furthermore, odds ratio of C/C genotype was significant when analyzed, using regression method according to age (Table 2). This indicates age as an insignificant source of variation. We also calculated "power" of the test of the null hypothesis by $SPSS^R$ and found a power of 89% to yield

a statistically significant result with this sample size.

Table 2. Age-adjusted tests for genotypes of VEGF-460 gene polymorphism

Genotype	Odds ratio (95% CI)[+]	
	Unadjusted	Age-adjusted
C/C	1* (2.3-24.60	8.5* (2.4-29.5)
C/T	1	1
T/T	1.4*(0.8-2.6)	1.8*(0.9-3.5)

[+]CI denotes confidence interval. *p<0.05

4. Discussion

Hypoxia and NO play pivotal roles in POAG pathogenesis. Regardless, VEGF appears as a key factor in POAG development. Ankeno N et al. demonstrated hypoxia transcriptionally activating VEGF expression by elevating level of basic helix-loop-helix (bHLH)-PAS transcription factor.[13] We suspect hypoxia inducing optic axon apoptosis, possibly influenced by altering VEGF transcription. Kimura H et al. proposed NO and hypoxic pathways of VEGF induction sharing common traits and NO mediating transcription by a mechanism distinct from hypoxia.[14] Regardless of pathways, the fact that hypoxia and NO activate VEGF transcription suggests expression of VEGF as closely related to POAG. Yet VEGF-induced angiogenesis might not be the primary factor in this relationship. VEGF is a cytokine, and our laboratory has demonstrated POAG's positive association with many cytokines: e.g., tumor necrosis factor alpha[18] and interleukin-1.[19] Pharmacological neuroprotection via inhibition of NO and hypoxia may prove useful in treating glaucoma.[5,6] We suspected that VEGF polymorphisms render optic nerve axons less capable of tolerating hypoxic and NO damage and predispose POAG patients to optic neuropathy. Excluding effects of hypoxia and NO, POAG is characterized by optic nerve death, known as mediated by apoptosis.[19,20] VEGF may also alter apoptotic conditions in optic axons through autocrine and paracrine mechanisms, yielding further evidence of a connection between POAG and VEGF, but we do not claim VEGF as direct cause. We suggest an association between them. Precise effect of VEGF on POAG is unknown and may warrant resolution via future use of "proteomic" analysis to identify factors as critical to pathological mechanisms. Our study noted starkly different distribution of VEGF-460 polymorphism between control and POAG groups. Ratio of C/C homozygote is 0% in controls, indicating C/C homozygote as useful for predicting POAG. Association of single nucleotide polymorphism (SNPs) with disease does not indicate genes as directly causes. It should be understood that there is just correlation, while environment effects and post translation may allow full understanding of pathology. We probe candidate genes in order to determine their role in POAG. Likewise, only a fraction of SNPs of these genes were examined; we selected POAG patients who meet the criteria for this study. We can say that VEGF -460 gene polymorphisms are linked with Chinese POAG and can identify Chinese POAG patients. Still, we cannot say that polymorphisms worsen prognosis or alter drug response. Our laboratory has linked certain SNPs with POAG.[17,21] SNPs hold vital implications for human genetics. Understanding associated polymorphism is expected to lend insight into course and treatment of disease. Our ongoing studies correlate SNPs with glaucoma, using SNPs to map Chinese POAG.

Acknowledgments:

This study was funded by a grant (DMR-103-066) from China Medical University Hospital.

REFERENCES

[1] Galassi F, Sodi A, Ucci F, Renieri G, Pieri B, Masini E. Ocular haemodynamics and nitric oxide in normal pressure glaucoma. Acta ophthalmol Scand 2000; 78: 37-38.

[2] Chung HS, Harris A, Evans DW, Kagemann L, Garzozi HJ, Martin B. Vascular aspects in the pathophisology of glaucomatous optic neuropathy. Surv Ophthalmol 43(suppl.1): S43-50

[3] Levy AP, Levy NS, Wegner S, Goldberg MA. Transcriptional regulation of the rat vascular endothelial growth factor gene by hypoxia. J of Biol Chem 1995; 270:13333-40.

[4] Neufeld AH, Sawada A, Becker B. Inhibition of nitric-oxide synthase 2 by aminoguanidine provides neuroprotection of retinal ganglion cells in a rat model of chnonic glaucoma. Proc. Natl. Acad. Sci 1999; 96: 9944-48.

[5] Lin Y, Cox SR, Morita T, Kourembanas S. Hypoxia regulates vascular endothelial growth factor gene expression in endothelial cells. Identification of a 5' dnhancer Circ Res 1995;77: 638-43.

[6] Chung HS, Harris A, Evans DW, Kagemann L, Garzozi HJ, Martin B. Vascular aspects in the pathophisology of glaucomatous optic neuropathy. Surv Ophthalmol 43 (suppl. 1)1999:S43-50.

[7] Nathanson JA. Mckee M. Alternations of ocular nitric oxide synthase in human glaucoma. Invest Ophthalmol Vis Sci. 1995; 36: 1774-84.

[8] Armaly MF, Krueger DE, Maunder L, Becker B, Hetherington J, Jr Kolker AE, Levene RZ, Maumenee AE, Pollack IP, Shaffer RN. Biostatistical analysis of the collaborative glaucoma study. Summary report of the risk factors. Arch Ophthalmol 1980; 98: 2163-71

[9] Kimura H, Weisz A, Kurashima Y, Hashimoto K, Tsutomu Ogura, Fulvio D'Acquisto, Raffaelo Addeo, Masatoshi Makundri, Esumi H. Hypoxia response element of the human vascular endothelial growth factor gene mediates transcriptional regulation by nitric oxide: control of hypoxia-inducible factor-1 activity by nitric oxide. Blood 2000; 95: 189-97.

[10] Guang L. Wang GL, Semenza GL. Characterization of hypoxia-inducible factor. 1 and regulation of DNA binding activity by hypoxia. J of Biol Chem 1993; 29: 21513-18.

[11] Steinbrech DS, Mehrara BJ, Saadeh PB, Greenwald JA, Spector JA, Gittes GK, MT. VEGF expression in an osteoblast-like cell line is regulated by a hypoxia response mechanism. Am J Physical Cell Physiol. 2000; 278: C853-60.

[12] Kimura H, Weisz A, Ogura T, Hitomi Y, Kurashima Y, Hashinoto K, D'Acquists F, Makunchi M, Esumi H. Identification of hypoxia-inducible factor-1 Ancillary sequence and its function in Vascular endothelial growth factor gene induction by hypoxia and nitric oxide. J Biol Chem 2001; 276: 2292-98.

[13] Akeno N, Czyzyk-Krzeska MF, Gross TS, Clemens TL. Hypoxia induces vascular endothelial growth factor gene transcription in human osteoblast like cells through the hypoxia inducible factor 2α. Endocrinology 1991; 142: 959-62.

[14] Hideo Kimura H, Weisz A. Kurashima Y, Hashimoto K, Ogura T, D'Acquisto F, Addeo R, Makuuchi M, Esumi H. Hypoxia response element of the human vascular endothelial growth factor gene mediates transcriptional regulation by nitric oxide: control of

hypoxia-inducible factor-1 activity by nictric oxide. Blood 2000; 95: 189-97.
[15] Klagsbrun M, D'Amore PA. Vascular endothelial growth factor and its receptors. Cytokine Growth Factor Rev 1996; 7: 259-70
[16] Jackson MW, Bentel JM, Tilley WD. Vascular endothelial growth factor (VEGF) expression in prostate cancer and begin prostatic hyperplasia. J Urol 1997; 157: 2323-8
[17] Lin HJ, Tsai FJ, Chen WC, Hsu CD, Tsai SW. Association of Interleukin - I Beta and Receptor Antagonist Gene Polymorphisms with Primary Open Angle Glaucoma. Ophthalomiga 2003; 217: 358-64.
[18] Lin HJ, Tsai FJ, Chen WC, Shi YR, Hsu Y, Tsai SW. Association of Tumor Necrosis Factor Alpha-308 Gene Polymorphism with Primary Open Angle Glaucoma in Chinese. Eye 2003; 17: 31-34.
[19] Stone EM, Fingert JH, Alward WLM, et al. Identification of a gene that causes primary open angle glaucoma. Science 1997; 275: 668-70.
[20] Nickells RW. Apoptosis of retinal ganglion cells in glaucoma: an update of the molecular pathways involved in cell death. Surv ophthalmol 1999; 43: S151-61.
[21] Lin HJ, Chen WC, Tsai FJ, Tsai SW. Distributions of p53 codon 72 polymorphism in primary open angle glaucoma. Br J Ophthalmol 2002; 86: 767-70

BioMedicine March 2014, Vol. 4, No. 1, Pages 24-28 DOI 10.7603/s40681-014-0005-2

Original article

Protective effects from *Houttuynia cordata* aqueous extract against acetaminophen-induced liver injury

Wei-ting Chen, Chieh-ling Yang, Mei-chin Yin*

Department of Nutrition, China Medical University, Taichung City, Taiwan

Received 30th of December 2013 Accepted 14th of January 2014

Keywords:
Hepatotoxicity;
Houttuynia cordata;
Acetaminophen;
MCP-1;
CYP2E1

ABSTRACT
Background: Protective effects of *Houttuynia cordata* aqueous extract (HCAE) against acetaminophen-induced hepatotoxicity in Balb/cA mice were examined.
Methods: HCAE, at 1 or 2 g/L, was added into the drinking water for 4 weeks. Acute liver injury was induced by acetaminophen treatment intraperitoneally (350 mg/kg body weight).
Results: Acetaminophen treatment significantly depleted hepatic glutathione (GSH) content, increased hepatic malonyldialdehyde (MDA), reactive oxygen species (ROS) and oxidized glutathione (GSSG) levels, and decreased hepatic activity of glutathione peroxidase (GPX), catalase and superoxide dismutase (SOD) (p<0.05). The pre-intake of HCAE alleviated acetaminophen-induced oxidative stress by retaining GSH content, decreasing MDA, ROS and GSSG production, and maintaining activity of GPX, catalase and SOD in liver (p<0.05). The pre-intake of HCAE also significantly lowered acetaminophen-induced increase in cytochrome P450 2E1 activity (p<0.05). Acetaminophen treatment increased hepatic release of interleukin (IL)-6, IL-10, tumor necrosis factor (TNF)-alpha and monocyte chemoattractant protein-1 (p<0.05). HCAE intake significantly diminished acetaminophen-induced elevation of these cytokines (p<0.05).
Conclusion: These results support that HCAE could provide hepato-protection

1. Introduction

Acetaminophen is an antipyretic and analgesic drug, and metabolized by cytochrome P450 system, which leads to the formation of. n-acetyl-p-benzoquinoneimine (NAPQI) [1,2] A large dose of this drug causes depletion of cellular glutathione (GSH) in liver because NAPQI reacts rapidly with GSH, which consequently enhances oxidation stress in conjunction with mitochondrial dysfunction, and leads to massive hepatocyte necrosis, liver failure or death [3,4]. On the other hand, it is known that cytochrome P450 2E1 (CYP2E1) regulates the metabolic activation of this drug both in human and rodents [5]. The increased CYP2E1 activity not only promotes NAPQI formation but also causes excessive reactive electrophiles and free radicals such as reactive oxygen species (ROS) to augment oxidative stress [6,7]. Thus, the agent(s) with GSH reserving ability and/or inhibitory effect upon CYP2E1 activity may provide preventive and/or alleviative effects for liver against the progression of acetaminophen-induced hepatocellular oxidative injury.

It is reported that interleukin-6 (IL-6) and tumor necrosis factor (TNF)-alpha are involved in acetaminophen-induced hepatotoxicity [8,9]. The increased release of these inflammatory cytokines, partially from the stimulation of oxidative stress [10], could consequently cause cytokine imbalance, immune dysfunction and even liver cell apoptosis. MCP-1 is generated at the site of infection or injury, and acts as a chemokine for monocyte recruitment and lymphocytes activation [11]. The increased hepatic mRNA expression of this chemokine has been observed in acetaminophen-treated mice, which facilitates the inflammatory response of liver innate immune system [12]. Thus, any agent(s) with suppressive effects on these inflammatory cytokines and/or chemokines may be able to improve acetaminophen-induced liver injury.

Houttuynia cordata is traditionally used as a medicinal plant in Asia countries including China, Taiwan, Japan and Thai [13]. It is reported that *Houttuynia cordata* provided anti-oxidative protection in mice against frying-oil and CCl_4-induced injury [14,15]. Our previous study found that *Houttuynia cordata* aqueous extract (HCAE) was rich in phenolic acids and flavonoids; and HCAE intake at 1 and 2% suppressed high fat diet induced oxidative and inflammatory stress in heart and liver via reducing malondialdehyde level, retaining GSH content and glutathione peroxidase activity, declining TNF-alpha, IL-1beta and IL-6 production [16]. Those previous studies suggest that HCAE may provide nutritional benefit for liver. However, it remains unknown that HCAE could protect liver against acetaminophen-induced oxidative and inflammatory damage.

The purpose of this animal study was to examine the protective effects of *Houttuynia cordata* aqueous extract on liver of acetaminophen treated mice. The influence of this extract upon CYP2E1 activity, associated antioxidant enzymes activities, and cytokines were also evaluated.

2. Materials and Methods

2.1 Materials

Fresh *Houttuynia cordata* leaves, harvested in summer, 2012, were

*Corresponding author, Department of Nutrition, China Medical University, 91, Hsueh-shih Rd., Taichung City, Taiwan
E-mail address:mcyin@mail.cmu.edu.tw (M.-c. Yin).

Published online: 13 February 2014

obtained from Nantou County, Taiwan. *Houttuynia cordata* aqueous extract (HCAE) was prepared by mixing 100 g chopped leaves and 250 mL sterile distilled water, homogenizing in a Waring blender and cooking for 20 min at 100℃. After filtrating through a Whatman No. 1 filter paper, the filtrate was further freeze-dried to a fine powder. Our previous study indicated that HCAE had total phenolic acids at 2175±210 mg/100 g dry HCAE. In our present study, the content of total phenolic Corresponding author, Department of Nutrition, China Medical University, 91, Hsueh-shih Rd., Taichung City, Taiwan

2.2. Animals and diets

Four- to five-week-old male Balb/cA mice were obtained from National Laboratory Animal Center (National Science Council, Taipei City, Taiwan). Mice were housed on a 12-h light-12-h dark schedule, and fed with water and mouse standard diet (PMI Nutrition International LLC, Brentwood, MO, USA). Use of the mice was reviewed and approved by the China Medical University animal care committee.

2.3. Experimental design

HCAE at 1 or 2 g/L was directly added into the drinking water. Two control groups of mice consumed distilled water, and all mice consumed normal diet. After 4 weeks supplement, HCAE treated mice and one control group were treated by APAP intraperitoneally (ip 350 mg/kg body weight), and all mice were sacrificed after 24 h. Liver from each mouse was collected and weighted. Blood was also collected, and plasma or serum was separated from erythrocyte immediately. Liver tissue, 100 mg, was homogenized on ice in 1 mL phosphate buffer (pH 7.2), and the filtrate was collected. Protein concentration of tissue homogenate was determined by a commercial assay kit (Pierce Biotechnology Inc., Rockford, IL, USA) with bovine serum albumin as standard. In all experiments, sample was diluted to a final concentration of 1 g protein /L.

2.4. Alanine aminotransferase (ALT), aspart ate aminotransferase (AST) and c-reactive protein (CRP) analyses

Serum activities of ALT and AST were determined by using commercial assay kits (Randox Laboratories Ltd., Crumlin, UK). CRP level (mg/L) was determined by a commercial ELISA kit (Anogen, ON, Canada).

2.5. GSH and oxidized glutathione (GSSG) levels, superoxide dismutase (SOD), catalase and glutathione peroxidase (GPX) activities assay

GSH and GSSG concentrations (nmol/mg protein) in liver were determined by commercial colorimetric GSH and GSSG assay kits (OxisResearch, Portland, OR, USA). Catalase, SOD and GPX activities (U/mg protein) in liver were determined by catalase, SOD and GPX assay kits (Calbiochem, Inc., San Diego, CA, USA)

2.6. Determination of lipid oxidation and ROS

Lipid oxidation in liver was determined by measuring the level of malondialdehyde (MDA, μmol/L) via an HPLC method [6]. The method described in Gupta et al. [17] was used to measure hepatic ROS level. Briefly, 10 mg liver was homogenized in 1 mL of ice cold 40 mM Tris–HCl buffer (pH 7.4), and further diluted to 0.25% with the same buffer. Then, samples were divided into two equal fractions. In one fraction, 40 μL 1.25 mM 2',7'-dichlorofluorescin diacetate in methanol was added for ROS estimation. Another fraction, in which 40 μL methanol was added, served as a control for auto fluorescence. After incubating for 15 min at 37 °C, fluorescence was determined at 488 nm excitation and 525 nm emission using a fluorescence plate reader.

2.7. Cytokines measurements

Hepatic levels of IL-6, IL-10, TNF-alpha and MCP-1 were measured by using cytoscreen immunoassay kits (BioSource International, Camarillo, CA, USA). Samples were run in duplicates according to manufacturer's instructions

.

2.8. Measurement of CYP2E1 activity

The activity of CYP2E1 in liver microsome was estimated by colorimetrically measuring the formation of 4-nitrocatechol, a product from p-nitrophenol hydroxylation catalyzed specifically by CYP2E1. The protein concentration of CYP2E1 was measured by ELISA, and a rabbit anti-CYP2E1 antibody (Calbiochem, Inc., San Diego, CA, USA) was used as the detect system. The formed 4-nitrocatechol was expressed as nmol/mg protein.

2.9. Statistical analyses

The effect of each treatment was analyzed from 10 mice (n=10) in each group. Data were subjected to analysis of variance (ANOVA). Differences with $p<0.05$ were considered to be significant.

3. Results

As shown in Table 1, the intake of HCAE did not affect daily water intake, feed intake, final body weight and liver weight ($P>0.05$). Plasma levels of ALT, AST and CRP are presented in Figure 1. The pre-treatments of HCAE alleviated acetaminophen-induced elevation of ALT and AST ($p<0.05$). HCAE intake only at 2 g/L significantly declined acetaminophen-induced increase in CRP ($p<0.05$).

Table 1 ─ Water intake (WI, mL/mouse/d), feed intake (FI, g/mouse/d), body weight (BW, g) and liver weight (LV, g) of mice consumed distilled water or HCAE at 1 or 2 g/L for 4 week. Data are mean ± SD (n=10).

	water	HCAE, 1	HCAE, 2
WI	2.7±0.2	2.9±0.3	2.6±0.3
FI	2.1±0.3	2.2±0.2	2.4±0.4
BW	25.3±1.2	24.8±1.0	25.0±0.8
LW	1.29±0.11	1.35±0.14	1.24±0.12

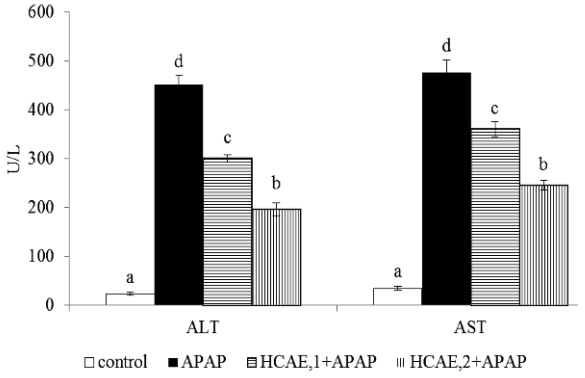

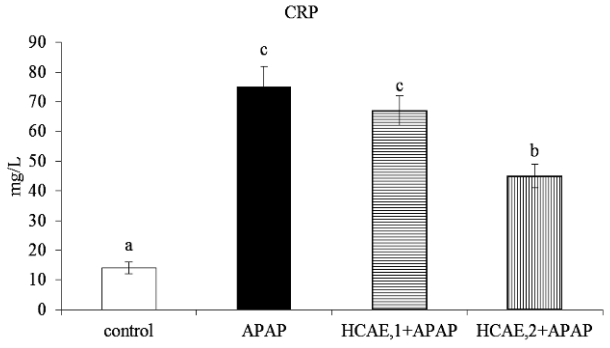

Fig. 1—Plasma ALT, AST and CRP levels in mice pre-treated by 0, 1 or 2 g/L HCAE, and followed with acetaminophen (APAP) treatment. Control group was mice without HCAE intake and without APAP treatment. Data are mean ± SD (n=10). [a-d]Means among bars without a common letter differ, $p<0.05$.

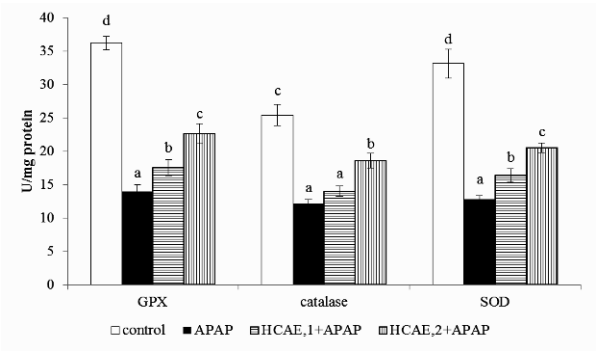

Fig.2—Hepatic GPX, catalase and SOD activities in mice pre-treated by 0, 1 or 2 g/L HCAE, and followed with acetaminophen (APAP) treatment. Control group was mice without HCAE intake and without APAP treatment. Data are mean ± SD (n=10). [a-d]Means among bars without a common letter differ, $p<0.05$.

Acetaminophen treatment significantly decreased hepatic GSH, and increased GSSG, MDA and ROS levels (Table 2, $p<0.05$); but the pre-intake of HCAE alleviated acetaminophen-induced GSH depletion, and reduced GSSG, MDA and ROS formation ($p<0.05$). As shown in Figure 2, acetaminophen treatment significantly reduced hepatic GPX, catalase and SOD activities ($p<0.05$). However, the pre-intake of HCAE significantly retained GPX and SOD activities ($p<0.05$). HCAE intake only at 2 g/L significantly maintained hepatic catalase activity ($p<0.05$). Acetaminophen treatment raised CYP2E1 activity (Figure 3), and HCAE pre-intake significantly suppressed subsequent acetaminophen-induced elevation of CYP2E1 activity ($p<0.05$). As shown in Table 3, acetaminophen treatment also significantly increased hepatic levels of TNF-alpha, IL-6, IL-10 and MCP-1 ($p<0.05$). The pre-intake of HCAE decreased acetaminophen-induced release of IL-6, IL-10 and MCP-1 ($p<0.05$). HCAE pre-intake only at 2 g/L significantly lowered hepatic TNF-alpha level ($p<0.05$).

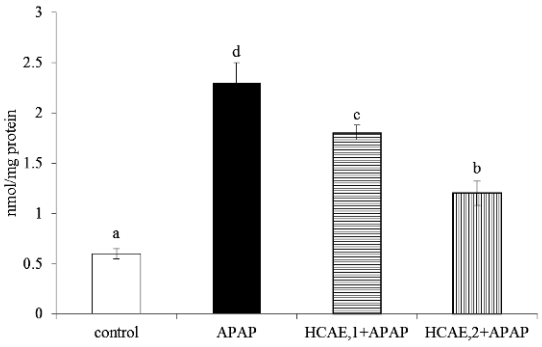

Fig.3—Liver microsomal CYP2E1 activity, determined as 4-nitrocatechol (nmol/mg protein), from mice pre-treated by 0, 1 or 2 g/L HCAE, and followed with acetaminophen (APAP) treatment. Control group was mice without HCAE intake and without APAP treatment. Data are mean ± SD (n=10). [a-d]Means among bars without a common letter differ, $p<0.05$.

Table 2—Hepatic content of GSH (nmol/mg protein), GSSG (nmol/mg protein), MDA (μmol/L) and ROS (nmol/mg protein) from mice pre-treated by 0, 1 or 2 g/L HCAE, and followed with acetaminophen (APAP) treatment. Control group was mice without HCAE intake and without APAP treatment. Data are mean ± SD (n=10).

	control	APAP	HCAE,1+APAP	HCAE,2+APAP
GSH	22.7±1.0[d]	12.1±0.5[a]	15.9±0.6[b]	18.0±0.8[c]
GSSG	0.26±0.05[a]	1.22±0.08[d]	0.96±0.10[c]	0.65±0.06[b]
MDA	0.51±0.07[a]	1.58±0.10[d]	1.21±0.09[c]	0.88±0.05[b]
ROS	0.34±0.03[a]	1.64±0.12[d]	1.25±0.06[c]	0.79±0.08[b]

[a-d]Means in a column without a common letter differ, $p<0.05$.

Table 3—Hepatic level (pg/mg protein) of TNF-alpha, IL-6, IL-10 and MCP-1 from mice pre-treated by 0, 1 or 2 g/L HCAE, and followed with acetaminophen (APAP) treatment. Control group was mice without HCAE intake and without APAP treatment. Data are mean ± SD (n=10).

	control	APAP	HCAE,1+APAP	HCAE,2+APAP
TNF-alpha	17±4[a]	523±21[c]	495±14[c]	407±17[b]
IL-6	16±2[a]	419±18[d]	366±10[c]	290±12[b]
IL-10	15±5[a]	303±15[d]	232±13	157±9[b]
MCP-1	14±3[a]	568±25[d]	475±18[c]	369±11[b]

[a-d]Means in a column without a common letter differ, $p<0.05$.

4. Discussion

Our previous study found that HCAE was rich in phenolic acids and flavonoids, and the intake of HCAE at 1 or 2% lowered hepatic and circulating lipid accumulation, as well as attenuated oxidative and inflammatory stress in liver from mice consumed high fat diet [16]. Our present study further found that the pre-intake of HCAE markedly protected liver against subsequent acetaminophen-induced oxidative and inflammatory injury via decreasing ALT and AST levels, increasing GSH retention, suppressing CYP2E1 activity, lowering IL-6 and MCP-1 release. These results support that HCAE is a potent hepatoprotective agent.

It is well known that acetaminophen at high dose causes GSH depletion, ROS accumulation and inflammatory cytokines release in liver [18,19]. The results from our present study agreed those previous studies. Furthermore, we found that the pre-intake of HCAE effectively alleviated acetaminophen-induced GSH depletion and GSSG increase in liver. It seems that hepatoprotective effects from HCAE could be partially ascribed to HCAE maintain hepatic GSH content. We also found that the pre-intake of HCAE retained the activity of three antioxidant enzymes in liver of acetaminophen-treated mice. Obviously, HCAE could provide hepatic anti-oxidative protection via enzymatic actions. CYP2E1 is the major isozyme responsible for the formation of NAPQI from acetaminophen [20,21]. A high dose of acetaminophen elevates CYP2E1 activity and facilitates this catalytic reaction, which in turn promotes ROS overproduction. In our present study, HCAE pre-intake markedly declined subsequent acetaminophen-induced CYP2E1 activity elevation, lowered ROS formation, and reduced acetaminophen-induced oxidative stress. These results implied that the protective action from HCAE was partially due to its suppressive effect on CYP2E1 activity.

IL-6 and TNF-alpha, proinflammatory cytokines, were central mediators for the regulation of several biomarkers such as CRP, especially at acute phase response [22]. In our present study, acetaminophen treatment increased the release of these proinflammatory cytokines and CRP; however, the pre-intake of HCAE decreased hepatic formation of these inflammatory cytokines and circulating CRP. Apparently, the anti-inflammatory protection from this extract was partially due to its inhibitory effects on the production of these cytokines. Dambach et al. [8] indicated that the increased IL-6 and TNF-alpha from acetaminophen treatment could induce neutrophil accumulation and activation at liver; stimulate macrophage and hepatocyte production of nitric oxide, which further enhance acetaminophen-induced hepatoxicity. MCP-1 is a chemotactic factor for activating monocytes and macrophages, and could recruit monocytes to the sites of injury [23,24]. In our present study, the increased hepatic MCP-1 and TNF-alpha levels indicated that the livers of these mice were injured, and implied that neutrophil and macrophage were activated to promote inflammatory reactions. However, the pre-intake of HCAE substantially decreased hepatic TNF-alpha and MCP-1 generation in acetaminophen-treated mice, which suggested that this extract might protect liver against inflammation via diminishing the activation of neutrophil, monocytes and macrophages, reducing the recruitment of monocytes. It is well known that oxidation and inflammation are closely interrelated in biological systems [25]. Since the pre-intake of HCAE already coped with acetaminophen-induced oxidative stress, it is reasonable to observe the lower levels of inflammatory cytokines in HCAE treated mice.

Our previous study reported that 8 phenolic acids and 7 flavonoids such as gallic acid, ellagic acid, ferulic acid, kaempferol, myricetin and quercetin could be detected in HCAE [16]. It is reported that these compounds possess anti-oxidative and/or anti-inflammatory activities [26,27]. Thus, the hepatic protection from this extract against acetaminophen as we observed could be due to the presence of these phenolic acids and flavonoids.

In conclusion, *Houttuynia cordata* aqueous extract may be considered as hepatoprotective agent because the pre-intake of this extract protected liver against subsequent acetaminophen-induced oxidative and inflammatory injury via retaining hepatic GSH content, maintaining GPX and SOD activities, suppressing CYP2E1 activity and decreasing production of IL-6 and MCP-1.

Acknowledgements

This study was supported by a grant from China Medical University, Taichung City, Taiwan (CMU 102-AWARD-04).

REFERENCES

[1] Song Z, McClain CJ, Chen T. S-adenosylmethionine protects against acetaminophen-induced hepatotoxicity in mice. Pharmacology 2004;71:199-208.

[2] Masubuchi Y, Suda C, Horie T. Involvement of mitochondrial permeability transition in acetaminophen-induced liver injury in mice. J Hepatol 2005;42:110-6.

[3] Oz HS, McClain CJ, Nagasawa HT, Ray MB, de Villiers WJ, Chen TS. Diverse antioxidants protect against acetaminophen hepatotoxicity. J Biochem Molecular Toxicol 2004;18:361-8.

[4] Hazai E, Vereczkey L, Monostory K. Reduction of toxic metabolite formation of acetaminophen. Biochem Biophys Res Commun 2002;291:1089-94.

[5] Manyike PT, Kharasch ED, Kalhorn TF, Slattery JT. Contribution of CYP2E1 and CYP3A to acetaminophen reactive metabolite formation. Clin Pharmacol Ther 2000;67:275-82.

[6] Hsu CC, Lin CC, Liao TS, Yin MC. Protective effect of s-allyl cysteine and s-propyl cysteine on acetaminophen-induced hepatotoxicity in mice. Food Chem Toxicol 2006;44:393-7.

[7] Williams CD, McGill MR, Farhood A, Jaeschke H. Fas receptor-deficient lpr mice are protected against acetaminophen hepatotoxicity due to higher glutathione synthesis and enhanced detoxification of oxidant stress. Food Chem Toxicol 2013;58:228-35.

[8] Dambach DM, Durham SK, Laskin JD, Laskin DL. Distinct roles of NF-kappaB p50 in the regulation of acetaminophen-induced inflammatory mediator production and hepatotoxicity. Toxicol Appl Pharmacol 2006;211:157-65.

[9] Ley K, Deem TL. Oxidative modification of leukocyte adhesion. Immunity 2005;22:5-7.

[10] Albano E. Free radical mechanisms in immune reactions associated with alcoholic liver disease. Free Radic Biol Med 2002;32:110-14.

[11] Takahashi K, Mizuarai S, Araki H, Mashiko S, Ishihara A, Kanatani A, et al. Adiposity elevates plasma MCP-1 levels leading to the increased CD11b-positive monocytes in mice. J Biol Chem 2003;278:46654-60.

[12] Liu ZX, Govindarajan S, Kaplowitz N. Innate immune system plays a critical role in determining the progression and severity of acetaminophen hepatotoxicity. Gastroenterology 2004;127:1760-74.

[13] Ji KM, Li M, Chen JJ, Zhan ZK, Liu ZG. Anaphylactic shock and lethal anaphylaxis caused by Houttuynia Cordata injection, a herbal treatment in China. Allergy 2009;64:816-7.
[14] Chen YY, Liu JF, Chen CM, Chao PY, Chang TJ. A study of the antioxidative and antimutagenic effects of Houttuynia cordata Thunb. using an oxidized frying oil-fed model. J Nutr Sci Vitaminol (Tokyo) 2003;49:327-33.
[15] Tian L, Shi X, Yu L, Zhu J, Ma R, Yang X. Chemical composition and hepatoprotective effects of polyphenol-rich extract from Houttuynia cordata tea. J Agric Food Chem 2012;60:4641-8.
[16] Lin MC, Hsu PC, Yin MC. Protective effects of Houttuynia cordata aqueous extract in mice consuming a high saturated fat diet. Food Funct 2013;4:322-7.
[17] Gupta R, Dubey DK, Kannan GM, Flora SJS. Concomitant administration of Moringa oleifera seed powder in the remediation of arsenic-induced oxidative stress in mouse. Cell Biol Inter 2007;31:44-56.
[18] Das J, Ghosh J, Manna P, Sil PC. Taurine protects acetaminophen-induced oxidative damage in mice kidney through APAP urinary excretion and CYP2E1 inactivation. Toxicology 2010;269:24-34.
[19] Yan SL, Wu ST, Yin MC, Chen HT, Chen HC. Protective effects from carnosine and histidine on acetaminophen-induced liver injury. J Food Sci 2009;74:H259-65.
[20] Walubo A, Barr S, Abraham AM, Coetsee C. The role of cytochrome-P450 inhibitors in the prevention of hepatotoxicity after paracetamol overdose in rats. Hum Exp Toxicol 2004;23:49-54.
[21] Yamaura K, Shimada M, Nakayama N, Ueno K. Protective effects of goldenseal (Hydrastis canadensis L.) on acetaminophen-induced hepatotoxicity through inhibition of CYP2E1 in rats. Pharmacognosy Res 2011;3:250-5.
[22] Zambon A, Gervois P, Pauletto P, Fruchart JC, Staels B. Modulation of hepatic inflammatory risk markers of cardiovascular diseases by PPAR-alpha activators: clinical and experimental evidence. Arterioscler Thromb Vasc Biol 2006;26:977-86.
[23] Zimmermann HW, Trautwein C, Tacke F. Functional role of monocytes and macrophages for the inflammatory response in acute liver injury. Front Physiol 2012;3:56.
[24] Dragomir AC, Laskin JD, Laskin DL. Macrophage activation by factors released from acetaminophen-injured hepatocytes: potential role of HMGB1. Toxicol Appl Pharmacol 2011;253:170-7.
[25] Furnkranz A, Schober A, Bochkov VN, Bashtrykov P, Kronke G, et al. Oxidized phospholipids trigger atherogenic inflammation in murine arteries. Arter Thromb Vascular Biol 2005;25:633-8.
[26] Chao CY, Mong MC, Chan KC, Yin MC. Anti-glycative and anti-inflammatory effects of caffeic acid and ellagic acid in kidney of diabetic mice. Mol Nutr Food Res 2010;54:388-95.
[27] Nirmala P, Ramanathan M. Effect of kaempferol on lipid peroxidation and antioxidant status in 1,2-dimethyl hydrazine induced colorectal carcinoma in rats. Eur J Pharmacol 2011;654:75-9.

BioMedicine March 2014, Vol. 4, No. 1, Pages 29-33 DOI 10.7603/s40681-014-0006-1

Original article

Metabolic Abnormality and Sleep Disturbance are Associated with Clinical Severity of Patients with Schizophrenia

Chung-Chieh Hung [a,b], Chin-Chih Liao[b], Po-Lun Wu [a,b], Shin-Da Lee [c,d] Hsien-Yuan Lane [a,b]*

[a]Graduate Institute of Clinical Medical Science, China Medical University, Taichung, Taiwan
[b]Department of Psychiatry, China Medical University Hospital, Taichung, Taiwan
[c] Graduate Institute of Rehabilitation Science, China Medical University, Taichung, Taiwan
[d]Department of Physical Therapy, China Medical University Hospital, Taichung, Taiwan

Received 4th of January 2014 Accepted 29th of January 2014

Keywords:
Schizophrenia;
Metabolic syndrome;
Sleep disturbance;
Slow wave sleep;
Body weight;
Neck circumference

ABSTRACT

Schizophrenic patients suffer from more metabolic or sleep problems. Little is known about risk factors. We recruited 17 patients with chronic schizophrenia from the rehabilitation center in a medical center in Taiwan and measured their demographic data, cognitive performance, and physical fitness, metabolic profiles and sleep parameters. They were divided into two groups according to clinical severity, then compared in terms of metabolic and sleep parameters.

Those with more severe symptomatology had more metabolic abnormality and shorter slow wave sleep (SWS).

Our findings suggest clinical symptoms as linked with heavier body weight, wider neck circumference, elevated blood pressure, and shorter SWS. Further studies are warranted to confirm the preliminary finding and to elucidate the underlying mechanism

1. Introduction

Schizophrenia, a psychiatric disorder causing deterioration of cognitive and daily function, is associated with obesity and metabolic syndrome, rendering patients vulnerable to morbidity and mortality[1].[1] Biological factors, lifestyle, and antipsychotics all contribute to obesity of patients[2], [3], which influences their sleep quality[4]. Prevalence of poor sleepers among schizophrenics is around 45%, related to adverse events of medication and accompanying depression and psychological distress[5], [6]. Metabolic abnormality and sleep disturbance seem correlated. Consequently, these patients reportedly have poor life quality; correlation between clinical symptoms and sleep quality remains unclear. We hypothesize patients with severe clinical symptoms as more likely to have metabolic abnormality and sleep disturbance.

2. Methods

Study was approved by China Medical University Hospital Institutional Review Board (IRB). All participants gave written informed consent.

2.1. Participants

We recruited 17 schizophrenic patients from the Rehabilitation Center of the China Medical University Hospital Psychiatric Department. All met criteria of schizophrenia, paranoid type, according to DSM-IV-TR[7]. We rated the subjects by Positive and Negative Syndrome Scale (PANSS) [8], with respective items scored from 1(absent) to 7(extreme severity). We rated their depressive symptoms by Hamilton Depression Rating Scale[9], and quality of life by Quality of Life Scale (QLS) [10]. Extrapyramidal symptoms were rated by Abnormal Involuntary Movement (AIMS) [11], Simpson-Angus (SAS) [12], and Barnes Rating Scale (BARS) [13]. Daily antipsychotic doses were recorderd as chlorpromazine equivalents [14],[14] and daily benzodiazepine doses as diazepam equivalents [15].

Inclusion criteria included (1) schizophrenic patients stable under current antipsychotics and benzodiazepine for at least three months; (2) engaged in regular rehabilitation program for at least three months; (3) aged between 20 and 50; (4) Han Taiwanese who speak Chinese fluently and understand this study well

Exclusion criteria included histories of (1) cerebrovascular, cardiovascular, and metabolic disorders (stroke, hypertension, diabetes mellitus); (2) neurologic disorders like epilepsy and traumatic brain injury; (3) physical disability (eg, fractures); (4) current DSM-IV-TR diagnosis of substance dependence (such as nicotine); (5) a DSM-IV-TR diagnosis of mental retardation, and (6) acute suicide or aggressive behaviors and (7) regular exercise.

2.2. Cognitive performance testing

Schizophrenic patients show impaired cognitive function [16], [17]. Our study included trail making, semantic association of verbal fluency, maze, verbal and non-verbal working memory, instant word list, delay word list, instant and, delayed visual reproduction, and digit symbol coding, as conducted by well-trained psychologists.

2.3. Cardiometabolic parameters and physical fitness

Patients' weight and height, body mass index (BMI), neck circumference (NC), waist circumference, hip circumference, and waist-hip ratio (WHR) were recorded. Body fat was assessed by Omron body fat scale. Physical fitness was gauged according to a profile distributed by Bureau of Health Promotion, Department of Health, Taiwan. First, we checked sit-up frequency in one minute. Second, they underwent three-minute 35-centimeter-ladder climbing. We checked post-exercise heart rate

* Corresponding author.. Institute of Clinical Medical Science, College of Medicine, China Medical University, Taichung, Taiwan No.91 Hsueh-Shih Road, Taichung 404, Taiwan
E-mail address: hylane@gmail.com (H.-Y. Lane)

Published online: 13 February 2014

(PEHR) at the end of the first minute (PEHR1), the second minute (PEHR2), and the third minute (PEHR3) while they stopped exercise. PEHR2 and PEHR3 were checked via similar method with total climbing time recorded.

Heart rate, systolic and diastolic blood pressure were measured before blood examination. Blood samples were taken at 8:00 a.m. after a 12-hour overnight fast, with subjects' blood withdrawn from an antecubital vein to measure plasma levels of glucose, insulin, total cholesterol, triglyceride, HDL-cholesterol, LDL-cholesterol, and cortisol. Insulin was quantified by chemiluminescent immunoassay sandwich method, and serum glucose by glucose-oxidase-based assay. We rated insulin resistance by homeostasis model assessment of insulin resistance (HOMA-IR), assessed by the formula of fasting insulin (μU/ml) × fasting glucose (mg/dl)/405 [18].

The presence of metabolic syndrome was recorded as defined by National Cholesterol Education Program (NCEP) guidelines: waist circumference≧102 cm (male) and≧88 cm (female), triglyceride (TG) ≧150 mg/dl, HDL-cholesterol <40 mg/dL (male) and < 50 mg/dL (female), blood pressure≧130/85 mmHg, and fasting glucose≧110 mg/dl[19]. Metabolic syndrome index was summated by the above criteria.

2.4 Sleep measurement

Sleep rating scales were self-recorded by all subjects preceding polysomnography examination: Pittsburgh Sleep Quality Index (PSQI) [20], Insomnia Severity Index (ISI) [21], Epworth Sleepness Scale (ESS) [22], and Pre-Sleep Arousal Scale (PSAS) [23]. Polysomnography (PSG) followed standardized techniques: digital electroencephalography (EEG), electromyography, and electrooculography signals acquired with Alice 4 system. PSG electrode montage was utilized, composed of EEG sites F3 and C3 (referenced to A2) and F4 and C4 (referenced to A1). PSG data were scored manually on a small monitor, using 30-second epochs for staging and arousal detection, as well as 2- or 5-minute respiratory data. We drew parameters from sleep polysomnography, including time in bed (TIB), total sleep time (TST), sleep latency, awakening time, sleep efficiency (TST/TIB).

Sleep architecture was assessed for each 30-second epoch coded as Wake, Stage 1, Stage 2, Stage 3+4 (slow wave sleep, SWS), and Rapid Eye-Movement (REM) sleep according to criteria made by Rechtschaffen and Kales [24]. Arousals were identified according to criteria of the American Sleep Disorders Association (ASDA) 1992 [25]. We identified apnea and hypopnea as flat air flow lower than 20% and 70% of the baseline, respectively, whose amplitude was measured during the nearest preceding period of regular breathing with stable oxygen saturation. We identified Apnea-hypopnea index as total apnea and hypopnea divided by total sleep time.

3. Data analysis

We divided participants into two groups according to severity of clinical manifestation Cut-off value was median number of the PANSS total scores. Student'-T test compared all variables between the two groups.

4. Results

Age and gender between groups were similar, as was duration of education and age at illness onset. Duration of illness of the H-PANSS group was longer. Clinical Global Impression (CGI) [11] tallied higher and Quality of Life Scale (QLS) lower in the H-PANSS group, depressive symptoms rated by Hamilton Depression Scale similar between groups (Table 1). Current medications calculated by chlorpromazine and Diazepam equivalents were also similar. There were no differences between the two groups in severity of EPS rated by Abnormal Involuntary Movement Scale, Barnes Akathsia Rating Scale, and Simpson-Angus Scale (Table 1).

Table 1. Demographic and clinical characteristics

Demographic characteristics	L-PANSS (n=8)	H-PANSS (n=9)	P value
Age (years)	35 ± 9.3	37 ± 9.6	0.801
Male/Female(male percentage)	2/6 (25%)	4/5 (44%)	0.434
Duration of education (years)	13.0 ± 3.3	11.6 ± 3.6	0.405
Age at illness onset (years) (years)	25.1 ± 7.5	22.3 ± 7.4	0.453
Duration of illness (months)	101.5 ± 71.8	186.7 ± 63.8	0.021 *
Clinical psychiatric condition rating scales			
Clinical Global Impression (CGI)	2.9 ± 0.4	3.7 ± 0.5	0.002 **
Quality of life scale (QLS)	63.3 ± 11.4	35.4 ± 14.0	<0.001 **
Hamilton Depression Rating scale	8.1 ± 5.2	12.7 ± 8.4	0.207
Medication amount			
Chlorpromazine equivalents	212.5 ± 64.1	237.2 ± 91.0	0.532
Diazepam equivalents	12.5 ± 16.9	5.0 ± 6.1	0.232
Extra-pyramidal symptoms rating scales			
Abnormal Involuntary Movement scale	4.1 ± 6.3	5.11 ± 4.5	0.712
Barnes Akathisia Rating scale	0.6 ± 1.2	2.1 ± 2.6	0.162
Simpson-Angus scale	5.8 ± 4.7	7.3 ± 3.5	0.440

All data were expressed as mean value ± standard deviation, except gender.

Low-PANSS (L-PANSS) group included schizophrenics with Positive and Negative Syndrome Scale (PANSS) total score below 65 (median of PANSS total scores of all 17 subjects); High-PANSS (H-PANSS) group included those with PANSS total scores 65 or higher.

***:P<0.05 and **:P<0.01, significance between groups**.

Cognitive performances between groups were similar. (Table 2)

Table 2. Cognition tests measured in two groups of patients

Parameters	L-PANSS (n=8)	H-PANSS (n=9)	P value
Trail making test	1.6 ± 0.9	2.0 ± 1.0	0.435
Digit symbol coding	4.9 ± 2.0	4.6 ± 3.1	0.807
Semantic association of verbal fluency	0.6 ± 0.5	0.4 ± 0.5	0.488
Maze	3.8 ± 1.6	4.2 ± 4.6	0.787
Verbal working memory	7.6 ± 3.9	8.7 ± 3.9	0.590
Non-verbal working memory	4.5 ± 3.1	5.6 ± 3.1	0.491
Instant word list	5.6 ± 2.8	5.1 ± 3.0	0.719
Delay word list	6.5 ± 2.6	6.6 ± 2.2	0.963
Instant visual reproduction	4.9 ± 2.2	4.8 ± 2.3	0.931
Delay visual reproduction	6.4 ± 2.6	5.1 ± 2.2	0.291

Data were expressed as mean value ± standard deviation. Low-PANSS (L-PANSS) group included schizophrenics with Positive and Negative Syndrome Scale (PANSS) total score below 65 (median of PANSS total scores of all 17 subjects); High-PANSS (H-PANSS) group comprised those with PANSS total scores 65 or higher. No significance appeared between groups

Body weight and neck circumference (NC) in the H-PANSS group were higher than those in the L-PANSS group. Body height, BMI, waist circumference, hip circumference, WHR and body fat between groups were similar, as was physical fitness measured by sit-up and climbing (Table 3). Both systolic and diastolic blood pressures in the H-PANSS group were higher. Metabolic index, heart rate, fasting sugar, insulin,

Homa-IR, cortisol, cholesterol, triglyceride, high-density lipoprotein, and low-density lipoprotein between groups were similar (Table 3).

Table 3. Cardiometabolic parameters and physical fitness

Physical parameters	L-PANSS (n=8)	H-PANSS (n=9)	P value
Body weight (BW) (kg)	65.4 ± 9.6	78.3 ± 9.2	0.013*
Body height (BH) (cm)	144.9 ± 12.5	161.1 ± 15.3	0.031*
Body mass index (BMI) (kg/m2)	31.5 ± 5.5	30.5 ± 4.1	0.653
Neck circumference (NC) (cm)	35.0 ± 2.6	38.6 ± 2.1	0.007**
Waist circumference (cm)	91.5 ± 10.5	95.8 ± 9.2	0.386
Hip circumference (cm)	104.4 ± 9.1	106.8 ± 6.5	0.537
Waist-hip ratio (WHR)	0.89 ± 0.07	0.87 ± 0.05	0.652
Body fat (%)	33.8 ± 5.1	32.1 ± 6.7	0.564
Physical fitness			
Sit-up (/min)	14.5 ± 12.7	14.2 ± 9.4	0.959
Stair-climbing PEHR 1 (/min)	52.9 ± 10.4	53.1 ± 8.7	0.960
PEHR 2 (/min)	48.4 ± 9.6	47.9 ± 8.5	0.913
PEHR 3 (/min)	47.0 ± 8.2	45.8 ± 8.3	0.765
Climbing time (s)	114.8 ± 57.4	133.3 ± 39.2	0.443
Cardiometabolic parameters			
Heart rate (/minute)	83.3 ± 16.8	85.9 ± 6.9	0.671
Systolic blood pressure (mmHg)	107.8 ± 8.2	122.7 ± 6.3	<0.001**
Diastolic blood pressure (mmHg)	65.8 ± 7.1	77.8 ± 10.2	0.014*
Fasting sugar (mg/dL)	91.1 ± 9.6	100.7 ± 17.7	0.196
Insulin (uIU/mL)	9.62 ± 4.04	29.30 ± 54.06	0.322
Homa-IR	2.21 ± 1.01	8.48 ± 17.04	0.316
Cortisol (ug/dL)	13.4 ± 2.4	11.4 ± 4.9	0.309
Total cholesterol (mg/dL)	202.6 ± 35.0	215.1 ± 44.3	0.532
Triglyceride (mg/dL)	228.5 ± 164.3	144.6 ± 77.5	0.190
High-density lipoprotein (mg/dL)	43.9 ± 16.0	41.2 ± 7.2	0.661
Low-density lipoprotein (mg/dL)	115.0 ± 27.9	142.4 ± 37.4	0.111
Metabolic syndrome index	1.4 ± 1.1	1.8 ± 1.6	0.549

All data were expressed as mean value ± standard deviation.
Low-PANSS (L-PANSS) group included schizophrenics with Positive and Negative Syndrome Scale (PANSS) total score below 65 (median of PANSS total scores of all 17 subjects); High-PANSS (H-PANSS) group included those with PANSS total score 65 or higher. PEHR1, 2, 3: post-exercise heart rate in the first, second and third minute, Homa-IR: homeostasis model assessment of insulin resistance
***:P<0.05 and **:P<0.01, significance between groups.**

The mean scores of respective sleep questionnaires, including ESS, ISI, PAS, and PSQI, were similar between L-PANSS and H-PANSS groups (Table 4). Parameters of sleep continuity measured by PSG, including awakening time, bed time, sleep efficiency, sleep latency, and total sleep time between groups were all similar. Marginal difference between the two groups were noted in the ratio of stage 3 and 4 sleep (slow wave sleep) and oxygen saturation rates.

Table 4. Sleep parameter measurement

Sleep continuity	L-PANSS (n=8)	H-PANSS (n=9)	P value
Awakening time	7.0 ± 0.9	7.2 ± 0.4	0.673
Bed time	22.7 ± 1.8	20.9 ± 1.6	0.052
Sleep efficiency (%)	84.0 ± 12.0	63.0 ± 28.3	0.071
Sleep latency	30.9 ± 20.2	24.3 ± 19.4	0.505
Total sleep time	7.5 ± 0.7	8.4 ± 1.1	0.067
Sleep questionnaires			
Epworth Sleepness Scale	9.0 ± 5.2	8.0 ± 4.0	0.663
Insomnia Severity Index	9.1 ± 3.7	8.3 ± 3.2	0.646
Pre-Sleep Arousal Scale	32.9 ± 16.6	26.4 ± 11.5	0.363
Pittsburgh Sleep Quality Index	13.8 ± 7.1	14.3 ± 7.5	0.872
Sleep architecture			
NREM S1 (%)	12.5 ± 14.6	29.3 ± 3.5	0.190
NREM S2 (%)	62.8 ± 19.0	47.0 ± 21.3	0.129
NREM S3+4 (%)	8.0 ± 9.1	1.1 ± 2.9	0.047*
REM sleep (%)	16.6 ± 5.5	22.7 ± 16.6	0.337
Sleep obstruction parameters			
Apnea-hypopnea index	6.2 ± 8.8	8.8 ± 9.4	0.560
Mean SpO_2 (%)	96.6 ± 1.5	95.0 ± 1.5	0.046*
ALM (events/hour)	8.8 ± 8.1	19.4 ± 19.0	0.164
Leg movement	53.1 ± 109.2	11.6 ± 34.7	0.295

All data were expressed as mean value ± standard deviation.
Low-PANSS (L-PANSS) group included schizophrenics with Positive and Negative Syndrome Scale (PANSS) total score below 65 (median of PANSS total scores of all 17 subjects); High-PANSS (H-PANSS) group included those with PANSS total scores 65 or higher. NREM: non-rapid eye movement, REM: rapid eye movement, SpO_2: saturation of peripheral oxygen, ALM: arousal and limb movement. NREM S3+4 (SWS) in the H-PANSS group was lower. Intergroup NREM S1, S2 and REM sleep were similar (Table 4). Mean SpO2 in the H-PANSS group was lower. Apnea-hypopnea index, Arousal and Limb Movement, and leg movement between groups were similar (Table 4).
***:P<0.05 and **:P<0.01, significance between groups.**

4. Discussion

To our knowledge, this is the first study to suggest that severer clinical symptoms are associated with metabolic and sleep disturbance in patients with schizophrenia. In more detail, this study demonstrates that schizophrenia patients with severe symptomatology may have more metabolic abnormalities including heavier body weight, wider neck circumference, and elevated systolic/diastolic blood pressure. We found no intergroup statistical significance in terms of blood sugar, insulin, cortisol, and lipid profiles. This is the first study to suggest that schizophrenic patients with more severe symptoms might have decreased oxygen saturation. It also demonstrated that patients with more severe symptoms had reduced SWS when their sleep efficiency and total sleep time were similar to the low PANSS group. Results concurred with prior studies: positive symptoms of schizophrenia increased REM sleep eye movement density, short REM latency, reduced sleep efficiency and prolonged sleep latency [26], [27], [28], [29]. Conversely, negative symptoms relate to short REM latency and SWS deficit [30], [31]. cognitive symptoms to SWS deficit [28], [29]. Sarkar et al. [32] found significant difference in SWS parameters (including increased Stage 3 and decreased Stage 4 latency between patients and controls.

The strength of this study is control over two groups of patients similar in basic demographic data, cognitive function performance, and physical fitness. Limitations of the study included small sample size and cross-section design. In sum, this study suggests clinical symptoms as linked with heavier body weight, wider neck circumference, elevated blood pressure, and shorter SWS in schizophrenic pateints. Further studies must confirm preliminary findings and elucidate the underlying mechanism.

Acknowledgments

This study is supported in part by Taiwan Department of Health Clinical Trial and Research Center of Excellence (DOH103-TD-B-111-004).

REFERENCES

[1] McEvoy JP, Meyer JM, Goff DC, Nasrallah HA, Davis SM, Sullivan L, et al. Prevalence of the metabolic syndrome in patients with schizophrenia: baseline results from the Clinical Antipsychotic Trials of Intervention Effectiveness (CATIE) schizophrenia trial and comparison with national estimates from NHANES III. Schizophr Res. 2005; 80: 19-32.

[2] Green AI, Patel JK, Goisman RM, Allison DB, Blackburn G. Weight gain from novel antipsychotic drugs: need for action. Gen Hosp Psychiatry. 2000; 22: 224-35.

[3] Newcomer JW. Second-generation (atypical) antipsychotics and metabolic effects: a comprehensive literature review. CNS drugs 2005; 19 Suppl 1: 1-93.

[4] Palmese LB, DeGeorge PC, Ratliff JC, Srihari VH, Wexler BE, Krystal AD, et al. Insomnia is frequent in schizophrenia and associated with night eating and obesity. Schizophr Res. 2011; 133: 238-43.

[5] Ritsner M, Kurs R, Ponizovsky A, Hadjez J. Perceived quality of life in schizophrenia: relationships to sleep quality. Qual Life Res 2004; 13: 783-91.

[6] Ritsner M, Modai I, Ponizovsky A. Assessing psychological distress in psychiatric patients: validation of the Talbieh Brief Distress Inventory. Compr Psychiatry. 2002; 43: 229-34.

[7] Association AP. Diagnostic and Statistical Manual of Mental Disorders. 4 ed: American Psychiatric Association, Washington, DC.; 1994.

[8] Kay SR, Fiszbein A, Opler LA. The positive and negative syndrome scale (PANSS) for schizophrenia. Schizophr Bull. 1987; 13: 261-76.

[9] Hamilton M. A rating scale for depression. J Neurol Neurosurg Psychiatry. 1960; 23: 56-62.

[10] Heinrichs DW, Hanlon TE, Carpenter WT, Jr. The Quality of Life Scale: an instrument for rating the schizophrenic deficit syndrome. Schizophr Bull. 1984; 10: 388-98.

[11] Rockville M. Guy W. ECDEU Assessment Manual for Psychopharmacology: Revised (DHEW publication number ADM 76-338). US: Department of Health, Education and Welfare, Public Health Service, Alcohol, Drug Abuse and Mental Health Administration, NIMH Psychopharmacology Research Branch, Division of Extramural Research Programs; 1976.

[12] Simpson GM, Angus JW. A rating scale for extrapyramidal side effects. Acta Psychiatr Scand Suppl. 1970; 212: 11-19.

[13] Barnes TR. A rating scale for drug-induced akathisia. Br J Psychiatry. 1989; 154: 672-76.

[14] Woods SW. Chlorpromazine equivalent doses for the newer atypical antipsychotics. J Clin Psychiatry. 2003; 64: 663-67.

[15] Ashton H. The diagnosis and management of benzodiazepine dependence. Curr Opin Psychiatry. 2005; 18: 249-55.

[16] Kern RS, Nuechterlein KH, Green MF, Baade LE, Fenton WS, Gold JM, et al. The MATRICS Consensus Cognitive Battery, part 2: co-norming and standardization. Am J Psychiatry. 2008; 165: 214-20.

[17] Nuechterlein KH, Green MF, Kern RS, Baade LE, Barch DM, Cohen JD, et al. The MATRICS Consensus Cognitive Battery, part 1: test selection, reliability, and validity. Am J Psychiatry. 2008; 165: 203-13.

[18] Matthews DR, Hosker JP, Rudenski AS, Naylor BA, Treacher DF, Turner RC. Homeostasis model assessment: insulin resistance and beta-cell function from fasting plasma glucose and insulin concentrations in man. Diabetologia 1985; 28: 412-19.

[19] Expert Panel on Detection E, Treatment of High Blood Cholesterol in A. Executive Summary of The Third Report of The National Cholesterol Education Program (NCEP) Expert Panel on Detection, Evaluation, And Treatment of High Blood Cholesterol In Adults (Adult Treatment Panel III). JAMA. 2001; 285: 2486-97.

[20] Buysse DJ, Reynolds CF 3rd, Monk TH, Berman SR, Kupfer DJ. The Pittsburgh Sleep Quality Index: a new instrument for psychiatric practice and research. Psychiatry Res. 1989; 28: 193-213.

[21] CM. M. Insomnia: psychological assessment and management.: New York: Guilford Press; 1993.

[22] Johns MW. A new method for measuring daytime sleepiness: the Epworth sleepiness scale. Sleep 1991; 14: 540-45.

[23] Nicassio PM, Mendlowitz DR, Fussell JJ, Petras L. The phenomenology of the pre-sleep state: the development of the pre-sleep arousal scale. Behav Res Ther. 1985; 23: 263-71.

[24]Rechtschaffen A, Kales, A.A. A manual of standardized terminology, techniques and scoring system for sleep stages of human subjects. Washington, DC: Government Printing Office: NIH Publication; 1968.

[25] EEG arousals: scoring rules and examples: a preliminary report from the Sleep Disorders Atlas Task Force of the American Sleep

Disorders Association. Sleep 1992; 15: 173-84.
[26] Zarcone VP, Benson KL. BPRS symptom factors and sleep variables in schizophrenia. Psychiatry Res. 1997; 66: 111-20.
[27] Poulin J, Daoust AM, Forest G, Stip E, Godbout R. Sleep architecture and its clinical correlates in first episode and neuroleptic-naive patients with schizophrenia. Schizophr Res. 2003; 62: 147-53.
[28] Monti JM, Monti D. Sleep in schizophrenia patients and the effects of antipsychotic drugs. Sleep Med Rev. 2004; 8: 133-48.
[29] Yang C, Winkelman JW. Clinical significance of sleep EEG abnormalities in chronic schizophrenia. Schizophr Res 2006; 82: 251-60.
[30] Tandon R, Shipley JE, Eiser AS, Greden JF. Association between abnormal REM sleep and negative symptoms in schizophrenia. Psychiatry Res. 1989; 27: 359-61.
[31] Keshavan MS, Miewald J, Haas G, Sweeney J, Ganguli R, Reynolds CF. Slow-wave sleep and symptomatology in schizophrenia and related psychotic disorders. J Psychiatr Res. 1995; 29: 303-14.
[32] Sarkar S, Katshu MZ, Nizamie SH, Praharaj SK. Slow wave sleep deficits as a trait marker in patients with schizophrenia. Schizophr Res. 2010; 124: 127-33.

BioMedicine March 2014, Vol. 4, No. 1, Pages 34-37 DOI 10.7603/s40681-014-0007-0

Short communication

Case report of Chromosome 3q25 deletion syndrome or Mucopolysaccharidosis IIIB

Yu-Tzu Chang[a,b], Chung-Hsing Wang[c,d], I-Ching Chou[a,e] ,Wei-De Lin [f,g], Siew-Yin Chee[c], Huang-Tsung Kuo[a,h], Fuu-Jen Tsai [f,i,j,k,*]

[a] Division of Pediatric Neurology, Children's Medical Center, China Medical University Hospital, Taichung, Taiwan
[b] China Medical University, Taichung, Taiwan
[c] Division of Pediatric Genetics and Metabolism, Children's Medical Center, Taichung, Taiwan
[d] Graduate Institute of Clinical Medical Science, China Medical University, Taichung, Taiwan
[e] Graduate Institute of Integrated Medicine, College of Chinese Medicine, China Medical University, Taichung, Taiwan
[f] Department of Medical Research, China Medical University Hospital, Taichung, Taiwan
[g] School of Post Baccalaureate Chinese Medicine, China Medical University, Taichung, Taiwan
[h] Division of Children's Development and Behavior, Children's Medical Center, China Medical University Hospital, Taichung, Taiwan
[i] School of Chinese Medicine, China Medical University, Taichung, Taiwan
[j] Department of Medical Genetics, China Medical University Hospital, Taichung, Taiwan
[k] Department of Health and Nutrition Biotechnology, Asia University, Taichung, Taiwan

Received 28th of December 2013 Accepted 15th of January 2014

Keywords:
Chromosome 3q deletion;
Mucopolysaccharidosis

ABSTRACT

Interstitial deletions of the long arm of chromosome 3 have, to our knowledge, been reported in only eleven patients; detailed genotype- phenotype correlations are not well established. Here we describe a case with interstitial deletion involving 3q25.33 region. Dysmorphic features and developmental delay lead to clinical genetic and enzyme assessment. Low alpha-hexosaminidase level is also noted, which imply Mucopolysaccharidosis(MPS) IIIB.

1. Introduction

Interstitial deletions involving the long arm of chromosome 3 are rare and detailed genotype-phenotype correlations have not been well established to date. Proximal 3q deletion syndrome was delineated by Simovich et al. They concluded that these patients have a distinct recognizable facial dysmorphism and are at risk for developmental delay plus other structure abnormalities of the brain, genitor-urinary and musculoskeletal system. Furthermore, only 11 cases have been reported with distal deletions involving 3q25 regions. Among them, variable chromosomal breakpoints and deletion sizes located from 3q23 to 3q26.1 have been reported [1-11]. All patients presented facial dysmorphism and developmental delay, but other phenotypic features, such as cardiac defect, microcephaly, epicanthus and short stature were not always present.

We report a patient with interstitial deletion involving the 3q25.33 region and compare her phenotype with 11 previously reported cases. This report will add more specific clinical profiles to this unique disease spectrum.

Methods and Results

1.1 Clinical description

The eleven-year-old female patient was referred for evaluation of dysmorphic features and developmental delay at age eight. She was the first child of healthy and non-consanguineous parents; family history was not contributory. The pregnancy itself was not complicated, the child born by term vaginal delivery with no adverse perinatal events observed. Her birth body weight at birth was 3250 gm (50 percentile), her length 52 cm (85-97 percentile). She was noticeably overactive, talkative, easily distracted and emotionally labile since age three. Her school performance was poor. Facial abnormalities (Fig 1A&B) included a coarse face, hairy skin, synophrys, bilateral mild epicanthic folds, but no blepharophimosis. Nasal bridge was broad and flat, nasal tip bulbous in addition to having anteverted nostrils. Philtrum was smooth. Her mouth was observed as having a full lip and her palate intact. Ears were set low, with posterior rotation and mild dysplasy noted. She had normal palmer creases, no clinodactyly of fingers. She had facial hirsutism and hypertrichosis of limbs. All the patient's cardiovascular, abdominal, genito-urinary and neurologic examinations were normal. Neurodevelopmental assessment by Wechsler Preschool and Primary Scale of Intelligence-Revision (WPPSI-R) was 60 and Adaptive Behavior Assessment System (ABAS) revealed mild adaptive disability. Attention deficit hyperactivity disorder (ADHD) was also diagnosed during assessment. In addition, enzyme analysis for mucopolysaccharidosis was performed due to coarse facial features and developmental delay. Low alpha-hexosaminidase level was found with 0.16 nmol/17h/mg (normal range 17.2±6.4 nmol/17h/mg) in the whole blood leukocyte. Therefore, mucopolysaccharidosis (MPS) type IIIB was also diagnosed. She started rehabilitation, along with behavioral and art therapies, for treatment of ADHD.

1.2 Chromosome study

Chromosome preparation was performed from peripheral white blood cells, and trypsin-banding Giemsa was applied 550 band resolution. G-banding analysis revealed that the patient had a karyotype of 46, xx, deletion at cytoband 3q25.33 (Fig 2).

* Corresponding author. Department of Medical Genetics, Pediatrics and Medical Research, China Medical University Hospital, Number 2, Yuh-Der Road, 404 Taichung, Taiwan.
E-mail address: d0704@mail.cmuh.org.tw

Published online: 13 February 2014

Figure 1A&B:
This 11 year-old girl with (A) coarse face, hirsutism, hypertelorism, synophrys, bilateral mild epicanthic folds, broad and flat nasal bridge. (B) low set, posterior rotated and mild dysplastic ear.

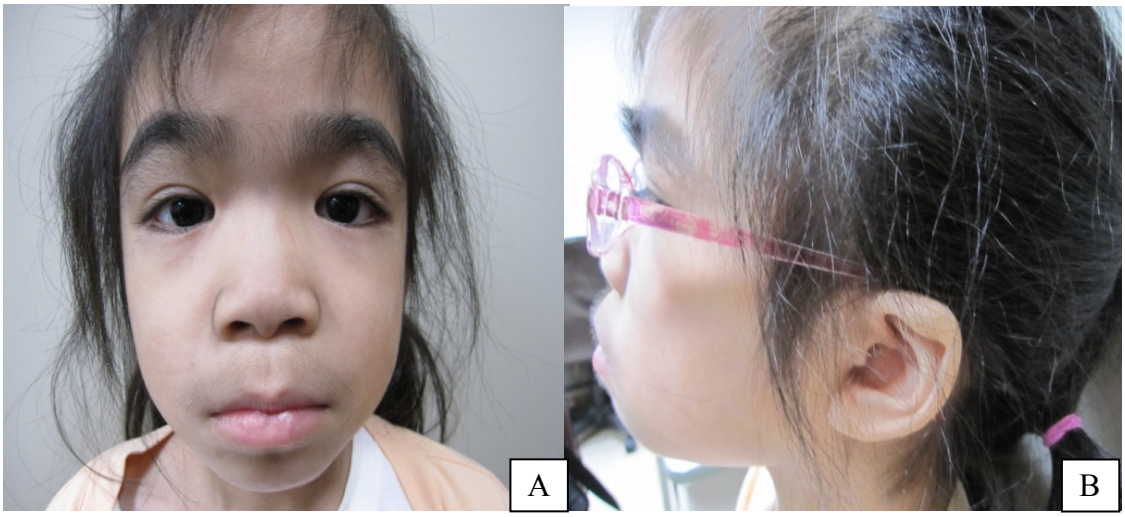

Figure 2:
Genome-Wide Human SNP Array 6.0 was performed and revealed a deletion at cytoband 3q25.33; physical position 160.277-160.450 Mb about the size of 173 Kb. Her father had the same cytogenic deletion

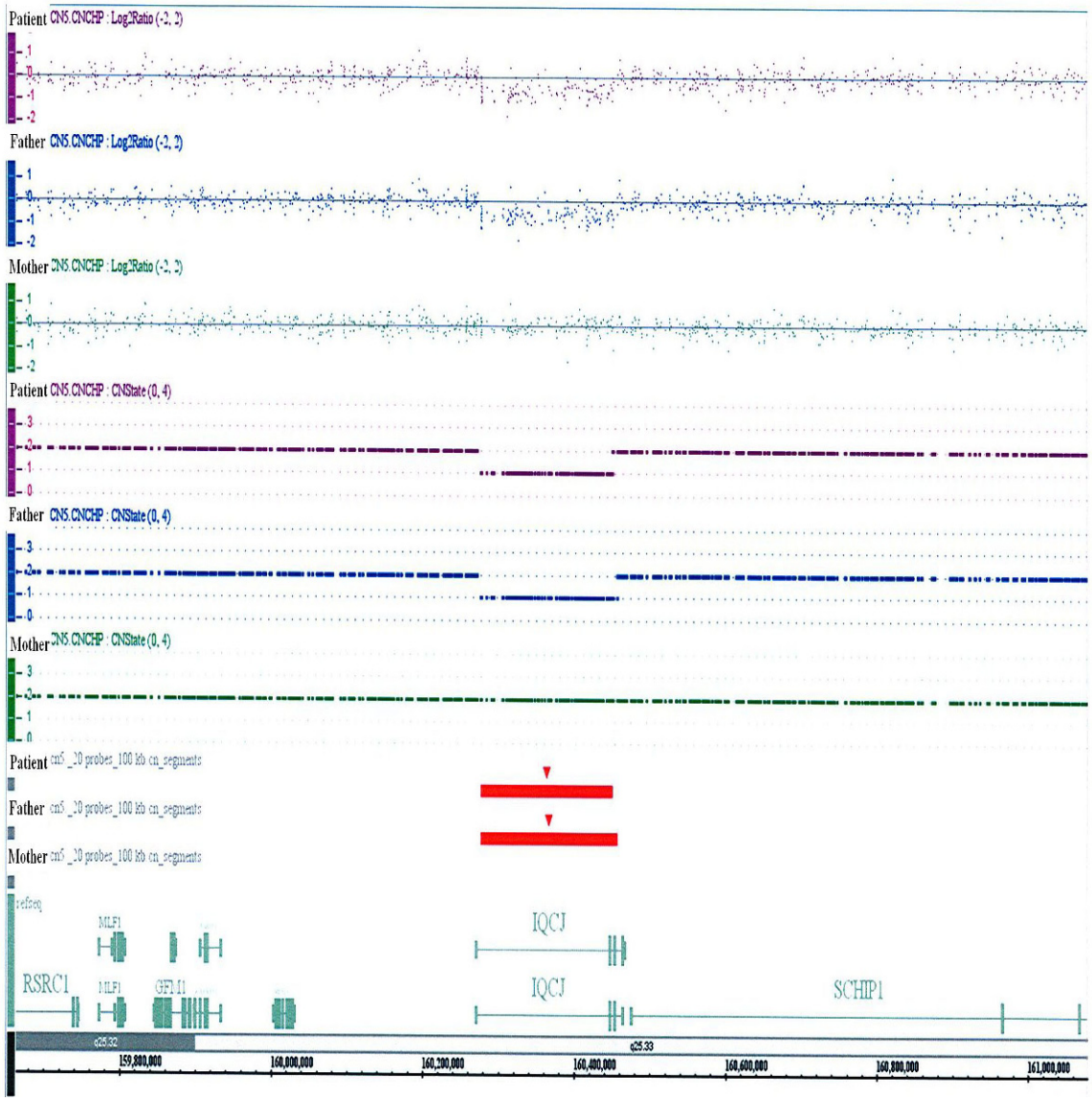

Discussion

Table 1 compares phenotype of our case with that of 11 previously reported 3q25 deletions [1-11]; female predominance was observed (10/12). Despite phenotypic variability, some clinical features, especially facial dysmorphism, were notable and comparable to cases reported earlier: e.g., synophrys, broad nasal bridge, large or abnormal ears. Developmental delay was also noted. Our patient had similar clinical facial features: synophrys, epicanthus, broad nasal bridge and ear abnormalities. Her parents also agreed to have genetic testing performed. Her mother's genotype was normal. Her father had the same deletion point at 3q25.33 but with normal appearance, which may suggest variable expressivity in 3q25 deletion syndrome.

Table 1. Clinical features of this and 11 additional previously reported patients with interstitial deletion in 3q25

	Previous 11 cases (%)	Present case
Sex	M/F (2/9)	F
Parental karyotypes normal	10/10 (100%)	Paternal inheritance
Developmental delay	11/11 (100%)	+
Micorcephaly	5/10 (50%)	-
Synophrys	6/8 (75%)	+
Epicanthus	7/11 (64%)	+
Ptosis	7/11 (64%)	-
Blepharophimosis	6/11 (55%)	-
Broad nasal bridge	11/11 (100%)	+
Ear abnormalities	10/10 (100%)	+
Cardiac defect	5/8 (63%)	-

+, present; -, absent; M, male; F, female

Associated neuropsychiatric disorder was only mentioned in one case report of autistic and obsessive behavioral traits involved with 3q25 deletion [10, 12]. In our patient, ADHD was noted with adaptive disability. Significance of attention deficit traits in the context of this chromosome deletion in our patient is uncertain at this time. However, specific behavioral phenotypes (like obsessive behavior) are recognized features of chromosomal deletion syndromes [13-14].

Another issue noted in this case was low alpha-hexosaminidase level, indicating that her as a possible victim of mucopolysaccharidosis. Mucopolysaccharidosis-IIIB (MPS- IIIB) or Sanfilippo-B syndrome is caused by deficiency of lysosomal α-N-acetylglucosaminidase that leads to accumulation of heparan-sulphate and degeneration of the central nervous system with progressive dementia, hyperactivity, and aggressive behavior [15-16]. Clinical dysmorphic features of MPS III are less pronounced than those of other MPS types. Individuals with MPS III typically have mildly "coarse" facial features, a large head (macrocephaly), lower abdomen (inguinal hernia), restless behavior and vision problems, which also resemble our present case. However, there was no other skeletal abnormalities, chronic diarrhea, recurrent upper airway infections, sleep disorder, hearing loss, nor hepatomegaly. Despite developmental delay, there was no sign of regression observed in our case. However, attenuated clinical phenotype was cited in a previous article [15]. In fact, they reported a large proportion (79%) MPS type IIIB showing as the attenuated type. Attenuated phenotype is characterized by significantly slower regression of intellectual and motor abilities. A majority of patients lived well into adulthood [15]. This probably emanated from the presence of low-level residual enzyme activity that delayed storage of heparan-sulphate and hence onset and progression of symptoms. Classical MPS type IIIB is caused by mutation in NAGLU at 17q21.1 [17-18]. Missense changes p.R643C, p.S612G, p.E634K, and p.L497V were found in patients with attenuated phenotype, exclusively. Further genetic testing for such regions is ongoing. Our review contains no report of MPS at mutation related to 3q25 region. It remains unclear as to whether the clinical phenomenon of this patient was partly influenced by other etiologies such as MPS.

Clinical facial dysmorphism appearance in our present case may resemble genetic disorders such as Donohue syndrome, 3q deletion syndrome or even storage diseases [17, 19-20]; final diagnosis may depend on genetic testing. Variable expressivity and phenotype heterogeneity does exist in many genetic disorders. At present, we cannot exclude possible causal relationship between these diseases. Long-term follow-up of details on natural disease course such as neurocognitive deterioration, combined with genotype correlation, may help to predict clinical course of the disease and establish definitive diagnosis.

Declaration of Interest: Authors declare no conflicts of interest for this work.

Acknowledgments

This study was supported in part by grant from China Medical University Hospital (DMR-96-004).

REFERENCES

[1] Moortgat S, Verellen-Dumoulin C, Maystadt I, Parmentier B, Grisart B, Hennecker JL, et al. Developmental delay and facial dysmorphism in a child with an 8.9 Mb de novo interstitial deletion of 3q25.1-q25.32: Genotype-phenotype correlations of chromosome 3q25 deletion syndrome. Eur J Med Genet 2011; 54: 177-80.

[2] Franceschini P, Cirillo Silengo M, Davi G, Bianco R, Biagioli M. Interstitial deletion of the long arm of chromosome 3 in a patient with mental retardation and congenital anomalies. Hum Genet 1983; 64:97.

[3] Martsolf JT, Ray M. Interstitial deletion of the long arm of chromosome 3. Ann Genet 1983; 26: 98-99.

[4] Al-Awadi SA, Naguib KK, Farag TI, Teebi AS, Cuschieri A, Al-Othman SA, et al. Complex translocation involving chromosomes Y, 1, and 3 resulting in deletion of segment 3q23-q25. J Med Genet 1986;23:91-92.

[5] Alvarado M, Bocian M, Walker AP. Interstitial deletion of the long arm of chromosome 3: case report, review, and definition of a phenotype. Am J Med Genet 1987; 27: 781-86.

[6] Chandler KE, de Die-Smulders CE, Engelen JJ, Schrander JJ. Severe feeding problems and congenital laryngostenosis in a patient with 3q23 deletion. Eur J Pediatr 1997; 156: 636-38.

[7] Ko WT, Lam WF, Lo FM, Chan WK, Lam TS. Wisconsin syndrome in a patient with interstitial deletion of the long arm of chromosome 3: further delineation of the phenotype. Am J Med Genet A 2003; 120A: 413-17.

[8] Rea G, McCullough S, McNerlan S, Craig B, Morrison PJ. Delineation of a recognisable phenotype of interstitial deletion 3 (q22.3q25.1) in a case with previously unreported truncus arteriosus. Eur J Med Genet 2010; 53: 162-67.

[9] Sudha T, Dawson AJ, Prasad AN, Konkin D, de Groot GW, Prasad C. De novo interstitial long arm deletion of chromosome 3 with facial dysmorphism, Dandy-Walker variant malformation and

hydrocephalus. Clin Dysmorphol 2001; 10: 193-96.
[10] Slavotinek AM, Huson SM, Fitchett M. Interstitial deletion of band 3q25. J Med Genet 1997; 34: 430-32.
[11] Robin NH, Magnusson M, McDonald-McGinn D, Zackai EH, Spinner NB. De novo interstitial deletion of the long arm of chromosome 3: 46,XX,del(3)(q25.1q26.1). Clin Genet 1993; 44: 335-37.
[12] Vardarajan BN, Eran A, Jung JY, Kunkel LM, Wall DP. Haplotype structure enables prioritization of common markers and candidate genes in autism spectrum disorder. Transl Psychiatry 2013; 3: e262.
[13] Dilts CV, Morris CA, Leonard CO. Hypothesis for development of a behavioral phenotype in Williams syndrome. Am J Med Genet Suppl 1990; 6: 126-31.
[14] Shprintzen RJ, Goldberg R, Golding-Kushner KJ, Marion RW. Late-onset psychosis in the velo-cardio-facial syndrome. Am J Med Genet 1992; 42: 141-42.
[15] Valstar MJ, Bruggenwirth HT, Olmer R, Wevers RA, Verheijen FW, Poorthuis BJ, et al. Mucopolysaccharidosis type IIIB may predominantly present with an attenuated clinical phenotype. J Inherit Metab Dis 2010;33:759-67.
[16] Saini AG, Singhi P, Sahu JK, Ganesan SL, Vyas S, Rao S, et al. Hyperactivity, Unexplained Speech Delay, and Coarse Facies—Is It Sanfilippo Syndrome? J Child Neurol 2013.
[17] Yogalingam G, Hopwood JJ. Molecular genetics of mucopolysaccharidosis type IIIA and IIIB: Diagnostic, clinical, and biological implications. Hum Mutat 2001; 18: 264-81.
[18] Zhao HG, Li HH, Bach G, Schmidtchen A, Neufeld EF. The molecular basis of Sanfilippo syndrome type B. Proc Natl Acad Sci U S A 1996; 93: 6101-05.
[19] de Bock M, Hayes I, Semple R. "Donohue syndrome". J Clin Endocrinol Metab 2012; 97: 1416-17.
[20] Simovich MJ, Bland SD, Peiffer DA, Gunderson KL, Cheung SW, Yatsenko SA, et al. Delineation of the proximal 3q microdeletion syndrome. Am J Med Genet A 2008; 146A: 1729-35.